Drug Design, Development and Therapy

Dovepress
Taylor & Francis Group

Open Access Full Text Article

REVIEW

Discovery of Pyrazoline Benzenesulfonamide Derivatives as Anticancer Agents: A Review

Dadang Muhammad Hasyim[1,2], Ida Musfiroh[3], Rudi Hendra[4], Ezatul Ezleen Kamarulzaman[5], Ritmaleni Ritmaleni[6], Muchtaridi Muchtaridi[3,7]

[1]Doctoral Program of Pharmacy, Faculty of Pharmacy, Universitas Padjadjaran, Sumedang, West Java, Indonesia; [2]Department of Pharmacy, STIKes Karsa Husada Garut, Garut, West Java, Indonesia; [3]Department of Pharmaceutical Analysis and Medicinal Chemistry, Faculty of Pharmacy, Universitas Padjadjaran, Sumedang, West Java, Indonesia; [4]Department of Chemistry, Faculty of Mathematics and Natural Sciences, Universitas Riau, Pekanbaru, Riau, Indonesia; [5]School of Pharmaceutical Sciences, Universiti Sains Malaysia, Gelugor, Pulau Pinang, Malaysia; [6]Department of Pharmaceutical Chemistry, Faculty of Pharmacy, Universitas Gadjah Mada, Sleman, Yogyakarta, Indonesia; [7]Research Collaboration Centre for Theranostic Radiopharmaceuticals, National Research and Innovation Agency (BRIN), Sumedang, West Java, Indonesia

Correspondence: Muchtaridi Muchtaridi; Ida Musfiroh, Department of Pharmaceutical Analysis and Medicinal Chemistry, Faculty of Pharmacy, Universitas Padjadjaran, Sumedang, West Java, Indonesia, Email muchtaridi@unpad.ac.id; ida.musfiroh@unpad.ac.id

Abstract: Pyrazoline benzenesulfonamide derivatives represent a distinctive class of heterocyclic compounds that synergistically combine the pharmacological versatility of the pyrazoline scaffold with the enzyme-inhibitory prowess of benzenesulfonamide moieties. These hybrids have emerged as promising candidates in anticancer drug discovery. This review systematically examines various synthetic strategies employed to prepare these derivatives, including classical Claisen–Schmidt condensation as well as modern ultrasound- and microwave-assisted protocols. These methods facilitate efficient structural diversification, incorporating a wide range of heterocyclic and aromatic substituents such as morpholine, pyrazole, benzodioxole, tetrazole, and ferrocene. Biological evaluations, integrating both in vitro cytotoxicity assays and in silico molecular docking studies, were analyzed to elucidate the anticancer potential and mechanistic insights of these compounds, particularly their selective inhibition of tumor-associated enzymes such as matrix metalloproteinases (MMP-2, MMP-9), carbonic anhydrase isoforms (hCA IX, hCA XII), and cyclooxygenase-2 (COX-2). The results reveal that several derivatives exhibit potent antiproliferative activity across multiple cancer cell lines, including lung (A549), breast (MCF-7), cervical (HeLa), colon (COLO 205), and oral squamous carcinoma, demonstrating significant tumor selectivity and low toxicity toward normal cells. Structure–activity relationship analyses further underscore the critical influence of electronic substituents and their positioning on aromatic rings in modulating both efficacy and selectivity. These findings highlight the therapeutic potential of pyrazoline benzenesulfonamide derivatives and support the continued optimization of synthetic strategies and mechanistic studies to facilitate their development as effective anticancer agents capable of overcoming clinical challenges such as drug resistance and adverse side effects.

Keywords: pyrazoline benzenesulfonamide, anticancer agents, synthesis, structure-activity relationships

Introduction

Cancer is a non-communicable disease that poses a significant global health burden. The disease is characterized by the loss of control over cell cycle regulation and cell homeostatic function in multicellular organisms, resulting in abnormal and uncontrolled cell proliferation.[1] As a result, cells will continue to proliferate, leading to the development of abnormal tissue growth and tumor growth. The process of cancer progression, or carcinogenesis, involves a series of microevolutionary changes in cancer growth that can occur over several months or years, progressing through various stages and ultimately leading to a malignant state.[2] Curing cancer remains highly challenging due to the complexity of its underlying molecular mechanisms. Current treatment strategies primarily aim to alleviate symptoms, improve the patient's quality of life, and minimize the risk of recurrence. Therapeutic approaches for cancer patients differ significantly from those for non-cancer patients. Cancer therapies encompass a broad range of interventions such as radiotherapy, chemotherapy, and hormone therapy, as well as surgery.[3,4]

Received: 20 August 2025
Accepted: 4 November 2025
Published: 27 December 2025

Cancer treatment with chemotherapy is probably the most recognized cancer treatment by the general public. Chemotherapy involves the administration of specialized drugs to patients, which aim to prevent the spread of cancer cells, slow their growth, and ultimately kill cancer cells. Various anticancer drugs have been developed, including drugs that stimulate the differentiation of cancer cells into benign cells, drugs that enhance the effectiveness of radiation, and drugs that modulate the immune response against cancer cells.[5,6] Additionally, numerous drugs have been developed based on the molecular characteristics of cancer cells. However, these therapies often face challenges such as drug resistance, reduced tolerance, limited selectivity, and a range of adverse side effects. A variety of drugs have been used in cancer treatment, including epirubicin, doxorubicin, vinorelbine, docetaxel, sorafenib, cisplatin, and busulfan.

Pyrazolines are an intriguing class of heterocyclic compounds that have attracted significant attention in drug design and development. Their importance lies in their ability to serve as isosteres of other heterocyclic rings, such as imidazole, thiazole, tetrazole, isoxazole, and oxazole.[7] This property enables pyrazolines to modulate the physicochemical properties and biological activities of these compounds, resulting in a diverse range of lead compounds with potential therapeutic applications. Structurally, pyrazoline comprises a five-membered ring containing two adjacent nitrogen atoms and one endocyclic double bond. Pyrazoline can exist in three different isomeric forms, 1-pyrazoline, 2-pyrazoline, and 3-pyrazoline, depending on the position of the double bond in the ring, as shown in Figure 1. Among these, 2-pyrazoline has been studied most extensively due to its greater stability compared to the other two forms.[8] Pyrazoline derivatives have garnered significant attention in medicinal chemistry due to their diverse range of biological activities. These compounds exhibit a broad spectrum of pharmacological properties, making them attractive targets for drug discovery and development. A wide range of biological activities of pyrazoline derivatives have been reported, including anticancer,[9–11] anti-Alzheimer,[12,13] antitubercular,[14,15] anticonvulsant,[16,17] anti-inflammatory,[18–20] antidepressant,[21] antimicrobial,[14,22–24] anti-HIV,[25–27] antimalarial,[28] anti-Parkinson,[29,30] antioxidant,[20,31,32] antiviral,[33] anti-amoebic,[34,35] anti-diabetic[36] (Figure 2).

Sulfonamides, particularly benzenesulfonamide derivatives, are another important class of pharmacophores in medicinal chemistry.[37] Characterized by a sulfonamide group attached to a benzene ring, benzenesulfonamide compounds are well known for their ability to form strong hydrogen bonds with biological targets, resulting in high binding affinity and improved pharmacokinetic profiles. These properties have made sulfonamide derivatives potent inhibitors of enzymes, such as carbonic anhydrases, which are often upregulated in tumor environments and play key roles in processes including cell proliferation, survival, and metastasis.[38,39] Various sulfonamide derivatives have been developed for biological purposes, including antibacterial,[40] antifungal,[41] antioxidant,[42] anti-inflammatory,[43] antidiabetic,[44] anticancer,[45–47] antihypertensive,[48] antimicrobial,[49] antimycobacterial,[50,51] antimalarial,[52] antiprotozoal[53] activities. Moreover, some benzenesulfonamide derivatives exhibit a broad spectrum of biological activities, such as carbonic anhydrase inhibitors,[54,55] herbicides and plant growth regulators,[56–58] elastase inhibitors,[59] and Clostridium histolyticum collagenase inhibitors.[60]

The objective of this review is to comprehensively examine recent developments in the discovery and synthesis of pyrazoline benzenesulfonamide derivatives as potent anticancer agents against various types of cancer to date. This

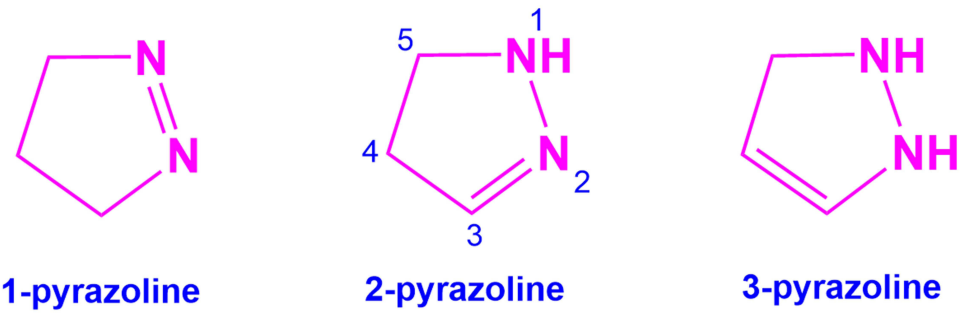

Figure 1 Chemical structures of 1-pyrazoline, 2-pyrazoline, and 3-pyrazoline isomers.

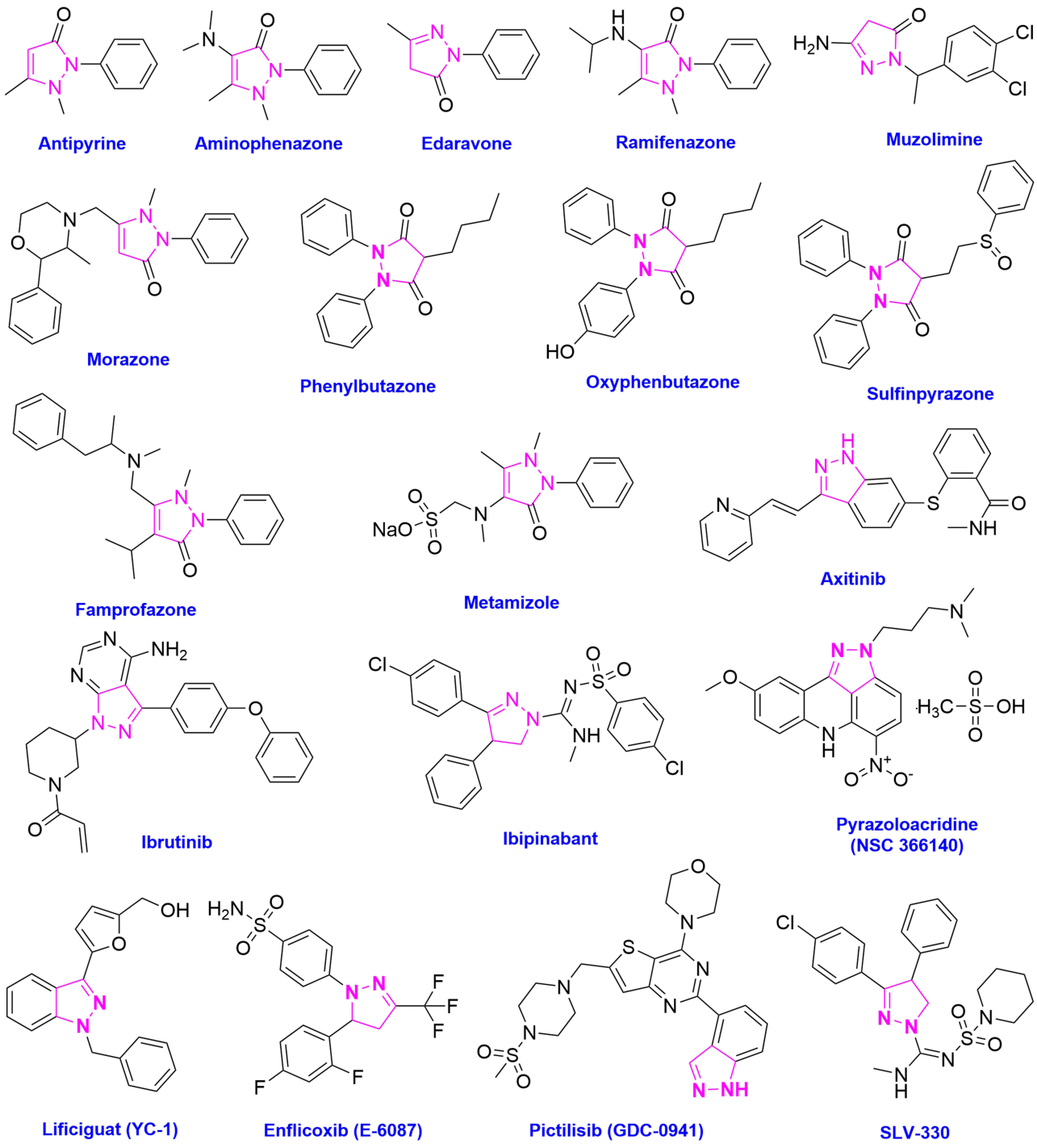

Figure 2 Overview of the biological activities of pyrazoline derivatives.

information will assist chemists and biologists in identifying promising structural frameworks, thereby guiding chemical synthesis efforts toward the discovery and development of more effective anticancer agents.

Clinically Available Drugs and Under Developments Containing Pyrazoline

The pyrazoline ring system represents a prominent structural motif widely found in clinically approved pharmaceuticals targeting a broad spectrum of diseases. Numerous marketed drugs, as shown in Figure 3, including antipyrine, phenylbutazone, edavarone, axitinib, and others, feature the pyrazoline moiety, underscoring its significance as

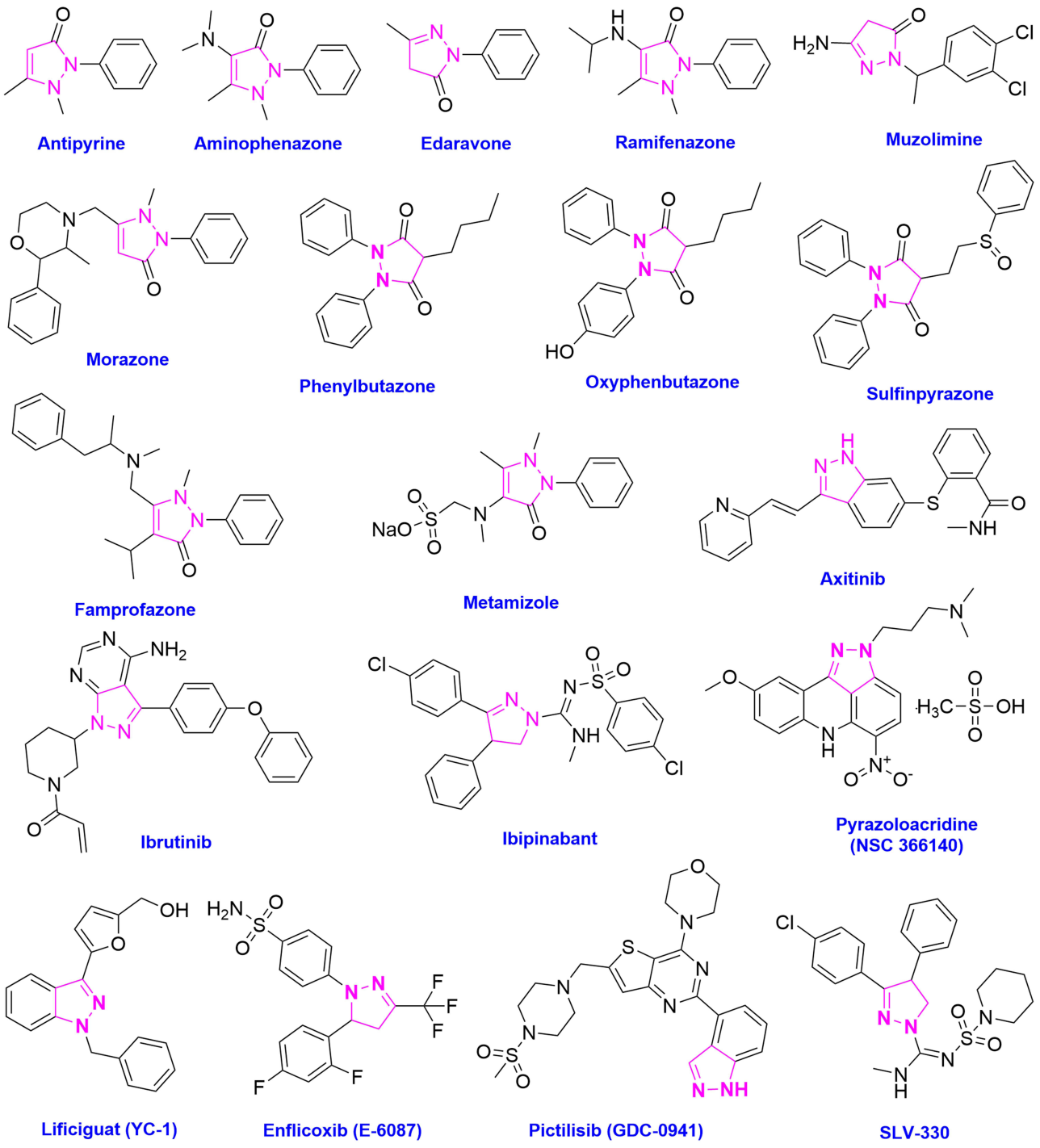

Figure 3 Representative clinically used and investigational drugs with a pyrazoline scaffold.

a privileged scaffold in medicinal chemistry. The versatility of the pyrazoline core is attributed to its broad spectrum of biological activities, which encompass anti-inflammatory, anticancer, analgesic, and cardiovascular effects, among others. This remarkable pharmacological profile has sparked sustained scientific interest and extensive research efforts aimed at developing novel pyrazoline derivatives with enhanced efficacy and safety. Consequently, beyond approved therapeutics, a diverse array of new pyrazoline-based compounds is in various stages of preclinical and clinical evaluation, highlighting the ongoing expansion of this class for therapeutic innovation.

Phenazone, also known as antipyrine, is a non-steroidal anti-inflammatory drug (NSAID) with analgesic and antipyretic properties. Its effects are believed to be mediated through the inhibition of cyclooxygenase isoforms, specifically COX-1, COX-2, and COX-3, which are involved in prostaglandin (PG) synthesis.[61,62] Phenylbutazone is another NSAID that exhibits analgesic and antipyretic activities and is used in some instances related to acute pain and musculoskeletal disorders, such as ankylosing spondylitis and rheumatoid arthritis.[63,64] Ramifenazone is a pyrazole derivative that acts as a non-steroidal anti-inflammatory drug, exhibiting analgesic, antipyretic, anti-inflammatory, and antimicrobial properties.[65] Famprofazone is an NSAID with analgesic, anti-inflammatory, and antipyretic effects and is notable for being metabolized to methamphetamine and/or amphetamine.[66,67]

Morazone is an NSAID used as an analgesic and is metabolized into phenmetrazine.[68] Oxyphenbutazone is a metabolite of phenylbutazone possesses anti-inflammatory effects. It is an orally active, non-selective COX inhibitor that has been shown to kill non-replicating Mycobacterium tuberculosis selectively.[69,70] Aminophenazone is another NSAID used as analgesics, antipyretics, and anti-inflammatories.[71] Its mechanism of action involves inhibiting COX-1 and COX-2 enzymes.[72] Metamizole is an analgesic, antipyretic, and spasmolytic drug used to treat both acute and chronic pain and fever. The most important side effect of metamizole is the development of agranulocytosis.[73] Edaravone is a free radical scavenger used as a neuroprotective agent in patients with acute ischemic stroke and amyotrophic lateral sclerosis.[74,75]

Sulfinpyrazone is an oral uricosuric agent used to treat chronic or intermittent gouty arthritis. It competitively inhibits the reabsorption of uric acid at the proximal convoluted tubule, thereby facilitating urinary excretion of uric acid and reducing plasma urate concentrations.[76,77] Muzolimine is a diuretic that has been proposed for the treatment of hypertension, known for its high ceiling effect similar to loop diuretics.[78] It can also be used in cardiovascular disease research.[79] Ibrutinib is a Bruton's tyrosine kinase inhibitor used in the treatment of lymphoid cancers, including chronic lymphocytic leukemia, Waldenström macroglobulinemia, and mantle cell lymphoma.[80] Ibipinabant is a potent, selective, and orally active antagonist of the cannabinoid CB1 receptor with potential applications in obesity and diabetes research.[81,82] Axitinib is a potent and selective antagonist inhibitor of vascular endothelial growth factor receptor (VEGFR) tyrosine kinases. It can suppress tumor growth and metastasis by inhibiting both angiogenesis and lymphangiogenesis. Additionally, it exerts antitumor effects through mechanisms involving the induction of apoptosis in tumor cells.[83]

Enflicoxib (E-6087) is a new pyrazoline derivative and an NSAID used for the treatment of pain and osteoarthritis. It functions as a selective COX-2 inhibitor with potent anti-inflammatory and analgesic activity.[84,85] SLV-330 is a drug candidate for the treatment of central nervous system (CNS) disorders and acts as a cannabinoid CB1 receptor antagonist.[86] Lificiguat (YC-1) was initially identified as an activator of NO-independent soluble guanylyl cyclase. It inhibits platelet aggregation and prevents vascular contraction. Additionally, it exhibits potent anticancer activity through various mechanisms in multiple cancer cell lines.[87,88] Pictilisib (GDC-0941) is a specific PI3K inhibitor with good clinical tolerability and promising anti-neoplastic activity in adult cancers; it also demonstrates anti-proliferative and pro-apoptotic effects in pediatric human medulloblastoma cell lines.[89] Pyrazoloacridine (NSC 366140) is a pyrazoline-fused acridine analogue currently under investigation in Phase II clinical trials as an anticancer agent.[90]

Synthetic Approaches for the Preparation of Pyrazoline Benzenesulfonamide Derivatives

Pyrazoline derivatives can be synthesized using either one-pot or two-pot techniques, as illustrated in Figure 4. The one-pot technique entails a multicomponent reaction in a single vessel, wherein an aromatic ketone, an aromatic aldehyde, and hydrazine are combined directly to afford the corresponding pyrazoline scaffold.[91–93] In contrast, the two-pot technique involves of multiple reaction steps and is more commonly reported for the synthesis of pyrazoline derivatives than the one-pot technique.[94] The two-pot technique consists of two synthetic steps. It first involves the preparation of chalcones, followed by cyclization with hydrazine under suitable reaction conditions.[95,96] This is supported by other studies, which report that pyrazoline derivatives are generally obtained by first synthesizing chalcones, followed by the formation of pyrazolines in acidic or basic medium or alcoholic solvents.[97] A widely accepted mechanism for chalcone synthesis is the Claisen-Schmidt condensation, which involves a base-catalyzed cross-aldol reaction between aromatic aldehydes and ketones. Under basic conditions, the enolate ion derived from the ketone attacks the carbonyl carbon of the

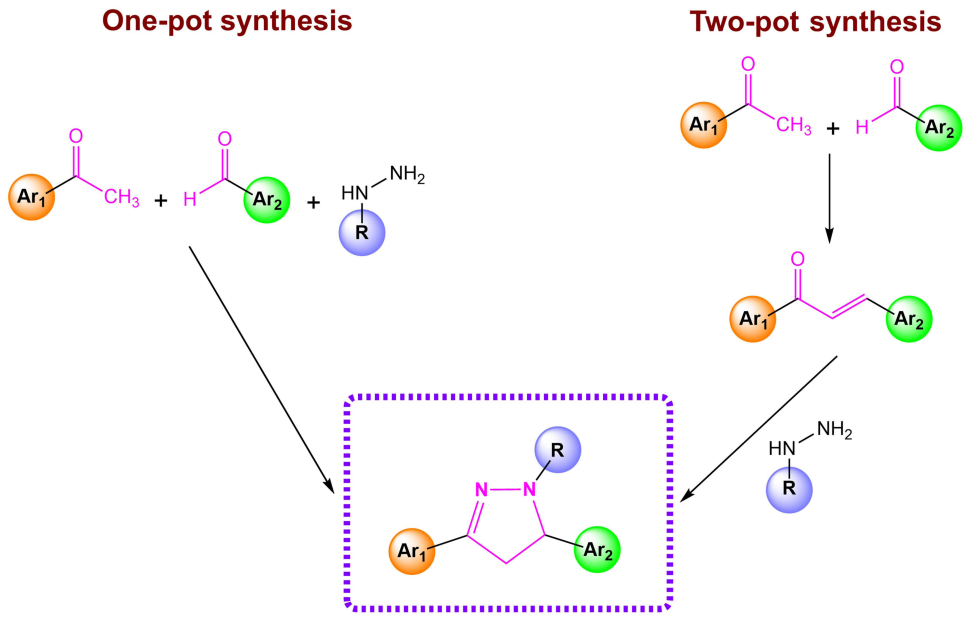

Figure 4 Schematic representation of one-pot and two-pot synthetic strategies for pyrazoline derivatives.

aldehyde, leading to the formation of a β-hydroxyketone intermediate, which subsequently undergoes dehydration to yield the corresponding chalcone,[98] as illustrated in Figure 5.

Multiple synthetic strategies have been established for the construction of pyrazoline derivatives, with the Knoevenagel and Fisher methods being among the most extensively utilized. These approaches enable efficient synthesis of structurally diverse pyrazolines, commonly achieved through the reaction of α,β-unsaturated carbonyl compounds with hydrazine or phenylhydrazine in the presence of acetic acid.[99,100] As illustrated in Figure 6, two mechanistic pathways have been proposed for the cyclization of α,β-enones with hydrazine derivatives, contingent on variables such as reaction conditions, catalyst, and substrate structure. The first route proceeds via formation of a hydrazone intermediate, followed by intramolecular cyclization to yield the desired 2-pyrazoline scaffold. Alternatively, the reaction may proceed through an aza-Michael addition, forming an aza-Michael intermediate that subsequently undergoes cyclization and water elimination to afford the 2-pyrazoline core. Both mechanisms reflect the strategic versatility available for the tailored synthesis of pyrazoline compounds.[97,101,102]

The synthesis of pyrazoline derivatives can be carried out using various heating methods, including microwave irradiation, ultrasonic irradiation, grinding techniques, ionic liquids, and conventional methods.[103–105] These methods offer several improvements over traditional protocols, notably faster reaction rates, higher yields, and greater environmental compatibility. Additionally, a wide range of solvents can be used, such as methanol, ethanol, toluene, pyridine, polyethylene glycol (PEG), dimethylformamide (DMF), tetrahydrofuran (THF), and dimethyl sulfoxide (DMSO).[106–108] These solvents are selected based on their specific properties, such as polarity and their ability to dissolve reactants, which can significantly influence the reaction's efficiency and outcome. Various catalysts have also been reported for the synthesis of pyrazoline derivatives. These include acids such as formic acid, acetic acid, glacial acetic acid, hydrochloric acid, chloroacetic acid, propionic acid, acetic anhydride, butyric acid, gallic acid, sulfuric acid,[109–112] as well as bases such as sodium hydroxide, potassium hydroxide, potassium carbonate, and triethylamine (TEA).[113–115] The choice of catalyst depends on the specific reaction conditions and the desired outcome. Hydrazines are the most frequently used reactants, as they provide both nitrogen atoms in the 2-pyrazoline ring.

Pyrazoline benzenesulfonamide derivatives can be synthesized via one-step, two-step, or multi-step reactions. A one-step approach, such as a one-pot reaction, can directly yield pyrazoline compounds using suitable reactants like acetophenone, benzaldehyde, and 4-hydrazinylbenzenesulfonamide. The two-step reaction typically involves a Claisen-Schmidt condensation reaction followed by cyclization with 4-hydrazinylbenzenesulfonamide. Multi-step reactions

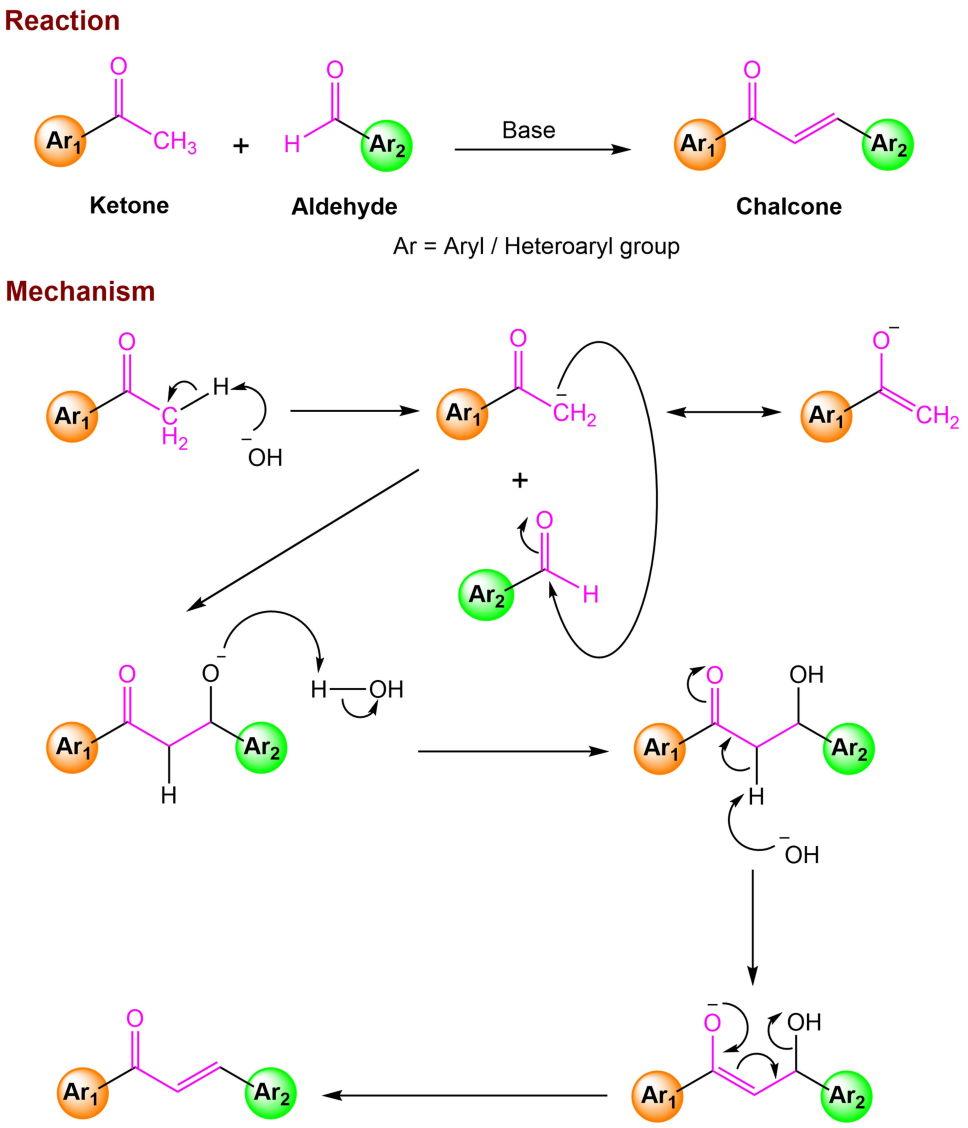

Figure 5 General reaction and mechanism of chalcone synthesis by base-catalyzed Claisen-Schmidt condensation.

involve multiple reactions to obtain the final pyrazoline derivative. For example, hydrazine or 4-hydrazinylbenzenesulfonamide (3) can be prepared from sulfanilamide (1) through a diazotization reaction with sodium nitrite ($NaNO_2$) in hydrochloric acid (HCl) to form a diazonium salt intermediate (2), followed by reduction using stannous chloride ($SnCl_2$) in hydrochloric acid (HCl), as depicted in Figure 7.[15,116,117]

Pyrazoline benzenesulfonamide derivatives can be synthesized via a one-pot, one-step reaction using a base catalyst, as depicted in Figure 8. The synthesis involves a direct reaction between aromatic ketones (1), aromatic aldehydes (2), and 4-hydrazinylbenzenesulfonamide (3) in the presence of sodium hydroxide (NaOH) as a base catalyst in absolute ethanol. The reaction is carried out in a sealed-vessel reactor (Monowave 50) equipped with a stir bar and pressure tube at 80°C for 2 hours, yielding 3,5-diphenylpyrazoline benzenesulfonamide derivatives (4), with yields ranging from 25% to 87%.[118] Another study reported that pyrazoline benzenesulfonamide derivatives can also be synthesized under catalyst-free conditions using microwave irradiation. In this case, the pyrazoline compounds were obtained through a two-step reaction, as depicted in Figure 9. In the first step, chalcones were prepared via the Claisen–Schmidt condensation reaction using a base catalyst in ethanol, or through an aldol condensation reaction catalyzed by thionyl chloride ($SOCl_2$) in absolute ethanol, involving the appropriate acetophenone (1) and appropriate benzaldehyde (2) at

https://doi.org/10.2147/DDDT.S562109

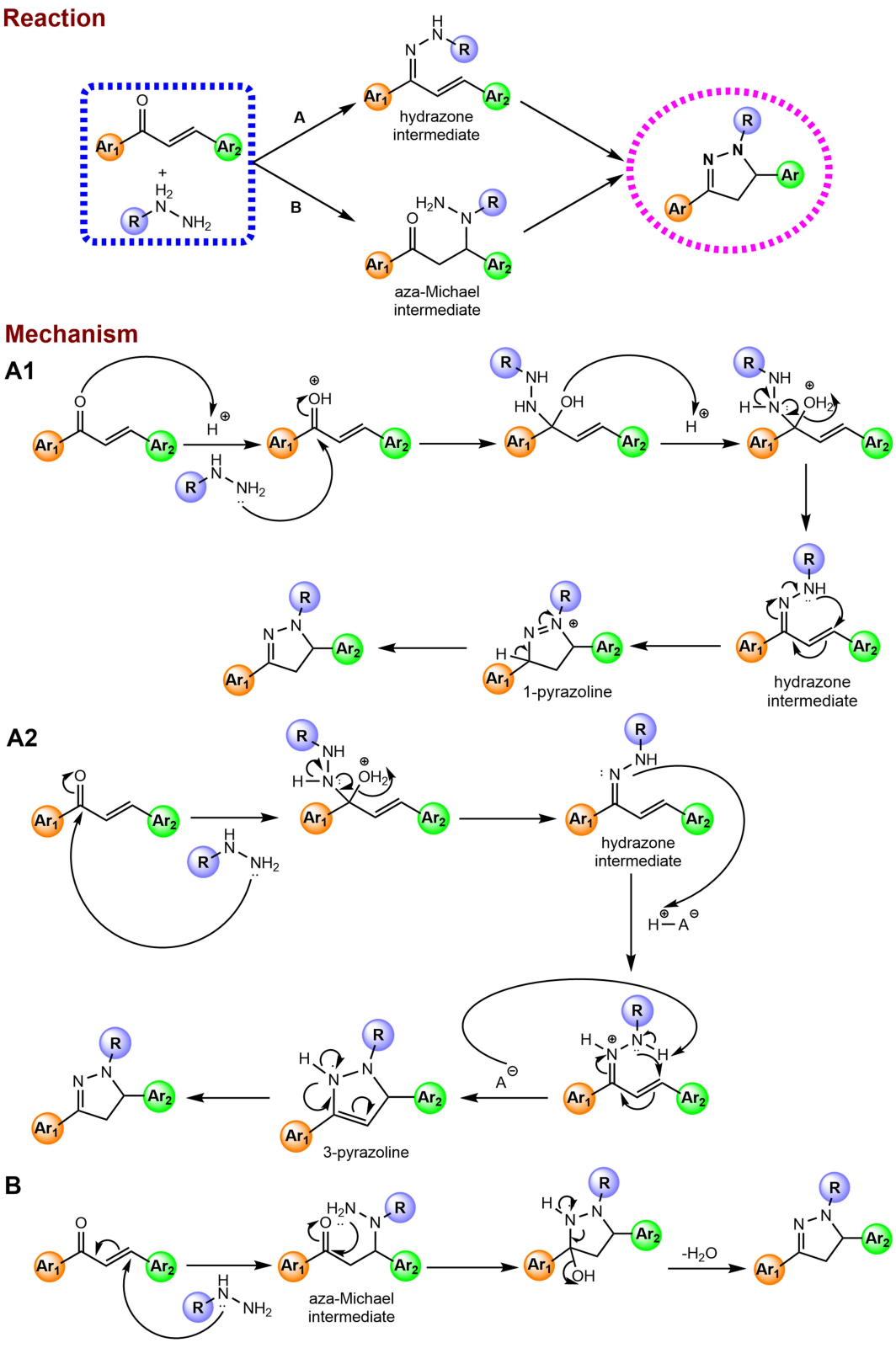

Figure 6 Reaction scheme and mechanistic pathways for the synthesis of 2-pyrazoline derivatives from chalcone and hydrazine. Top: Reaction overview showing the condensation of a chalcone and hydrazine to yield either a hydrazone or aza-Michael intermediate, leading to 2-pyrazoline. Bottom: Mechanism reaction pathways for 2-pyrazoline, (**A1**) the chalcone and hydrazine condense to form a hydrazone intermediate, which subsequently undergoes nucleophilic cyclization and proton transfers to yield 2-pyrazoline via intramolecular attack at the enone carbon, (**A2**) starting with the same hydrazone intermediate, ring closure occurs through a different cyclization route, with nucleophilic attack at the β-carbon, leading to the formation of 2-pyrazoline, (**B**) hydrazine directly adds to the α,β-unsaturated carbonyl of the chalcone via an aza-Michael reaction, forming an intermediate that cyclizes and then eliminates water to provide the 2-pyrazoline product.

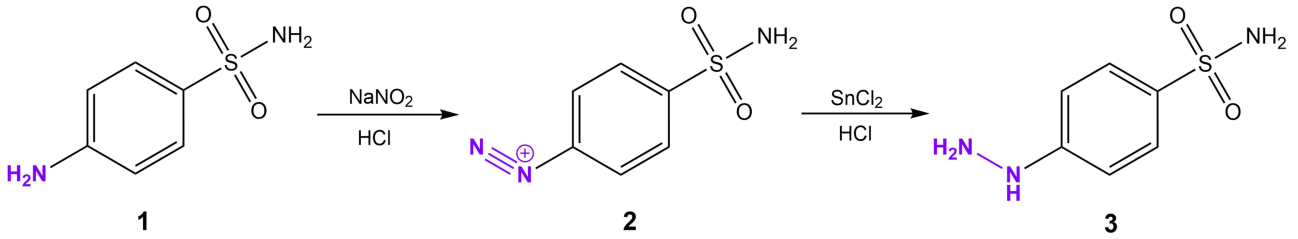

Figure 7 Synthesis of 4-hydrazinylbenzenesulfonamide. Sulfanilamide (1) was converted through a diazotization reaction to form a diazonium salt intermediate (2), followed by reduction to yield 4-hydrazinylbenzenesulfonamide (3).

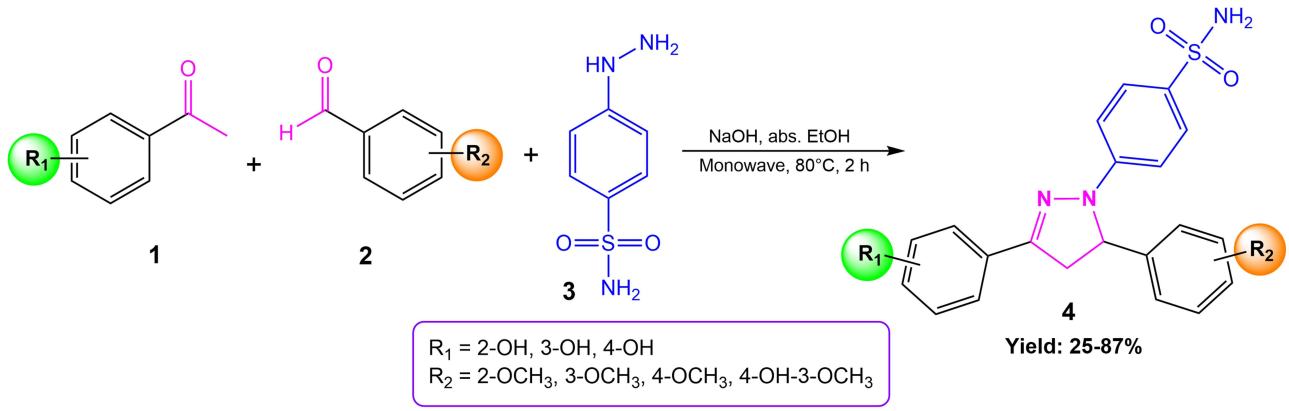

Figure 8 One-pot synthesis of 3,5-diphenyl pyrazoline benzenesulfonamide derivatives. Aromatic ketones (1), aromatic aldehydes (2), and 4-hydrazinylbenzenesulfonamide (3) were reacted under a sealed-vessel reactor (Monowave 50) to yield 3,5-diphenylpyrazoline benzenesulfonamide derivatives (4).

room temperature. In the second step, the suitable chalcone derivatives (3) were reacted with 4-hydrazinylbenzenesulfonamide hydrochloride (4) in methanol or ethanol under microwave irradiation for 7 to 60 minutes, affording pyrazoline benzenesulfonamide derivatives bearing substituted-diphenyl (5), substituted-phenyl and styryl (6), and thiophene and substituted-phenyl (7), with yields ranging from 4 to 98%.[119–121]

Pyrazoline benzenesulfonamide derivatives have also been synthesized under acidic conditions using ultrasound irradiation, through a stepwise process, as depicted in Figure 10. Initially, 2,4-dimethoxybenzaldehyde (1) reacts with methylmagnesium iodide (CH_3-MgI) to produce 1-(2,4-dimethoxyphenyl)ethanol (2). This intermediate is then oxidized in the presence of magnesium oxide (MgO) under reflux for 2 hours at 80°C, affording 2,4-dimethoxyacetophenone (3). Subsequent Claisen–Schmidt condensation of 2,4-dimethoxyacetophenone (3) with a substituted aromatic aldehyde (4) in ethanol at room temperature afforded chalcone derivatives (5). In parallel, 4-hydrazinylbenzenesulfonamide hydrochloride (6) is obtained from sulfanilamide via a diazotization-reduction sequence. In the final stage, the chalcones (5) are cyclized with 4-hydrazinylbenzenesulfonamide hydrochloride (6) using acetic acid as a catalyst under ultrasound irradiation at 65°C for 50–90 minutes in open vessels, affording pyrazoline benzenesulfonamide derivatives bearing 2,4-dimethoxyphenyl and thiophene (7), 2,4-dimethoxyphenyl and furan (8), and 2,4-dimethoxyphenyl and substituted-phenyl (9), with yields ranging from 72% to 85%.[116] This ultrasound-assisted method provides an efficient and environmentally benign pathway for generating structurally diverse pyrazoline benzenesulfonamide analogues.

A widely used conventional method for synthesizing pyrazoline benzenesulfonamide involves a two-step reaction. The first step involves a Claisen–Schmidt condensation reaction between an appropriate aromatic aldehyde and an aromatic ketone in the presence of a base or acid catalyst, yielding α,β-unsaturated carbonyl compounds known as chalcones. In the second step, the chalcone is then reacted with 4-hydrazinylbenzenesulfonamide hydrochloride in an acidic or basic medium, or simply in alcoholic solvents such as ethanol or methanol. The reaction mixture is typically heated under reflux for several hours or longer, depending on the substrate, to promote intramolecular cyclization and form the pyrazoline ring. After completion, the reaction mixture is cooled, and the crude product is isolated by filtration

https://doi.org/10.2147/DDDT.S562109

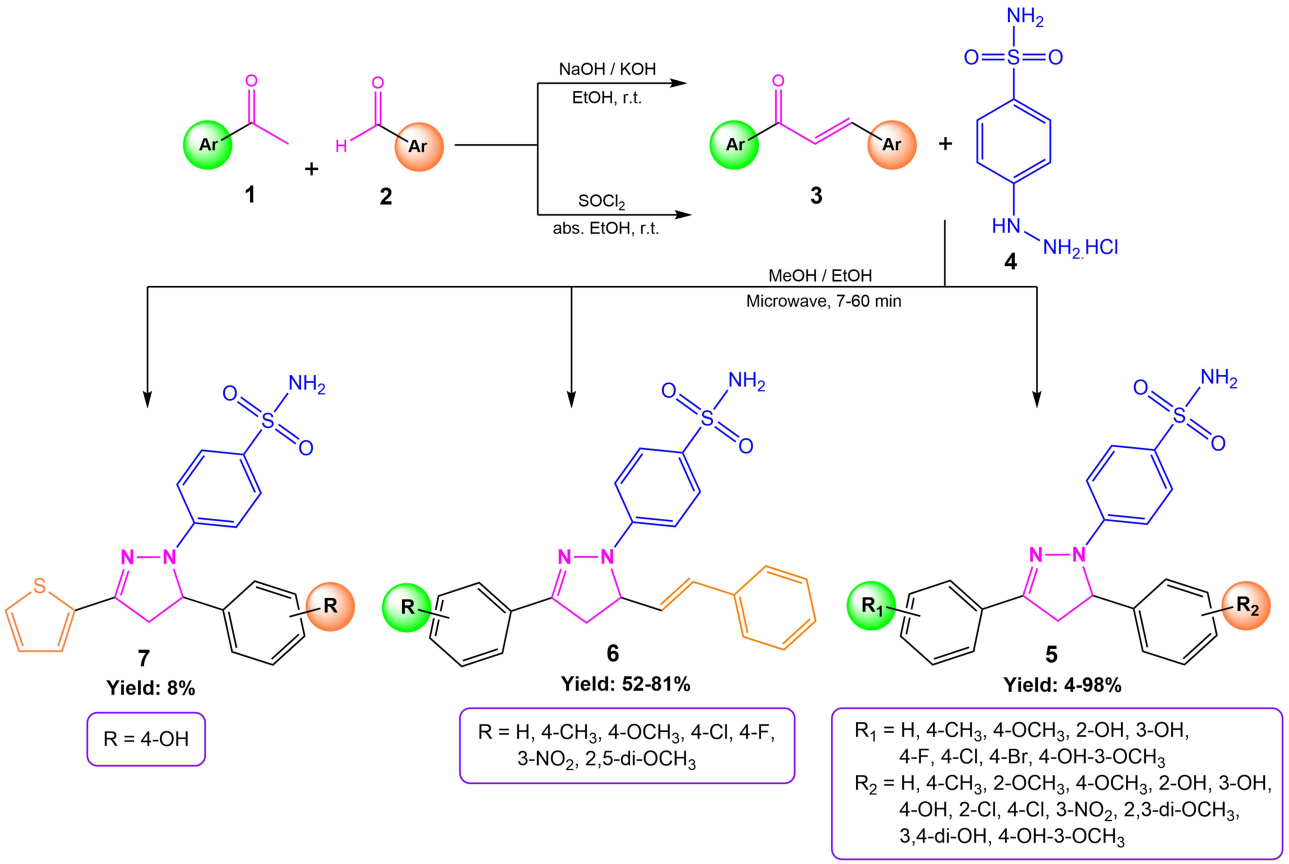

Figure 9 Microwave-assisted synthesis of various pyrazoline benzenesulfonamide derivatives. Appropriate acetophenone (1) condensed with appropriate benzaldehyde (2) to prepare chalcone derivatives (3), then reacted with 4-hydrazinylbenzenesulfonamide hydrochloride (4) under microwave irradiation to afford pyrazoline benzenesulfonamide derivatives bearing substituted-diphenyl (5), substituted-phenyl and styryl (6), and thiophene and substituted-phenyl (7).

and purified by recrystallization. This conventional synthetic approach is widely employed owing to its straightforward procedure and adaptability, allowing for diverse substitution patterns at the 3- and 5-positions of the pyrazoline core. This method facilitates the incorporation of a broad array of aromatic and heteroaromatic groups, including 1,5,6,7-tetrahydro-4*H*-indol-4-one,[122] naphthalene,[123] thiazole,[124] pyridine,[125,126] benzo[*d*][1,3]dioxole,[127,128] 2*H*-chromen-2-one,[129] pyrazole,[130,131] as well as phenoxybenzene and (benzyloxy)benzene.[132] In addition, substituents such as furan, thiophene, styrene, anthracene, and diphenyl[133–140] have also been introduced through this strategy. As illustrated in Figure 11, this versatile protocol provides access to structurally diverse pyrazoline benzenesulfonamide derivatives (1–18) with variable yields, highlighting its utility in generating novel analogues with potential pharmacological relevance.

The synthesis of pyrazoline benzenesulfonamide derivatives incorporating a ferrocene organometallic moiety is accomplished via a stepwise protocol, as depicted in Figure 12. Initially, a Claisen-Schmidt condensation is employed, wherein acetylferrocene (1) reacts with various substituted benzaldehydes (2) in the presence of potassium hydroxide (KOH) in ethanol at room temperature, affording the corresponding ferrocenyl chalcone intermediates (3). In the subsequent step, these intermediates undergo cyclization with 4-hydrazynylbenzenesulfonamide hydrochloride (4) in an ethanol–acetic acid mixture (1:2) at 100°C for 21–22 hours, yielding pyrazoline benzenesulfonamide derivatives bearing ferrocene and aryl groups (5) in moderate to good yields ranging from 49% to 74%.[141]

Pyrazoline benzenesulfonamide derivatives bearing benzodioxole and benzodioxane moieties can be efficiently synthesized through a sequential three-step process, as depicted in Figure 13. As reported by Yan et al,[142] the first step involves alkylation of protocatechuic aldehyde (1) with dibromomethane (2a) or 1,2-dibromoethane (2b) using anhydrous potassium carbonate (K_2CO_3) in dimethylformamide (DMF) at 70°C to afford benzo oxygen heterocyclic intermediates (3). The resulting intermediates undergo a Claisen–Schmidt condensation with various substituted

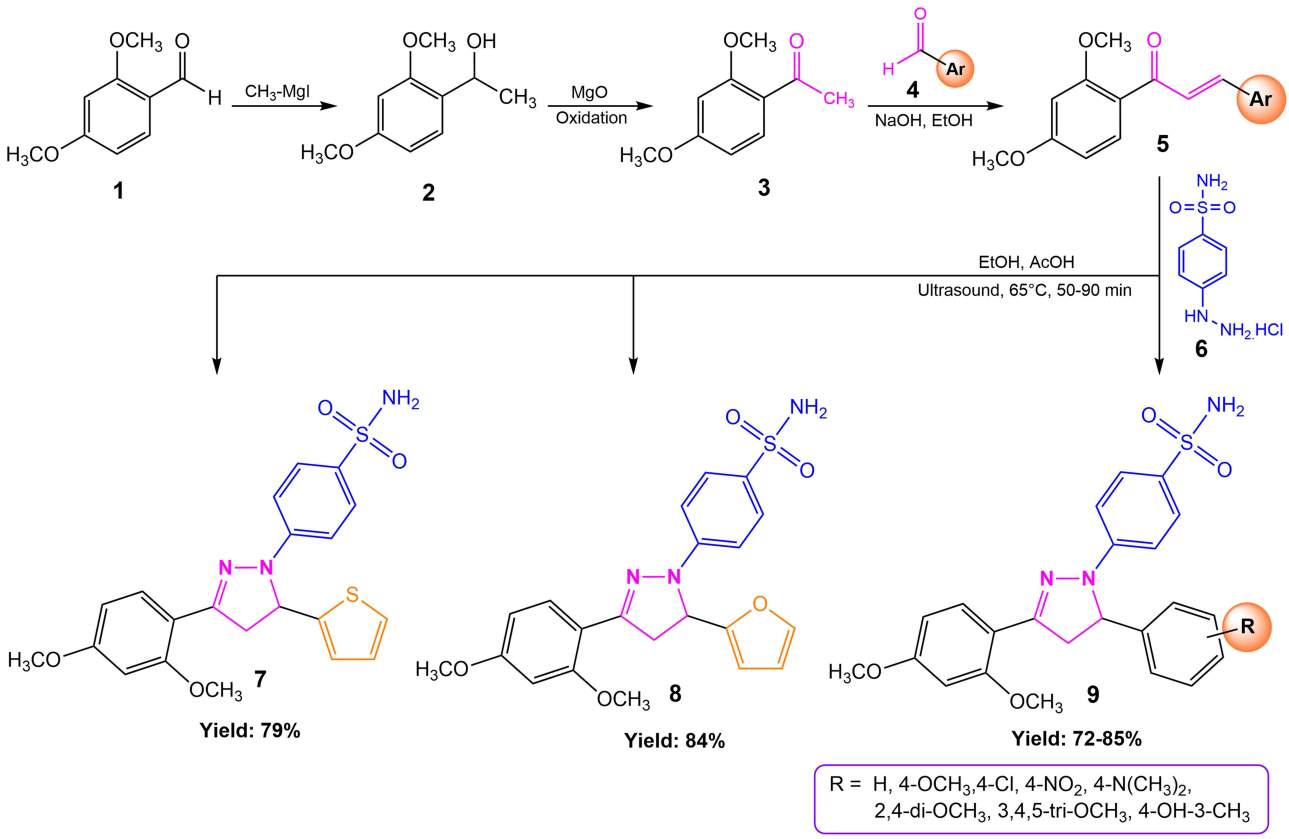

Figure 10 Ultrasound-assisted synthesis of pyrazoline benzenesulfonamide derivatives. 2,4-dimethoxybenzaldehyde (1) was converted to 1-(2,4-dimethoxyphenyl)ethanol (2), then oxidized to yield 2,4-dimethoxyacetophenone (3), then condensed with substituted aromatic aldehyde (4) to afford chalcone derivatives (5), which then reacted with 4-hydrazinylbenzenesulfonamide hydrochloride (6) under ultrasound irradiation to produce pyrazoline benzenesulfonamide derivatives bearing 2,4-dimethoxyphenyl and thiophene (7), 2,4-dimethoxyphenyl and furan (8), and 2,4-dimethoxyphenyl and substituted-phenyl (9).

acetophenones (4) in ethanol, catalyzed by potassium hydroxide (KOH), yielding the corresponding chalcone derivatives (5). In the final step, a cyclization reaction was performed on the resulting chalcone with 4-hydrazinylbenzenesulfonamide hydrochloride (6) in ethanol, using glacial acetic acid as a catalyst, under reflux overnight. This process affords pyrazoline benzenesulfonamide derivatives bearing benzodioxole (7) and benzodioxane (8) moieties, with yields of 59–78% and 60–76%, respectively.

The synthesis of tetrazole-bearing pyrazoline benzenesulfonamide derivatives was conducted using a systematic three-step process, as depicted in Figure 14. In the first step, 4-aminoacetophenone (1) was converted into a tetrazole-substituted acetophenone (2) through a cyclization reaction with sodium azide (NaN_3) and triethyl orthoformate (TEOF) in glacial acetic acid under reflux conditions for 12 hours. In the second step, acetophenone was condensed with substituted benzaldehydes (3), specifically 3,4-dimethoxybenzaldehyde and 3,4,5-trimethoxybenzaldehyde in the presence of potassium hydroxide (KOH) in absolute ethanol at room temperature for 10–12 hours. This reaction proceeds via an aldol condensation mechanism, yielding tetrazole-substituted chalcones (4). In the final step, cyclization was achieved by reacting the chalcone with 4-hydrazinylbenzenesulfonamide hydrochloride (5) in absolute ethanol under reflux conditions for 18 hours. This reaction affords pyrazoline benzenesulfonamide derivatives bearing a tetrazole moiety (6), with yields of 51% and 46%.[143]

The synthesis of morpholine-bearing pyrazoline benzenesulfonamide derivatives is accomplished through a sequential three-step process, as depicted in Figure 15. In the first step, morpholine (1) was reacted with 4-fluorobenzaldehyde (2) in dimethyl sulfoxide (DMSO) at 120°C for 4 hours to afford 4-morpholinobenzaldehyde (3). In the second step, the resulting aldehyde undergoes Claisen–Schmidt condensation with substituted acetophenone (4) in ethanol at 0°C, affording morpholine- substituted chalcone intermediates (5). In the final step, cyclization reaction of the resulting chalcone with

https://doi.org/10.2147/DDDT.S562109

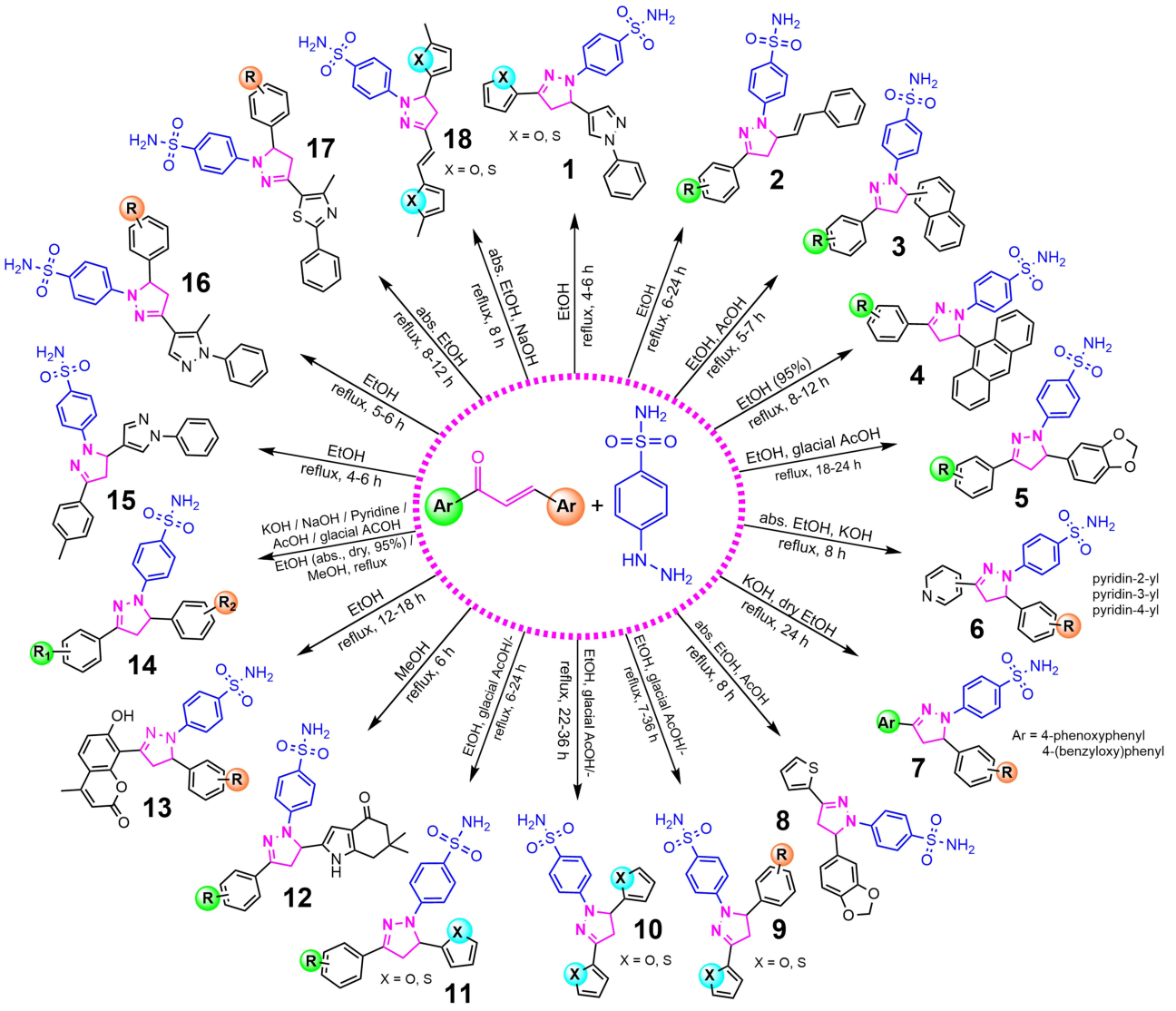

Figure 11 Synthesis of substituted pyrazoline benzenesulfonamide derivatives containing various heterocyclic and aromatic substituents using the conventional method. Appropriate acetophenone and appropriate benzaldehyde were condensed to prepare chalcone derivatives, which then reacted with 4-hydrazinylbenzenesulfonamide hydrochloride under reflux conditions to yield structurally diverse pyrazoline benzenesulfonamide derivatives. Structures 1–18 represent products bearing: furan/thiophene and pyrazole (1), substituted-phenyl and styryl (2), substituted-phenyl and naphthalene (3), substituted-phenyl and anthracene (4), substituted-phenyl and benzo[d]dioxole (5), pyridine and substituted-phenyl (6), phenoxybenzene or (benzyloxy)benzene and substituted-phenyl (7), thiophene and benzo[*d*]dioxole (8), furan/thiophene and substituted-phenyl (9), furan and/or thiophene (10), substituted-phenyl and furan/thiophene (11), substituted-phenyl and 1,5,6,7-tetrahydro-4H-indol-4-one (12), 2H-chromen-2-one and substituted-phenyl (13), substituted diphenyl (14), p-tolyl and pyrazole (15), pyrazole and substituted-phenyl (16), thiazole and substituted-phenyl (17), and 2-vinylfuran or 2-vinylthiophene and furan/thiophene (18).

4-hydrazinylbenzenesulfonamide (6) in ethanol, using glacial acetic acid as a catalyst, under reflux conditions at 80°C for 8 hours. This reaction affords pyrazoline benzenesulfonamide derivatives bearing a morpholine moiety (7).[144]

The synthesis of pyrazoline benzenesulfonamide derivatives featuring a methanesulfonamide moiety involves a concise three-step process, as depicted in Figure 16. In the first step, N-(4-acetylphenyl)-N-(methylsulfonyl)methanesulfonamide (3) was synthesized by reacting 4-aminoacetophenone (1) with methanesulfonyl chloride (2) in dichloromethane (CH_2Cl_2) using triethylamine (TEA) as a base. This intermediate is subsequently subjected to Claisen–Schmidt condensation with various substituted benzaldehydes (4) in absolute ethanol, catalyzed by sodium ethoxide at room temperature, yielding methanesulfonamide-bearing chalcone derivatives (5) in good yields. The final step, the cyclization of these chalcones with 4-hydrazinylbenzenesulfonamide hydrochloride (6) in absolute ethanol under reflux conditions for 6–24 hours, affords pyrazoline benzenesulfonamide derivatives featuring a methanesulfonamide moiety (7), with yields ranging from 41% to 42%.[145]

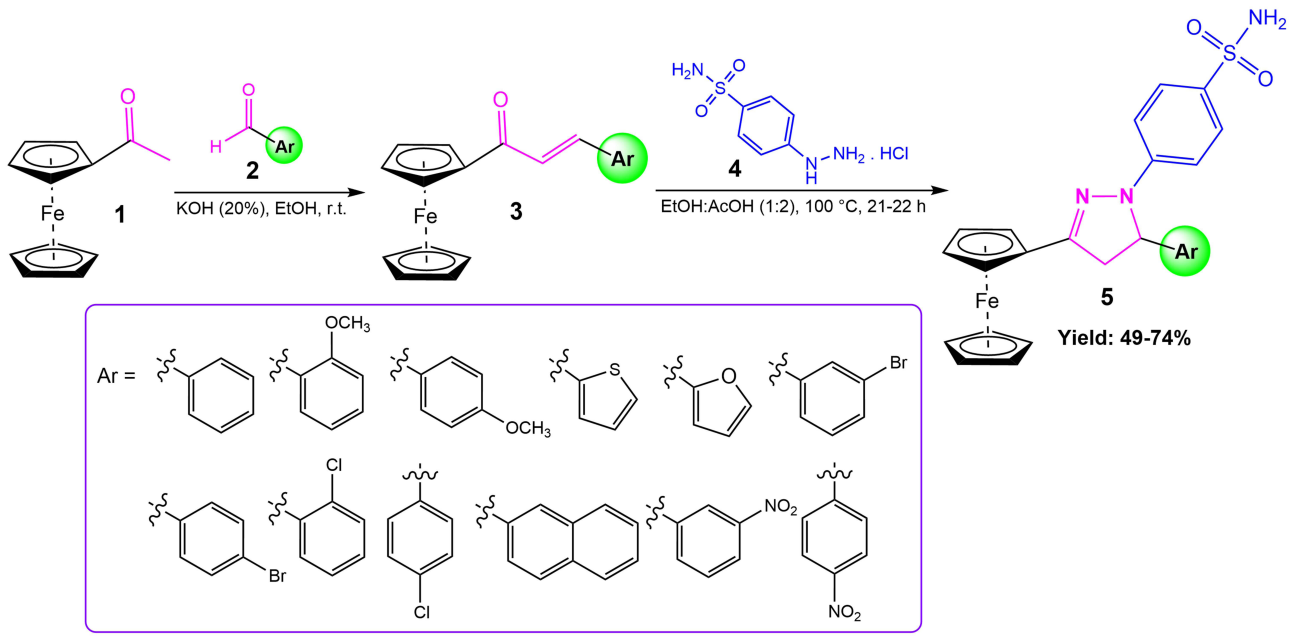

Figure 12 Synthesis of ferrocene-substituted pyrazoline benzenesulfonamide derivatives. Acetylferrocene (1) condensed with substituted benzaldehydes (2) to prepare ferrocenyl chalcones (3), which then reacted with 4-hydrazinylbenzenesulfonamide hydrochloride (4) to produce pyrazoline benzenesulfonamide derivatives bearing ferrocene and aryl moieties (5).

The synthesis of pyrazole-linked pyrazoline benzenesulfonamide derivatives proceeds through a multi-step sequence, as depicted in Figure 17. In the first step, substituted acetophenones (1) undergo condensation with phenylhydrazine (2) in ethanol using acetic acid as a catalyst at room temperature, forming hydrazone intermediates (3).[146] These intermediates are then subjected to the Vilsmeier–Haack reaction with phosphoryl chloride ($POCl_3$) and dimethylformamide (DMF) under reflux conditions in the presence of sodium bicarbonate ($NaHCO_3$), affording pyrazole carbaldehydes (4). Subsequent Claisen–Schmidt condensation of the pyrazole carbaldehydes with various substituted acetophenones (5) in methanol and sodium hydroxide (NaOH) yields chalcone intermediates (6) in good yields (56–79%). The final step involves the cyclization reaction of the resulting chalcone intermediates with 4-hydrazinylbenzenesulfonamide (7) in methanol, catalyzed by hydrochloric acid (HCl) under reflux conditions. This reaction affords pyrazole-linked pyrazoline benzenesulfonamide derivatives (8), with yields ranging from 54% to 76%.[145]

The synthesis of coumarin-linked pyrazoline benzenesulfonamide derivatives proceeds through a well-defined a multi-step process, as depicted in Figure 18. Initially, 7-hydroxycoumarin (1) was acetylated with acetic anhydride (2) under reflux for 5 hours, producing 7-acetoxycoumarin (3). Subsequent Friedel–Crafts acylation with aluminium chloride ($AlCl_3$) at 145°C for 1 hour affords 8-acetyl-7-hydroxycoumarin (4). This intermediate then undergoes methylation using methyl iodide (CH_3I) in dry acetone under reflux for 24 hours, yielding 8-acetyl-7-methoxycoumarin (5). In the next stage, the Claisen–Schmidt condensation of 8-acetyl-7-methoxycoumarin (5) with various aromatic aldehydes (6) in 10% sodium hydroxide (NaOH) solution in ethanol at room temperature for 24 hours generates coumarin–chalcone derivatives (7). Finally, the cyclization of these chalcones with 4-hydrazinylbenzenesulfonamide (8) in absolute ethanol under reflux for 16 hours afforded coumarin–pyrazoline benzenesulfonamide hybrids (9), which were obtained in yields ranging from 65% to 70%.[147]

The synthesis of oxazoline-based pyrazoline benzenesulfonamide derivatives was achieved through a structured multi-step synthetic strategy, as depicted in Figure 19. The synthesis begins with the O-alkylation of *p*-hydroxyacetophenone (1) using ethyl bromoacetate (2) as the alkylating agent in dry acetone, with potassium carbonate as base, under reflux conditions to afford ethyl 2-(4-acetylphenoxy)acetate (3). Subsequent hydrolysis of the ester group yields 2-(4-acetylphenoxy)acetic acid (4), followed by cyclization with ethanolamine in methanol under reflux conditions to afford the oxazoline intermediate (5). This intermediate is subjected to a Claisen–Schmidt condensation with various

https://doi.org/10.2147/DDDT.S562109

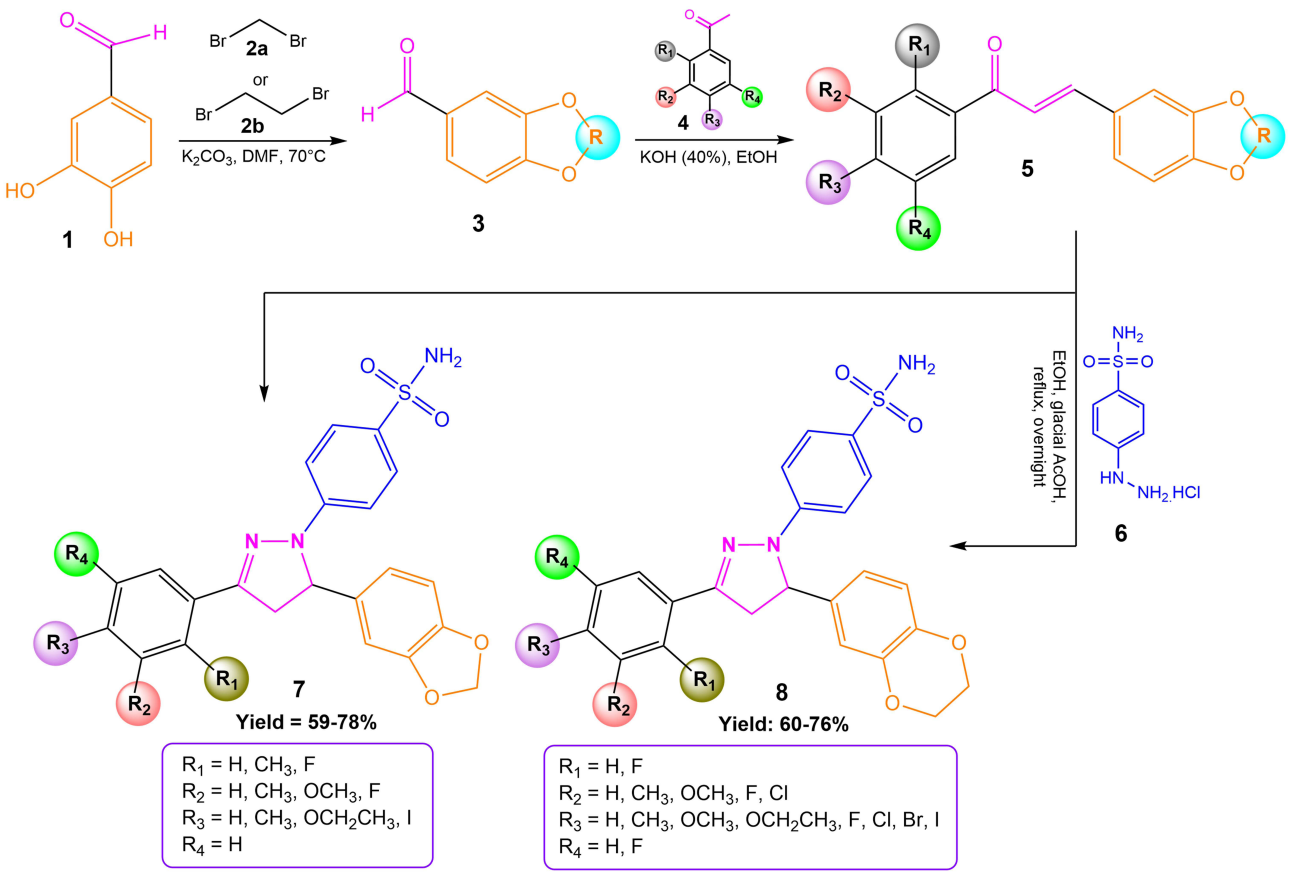

Figure 13 Synthesis of pyrazoline benzenesulfonamide derivatives bearing benzodioxole and benzodioxane moieties. Protocatechuic aldehyde (1) was alkylated with dibromomethane (2a) or 1,2-dibromoethane (2b) to yield benzo oxygen heterocyclic (3), then condensed with substituted acetophenones (4) to afford chalcone derivatives (5), which then reacted with 4-hydrazinylbenzenesulfonamide hydrochloride (6) to produce pyrazoline benzenesulfonamide derivatives bearing benzodioxole (7) and benzodioxane (8) moieties.

aromatic aldehydes (6) in methanol in the presence of sodium hydroxide (NaOH) to afford a series of oxazoline–based chalcone derivatives (7). The resulting chalcones undergo cyclization with 4-hydrazinylbenzenesulfonamide (8) in methanol under reflux, followed by the addition of hydrochloric acid (HCl), yielding oxazoline–based pyrazoline benzenesulfonamide derivatives bearing a phenyl group (9) and benzodioxane (10), with yields of 62–72% and 62%, respectively.[148]

The synthesis of chloropyrazole benzenesulfonamide–linked pyrazoline benzenesulfonamide derivatives, as reported by Gul et al[149] and Khloya et al,[150] was accomplished through a well-defined multi-step process, as depicted in Figure 20. The synthesis commences with the condensation of ethyl acetoacetate (2) with 4-hydrazinylbenzenesulfonamide hydrochloride (1) in ethanol under reflux, resulting in the formation of the pyrazolone intermediate (3). This intermediate then undergoes a Vilsmeier–Haack reaction using dimethylformamide (DMF) and phosphoryl chloride ($POCl_3$), which introduces a formyl substituent at the 4-position and a chloro substituent at the 5-position of the pyrazole ring, affording N-(5-chloro-4-formyl-3-methyl pyrazole)-4-phenylsulfonyl-N,N-dimethylformimidamide (4). During this process, the sulfonamide group is temporarily protected through conversion to an N-[(dimethylamino)methylidine] sulfonamide group. Subsequent acidic treatment removes the dimethylaminomethyl protecting group, regenerating the free sulfonamide moiety and yielding 5-chloro-3-methyl-4-formylpyrazole benzenesulfonamide (5). In the next step, this intermediate undergoes a Claisen–Schmidt condensation with substituted acetophenones (6) in ethanol, catalyzed by potassium hydroxide (KOH) to yield chalcone derivatives (7). In the final step, these chalcones undergo cyclization with 4-hydrazinylbenzenesulfonamide hydrochloride in ethanol, in the presence of glacial acetic acid under reflux conditions, yielding chloropyrazole benzenesulfonamide–linked pyrazoline benzenesulfonamide derivatives (8).

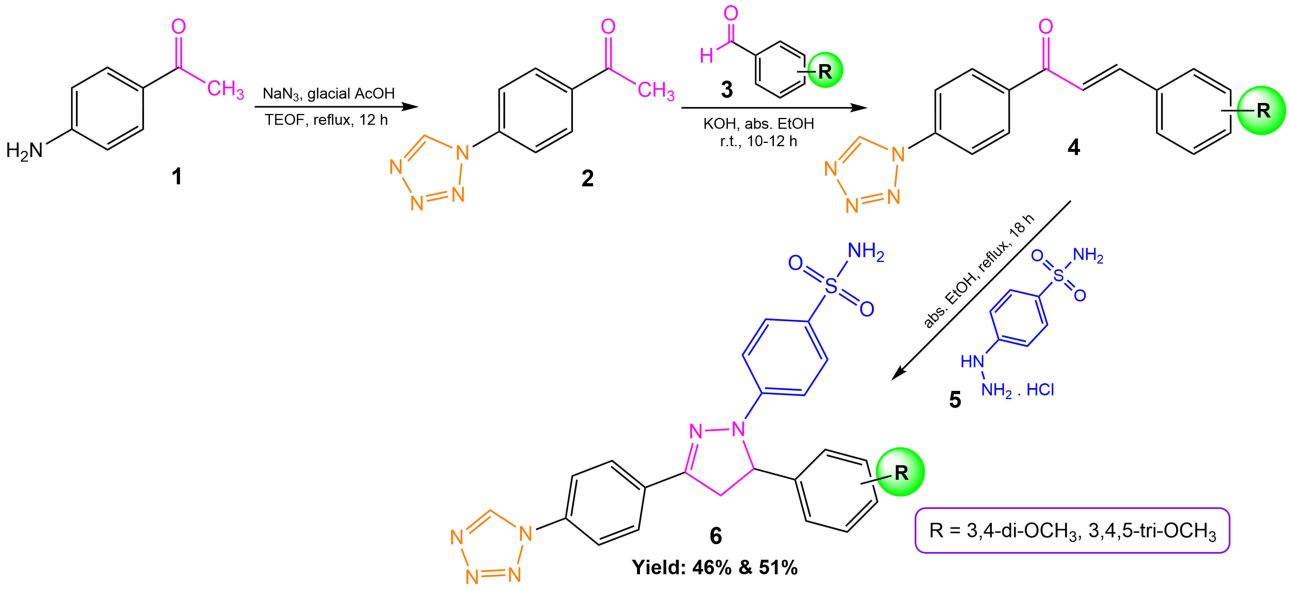

Figure 14 Synthesis of tetrazole–beraing pyrazoline benzenesulfonamide derivatives. 4-aminoacetophenone (1) was converted to a tetrazole–substituted acetophenone (2), then condensed with substituted benzaldehydes (3) to afford tetrazole–substituted chalcones (4), which then reacted with 4-hydrazinylbenzenesulfonamide hydrochloride (5) to produce pyrazoline benzenesulfonamide derivatives bearing a tetrazole moiety (6).

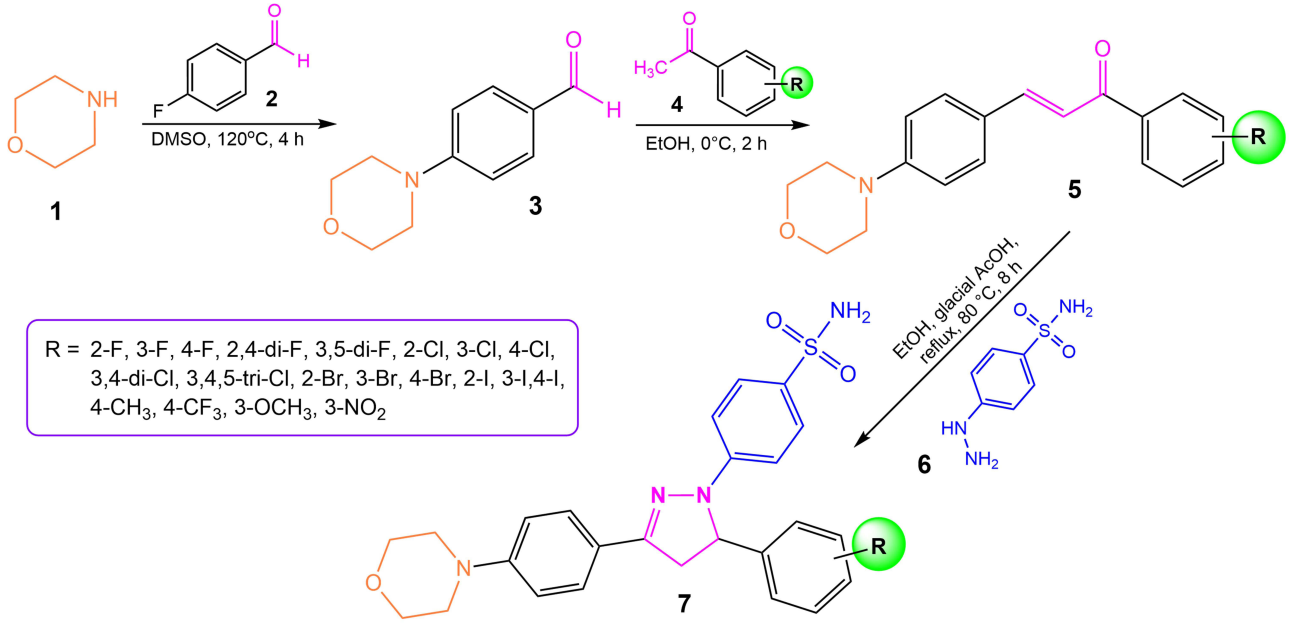

Figure 15 Synthesis of morpholine-bearing pyrazoline benzenesulfonamide derivatives. Morpholine (1) was reacted with 4-fluorobenzaldehyde (2) to yield 4-morpholino-benzaldehyde (3), then condensed with substituted acetophenone (4) to afford morpholine–substituted chalcone derivatives (5), which then reacted with 4-hydrazinylben-zenesulfonamide (6) to produce pyrazoline benzenesulfonamide derivatives bearing a morpholine moiety (7).

The synthesis of pyrazoline benzenesulfonamide derivatives containing pyrazole benzenesulfonamide, as reported by Kumar et al,[151] was achieved through a systematic multi-step process, as depicted in Figure 21. The first step involves the preparation of intermediate 4-formylpyrazole bearing a benzenesulfonamide substituent at the N-1 position (1), according to established procedures. This intermediates was then subjected to Claisen–Schmidt condensation with appropriate acetophenones (2) in a mixed solvent system of methanol and tetrahydrofuran (THF), with sodium hydroxide (NaOH) as base, yielding in the formation of chalcone derivatives (3) in moderate to good yields. Subsequently, cyclization of the

https://doi.org/10.2147/DDDT.S562109

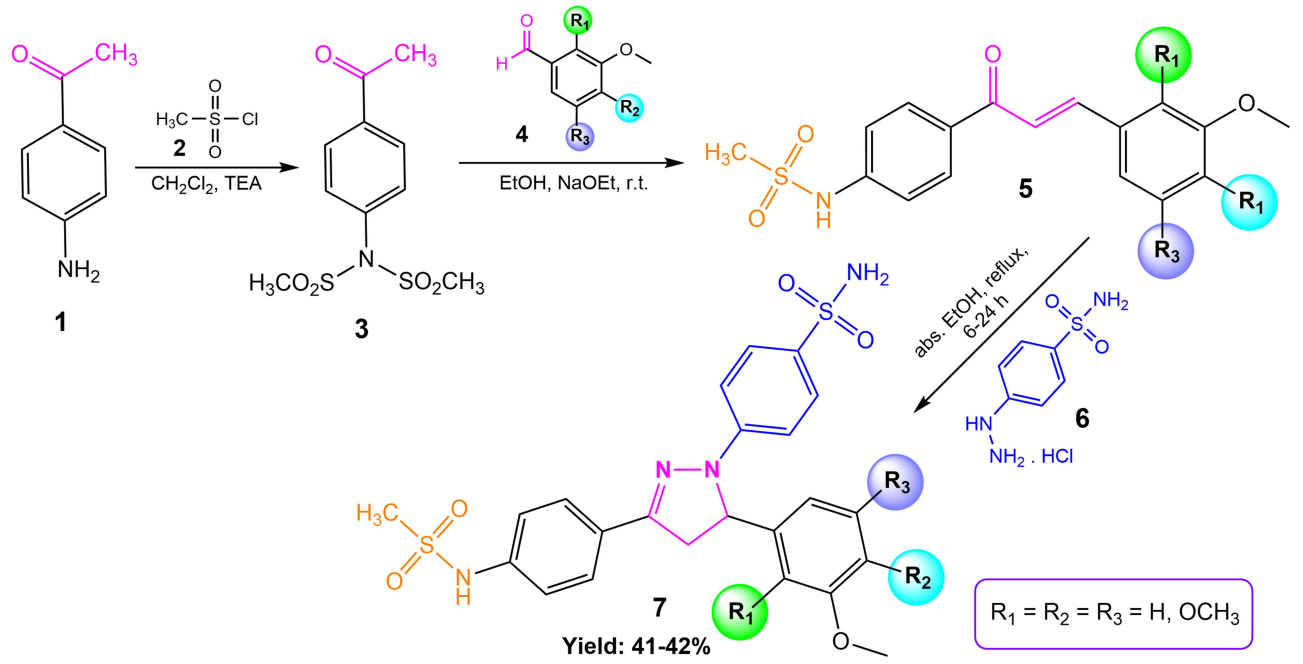

Figure 16 Synthesis of pyrazoline benzenesulfonamide derivatives featuring a methanesulfonamide moiety. 4-Aminoacetophenone (1) was reacted with methanesulfonyl chloride (2) to afford N-(4-acetylphenyl)-N-(methylsulfonyl)methanesulfonamide (3), then condensed with substituted benzaldehydes (4) to prepare methanesulfonamide–bearing chalcone derivatives (5), which then reacted with 4-hydrazinylbenzenesulfonamide hydrochloride (6) to produce pyrazoline benzenesulfonamide derivatives featuring a methanesulfonamide moiety (7).

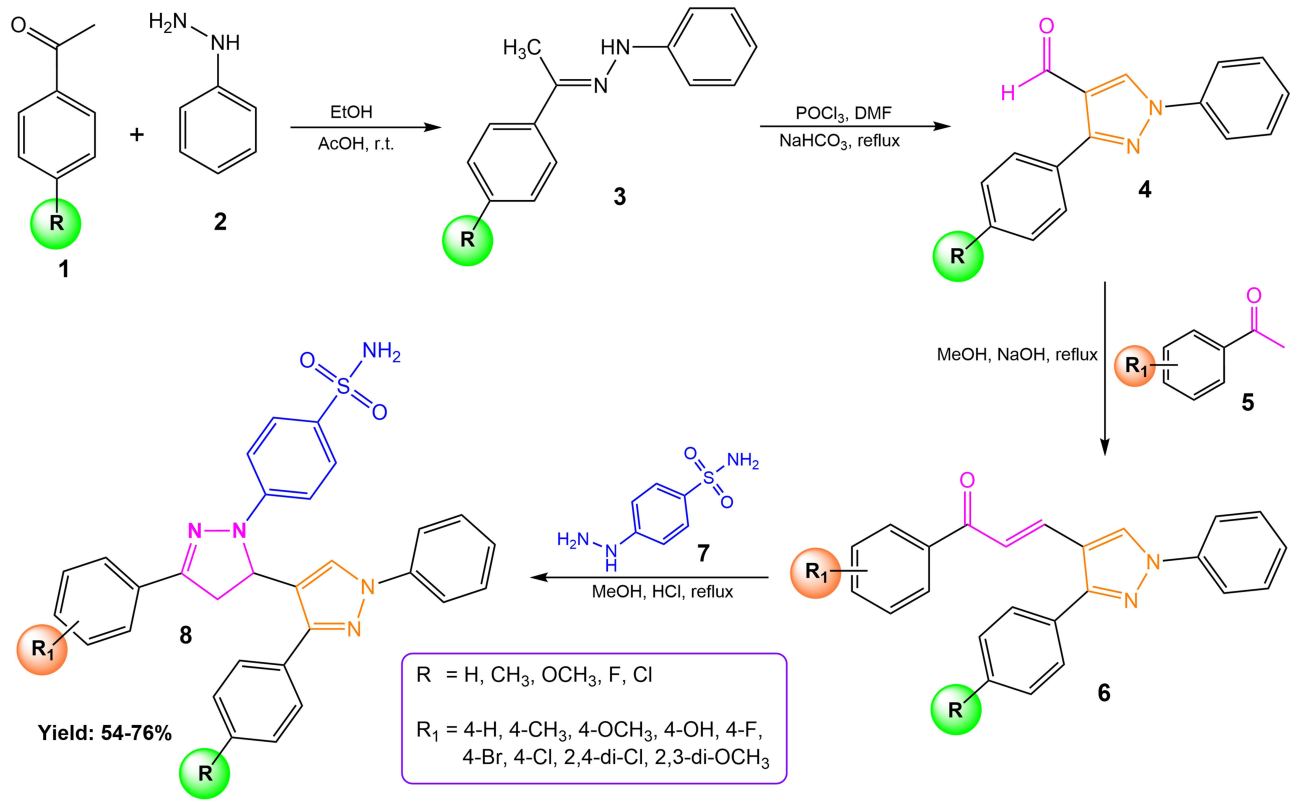

Figure 17 Synthesis of pyrazole-linked pyrazoline benzenesulfonamide derivatives. Substituted acetophenone (1) was condensed with phenylhydrazine (2) to form hydrazone intermediates (3), then subjected to the Vilsmeier–Haack reaction to afford pyrazole carbaldehydes (4), which then condensed with substituted acetophenones (5) to afford pyrazole–linked chalcone intermediates (6), which then reacted with 4-hydrazinylbenzenesulfonamide (7) to produce pyrazole–linked pyrazoline benzenesulfonamide derivatives (8).

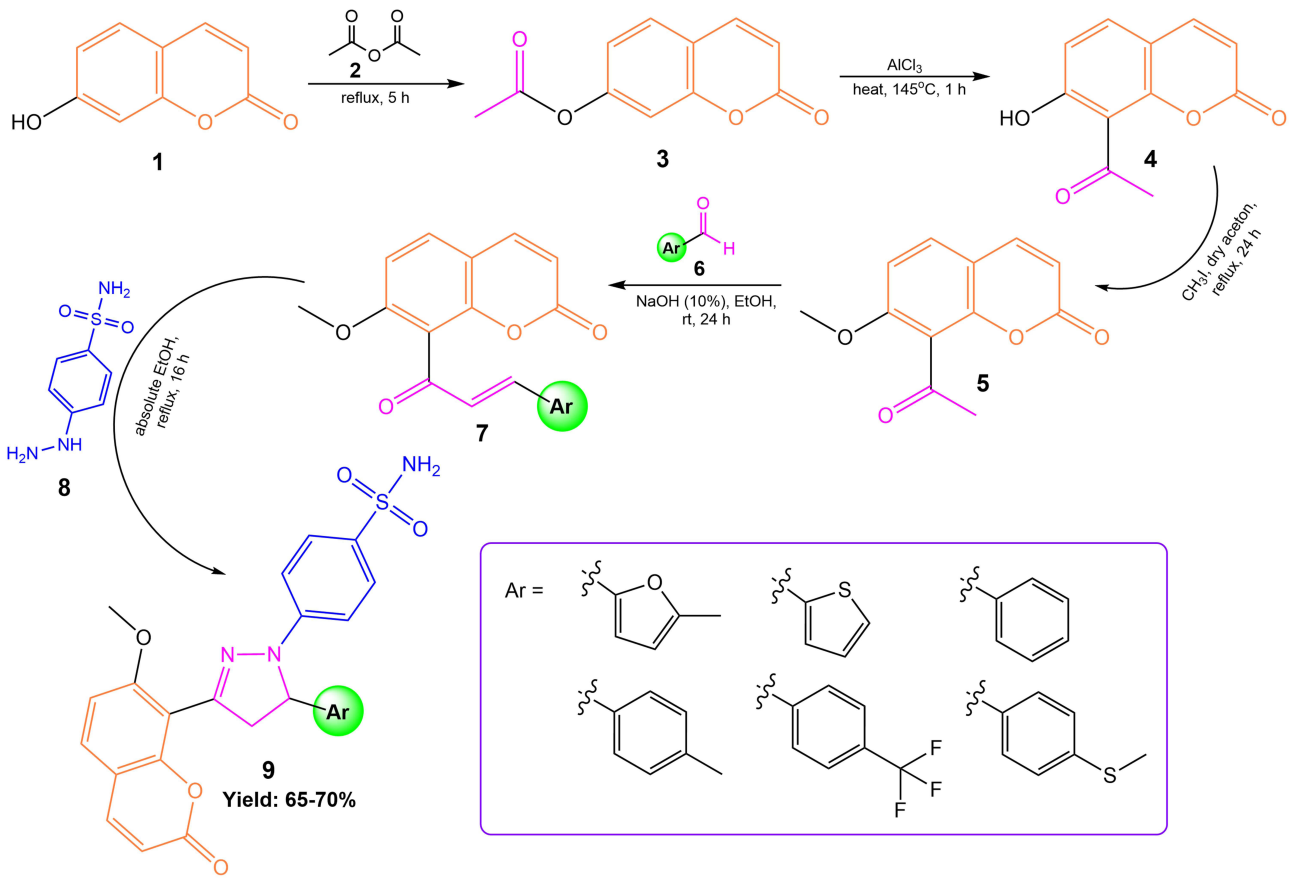

Figure 18 Synthesis of coumarin-linked pyrazoline benzenesulfonamide hybrids. 7-hydroxycoumarin (1) was acetylated with acetic anhydride (2) to yield 7-acetoxycoumarin (3), then acylated with aluminium chloride (AlCl3) to afford 8-acetyl-7-hydroxycoumarin (4), then methylated using methyl iodide (CH3I) to yield 8-acetyl-7-methoxycoumarin (5), then condensated with various aromatic aldehydes (6) generates coumarin–linked chalcone derivatives (7), which then reacted with 4-hydrazinylbenzenesulfonamide (8) to produce coumarin–linked pyrazoline benzenesulfonamide derivatives (9).

chalcone intermediates is carried out using 4-hydrazinylbenzenesulfonamide hydrochloride (4) under reflux in an ethanol/THF mixture, using a catalytic amount of acetic acid. This step affords pyrazoline benzenesulfonamide containing pyrazole benzenesulfonamide derivatives (5), with yields ranging from 65% to 84%.

The synthesis of pyrazoline benzenesulfonamide derivatives bearing benzofuran and pyrazole moieties, as reported by Ragab et al,[152] was achieved through a structured multi-step synthetic strategy, as depicted in Figure 22. For Scheme A, the synthesis commences with the alkaline hydrolysis of the natural furochromone precursor (1) in aqueous KOH (5%), affording 1-(6-hydroxy-4,7-dimethoxybenzofuran-5-yl)ethanone (2). This benzofuran–based ketone was then subjected to Claisen–Schmidt condensation with a pyrazole-4-carbaldehyde (3) in a sodium hydroxide–ethanol system at room temperature, resulting hydroxybenzofuranyl–pyrazolyl chalcone intermediates (4). Subsequently, cyclization of these chalcone intermediates with 4-hydrazinylbenzenesulfonamide hydrochloride (5) in ethanol under reflux for 16–48 hours, yielding pyrazoline benzenesulfonamide derivatives bearing pyrazole and benzofuran moieties (6), with yields ranging from 40% to 60%. Scheme B details a parallel pathway beginning with the Claisen–Schmidt condensation between appropriately substituted acetophenone (1) and pyrazole-4-carbaldehyde derivatives (2) in ethanol with sodium hydroxide (NaOH), generating pyrazolyl chalcone intermediates (3). Cyclization of these chalcone intermediates with 4-hydrazinylbenzenesulfonamide hydrochloride (4) under reflux in ethanol for 16–48 h, yielding pyrazoline benzenesulfonamide derivatives bearing a pyrazole moiety (5), with yields ranging from 30% to 55%. This synthetic pathway thus provides efficient access to novel benzofuran–pyrazole–pyrazoline benzenesulfonamide derivatives, supporting the exploration of new molecular scaffolds in drug discovery.

https://doi.org/10.2147/DDDT.S562109

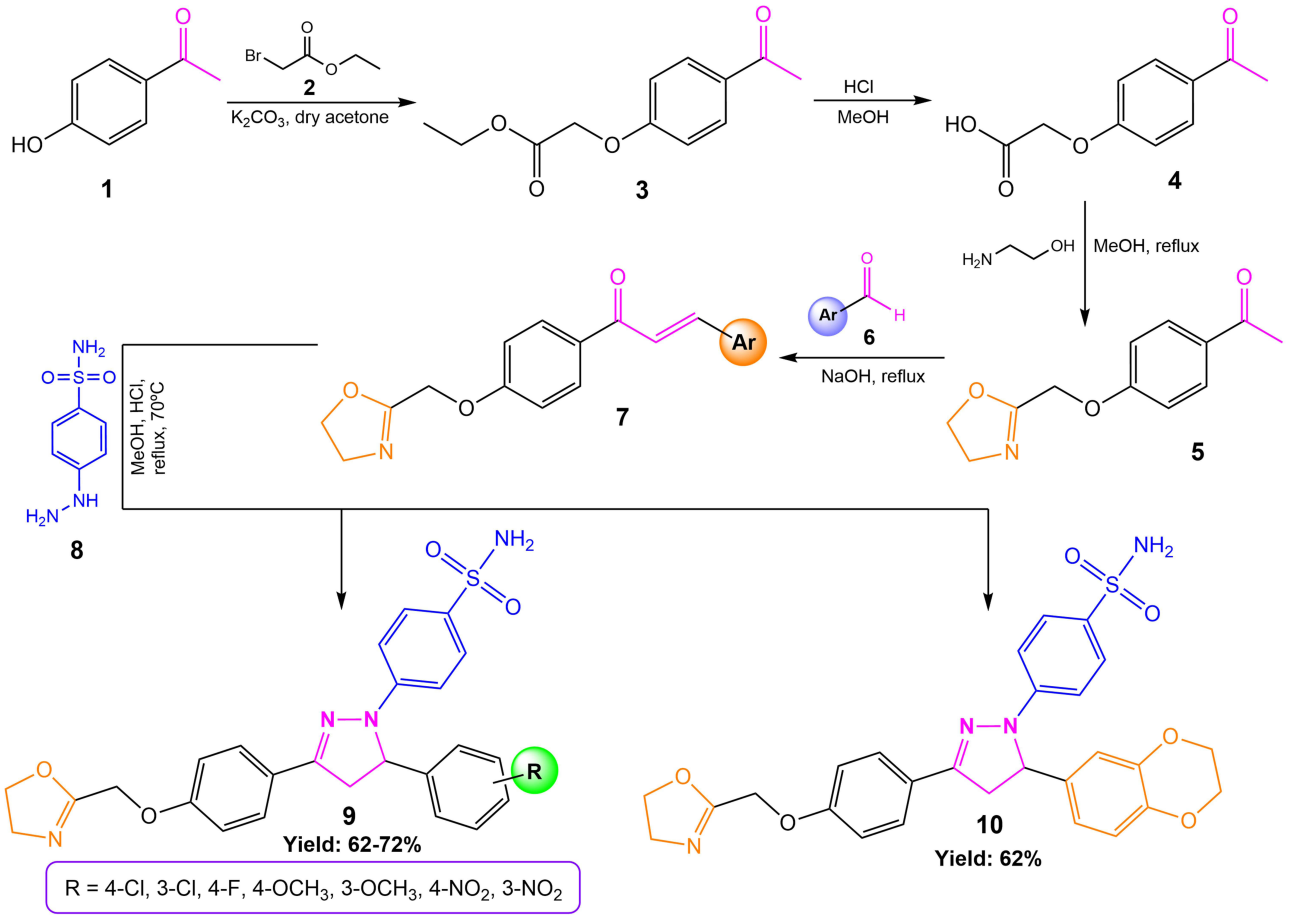

Figure 19 Synthesis of oxazoline-based pyrazoline benzenesulfonamide derivatives. p-Hydroxyacetophenone (1) was alkylated with ethyl bromoacetate (2) to afford ethyl 2-(4-acetylphenoxy)acetate (3), then hydrolysis of the ester group yields 2-(4-acetylphenoxy)acetic acid (4), followed by cyclization with ethanolamine to yield oxazoline–based acetophenone (5), then condensated with various aromatic aldehydes (6) to afford oxazoline–based chalcone derivatives (7), which then reacted 4-hydrazinylbenzenesulfonamide (8) to produce oxazoline–based pyrazoline benzenesulfonamide derivatives bearing a phenyl group (9) and benzodioxane (10).

The synthesis of pyrazoline benzenesulfonamide derivatives bearing pyrazole–quinoline scaffold substituted with either a furan or thiophene side chain, as reported by Zala et al,[15] proceeds via a convergent multi-step process, as depicted in Figure 23. The route initiates with the preparation of 7-chloro-4-hydrazinylquinoline (3), achieved by refluxing 4,7-dichloroquinoline (1) with hydrazine hydrate (2) in ethanol for 8 hours. In parallel, 4-hydrazinylbenzenesulfonamide (8) is synthesized through diazotization of sulfanilamide using sodium nitrite and hydrochloric acid at low temperature, followed by reduction with stannous chloride, as per established literature methods (not explicitly depicted in this scheme). The Vilsmeier–Haack formylation was then performed by reacting the quinoline hydrazine intermediate (3) with a suitable furan or thiophene acetyl (4) in the presence of dimethylformamide (DMF) and phosphoryl chloride ($POCl_3$) at 75–80°C for 6 hours, affording the corresponding pyrazole-4-carbaldehyde intermediates (5). These intermediates are subsequently subjected to Claisen–Schmidt condensation with various substituted acetophenones (6) in methanol, in the presence of sodium hydroxide (NaOH) at room temperature for 10–12 hours, generating chalcone intermediates (7). The final step involves cyclization, where the resulting chalcones are reacted with 4-hydrazinylbenzenesulfonamide (8) in ethanol using a catalytic amount of concentrated hydrochloric acid (HCl), under reflux at 75°C for 6–8 hours, yielding pyrazoline benzenesulfonamide derivatives bearing the central pyrazole–quinoline scaffold substituted with either a furan or thiophene side chain (9), with yields ranging from 78% to 86%.

Dekhane et al[153] reported an efficient and versatile synthetic protocol for the construction of pyrazoline benzenesulfonamide derivatives bearing 1,3,4-oxadiazole, 1,3,4-thiadiazole, 1,2,4-oxadiazole, and tetrazole rings, as depicted in Figure 24. The synthesis begins with the esterification of the potassium salt of 4-(4-chlorophenyl)-2-oxobut-3-enoic acid

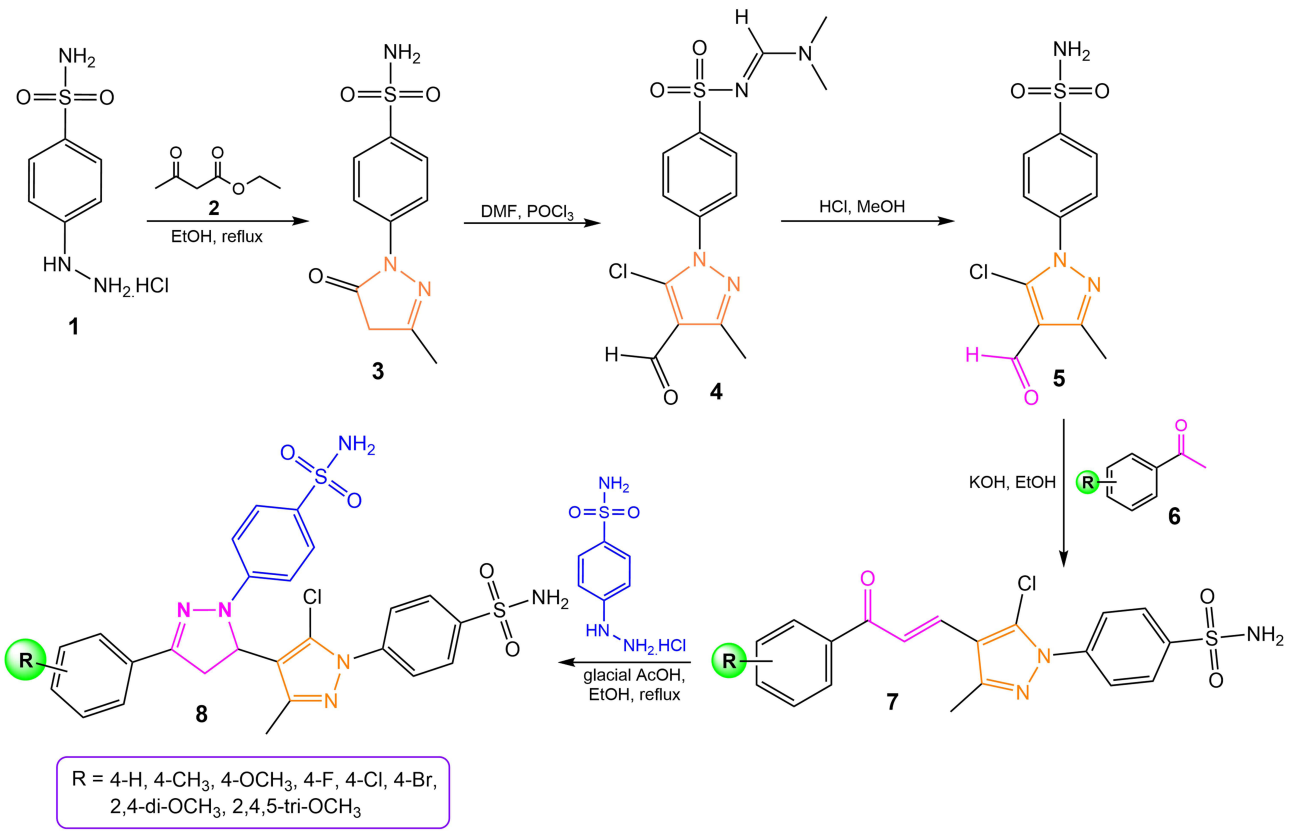

Figure 20 Synthesis of chloropyrazole benzenesulfonamide-linked pyrazoline benzenesulfonamide derivatives. 4-hydrazinylbenzenesulfonamide hydrochloride (1) reacted with ethyl acetoacetate (2) to form the pyrazolone intermediate (3), then undergoes a Vilsmeier–Haack reaction to afford N-(5-chloro-4-formyl-3-methyl pyrazole)-4-phenylsulfonyl-N, N-dimethylformimidamide (4), then removes the dimethylaminomethyl protecting group, regenerating the free sulfonamide moiety to yield 5-chloro-3-methyl-4-formylpyrazole benzenesulfonamide (5), then condensated with substituted acetophenones (6) to prepare chalcone derivatives (7), which then reacted with 4-hydrazinylbenzenesulfonamide hydrochloride to produce chloropyrazole benzenesulfonamide-linked pyrazoline benzenesulfonamide derivatives (8).

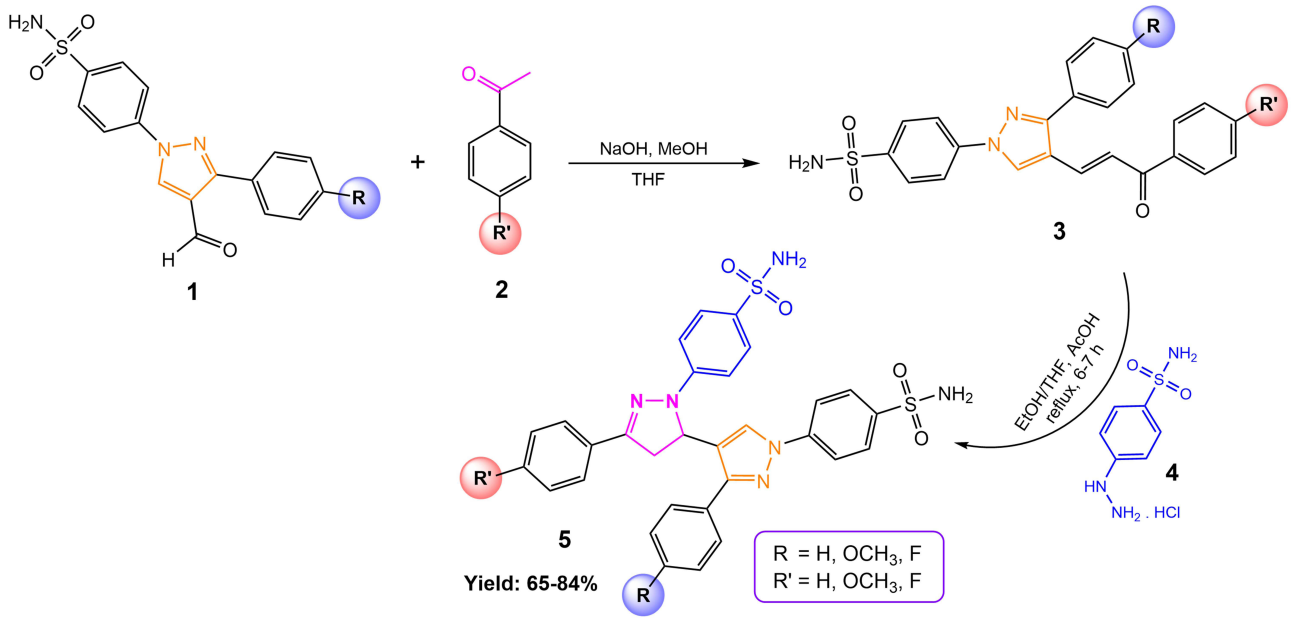

Figure 21 Synthesis of pyrazoline benzenesulfonamide derivatives containing pyrazole benzenesulfonamide. Preparation of intermediate 4-formylpyrazole bearing a benzenesulfonamide substituent at the N-1 position (1), then condensed with substituted acetophenones (2) to prepare chalcone derivatives (3), which then reacted with 4-hydrazinylbenzenesulfonamide hydrochloride (4) to produce pyrazoline benzenesulfonamide derivatives containing pyrazole benzenesulfonamide (5).

https://doi.org/10.2147/DDDT.S562109

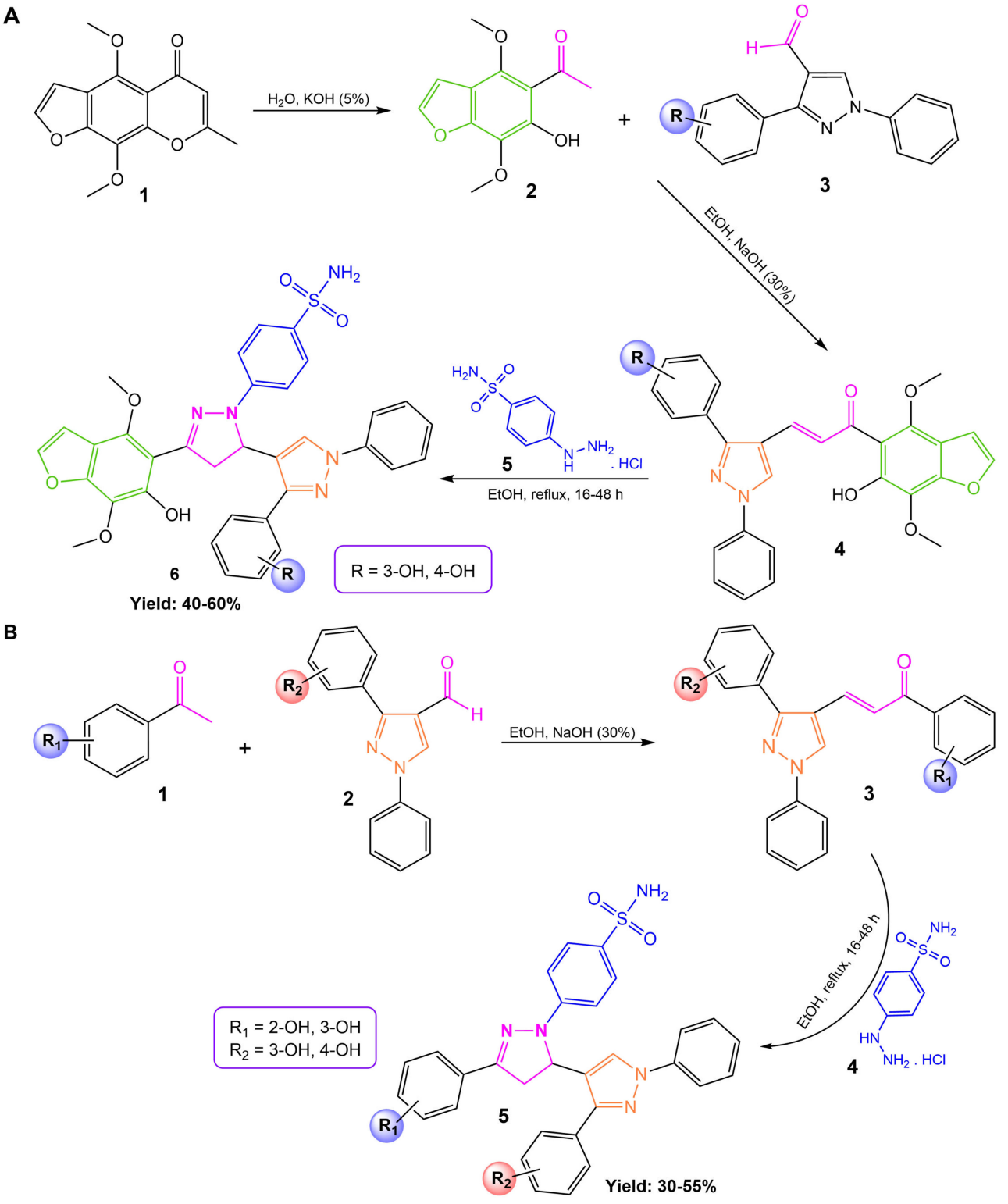

Figure 22 Synthesis of pyrazoline benzenesulfonamide derivatives bearing benzofuran and pyrazole moieties. (**A**) Natural furochromone (1) was converted to 1-(6-hydroxy-4,7-dimethoxybenzofuran-5-yl)ethanone (2), then condensed with pyrazole-4-carbaldehyde derivatives (3) to prepare hydroxybenzofuranyl–pyrazolyl chalcone intermediates (4), which then reacted with 4-hydrazinylbenzenesulfonamide hydrochloride (5) to produce pyrazoline benzenesulfonamide derivatives bearing pyrazole and benzofuran moieties (6). (**B**) Substituted acetophenone (1) was condensed with pyrazole-4-carbaldehyde derivatives (2) to prepare pyrazolyl chalcone intermediates (3), which then reacted with 4-hydrazinylbenzenesulfonamide hydrochloride (4) to produce pyrazoline benzenesulfonamide derivatives bearing a pyrazole moiety (5).

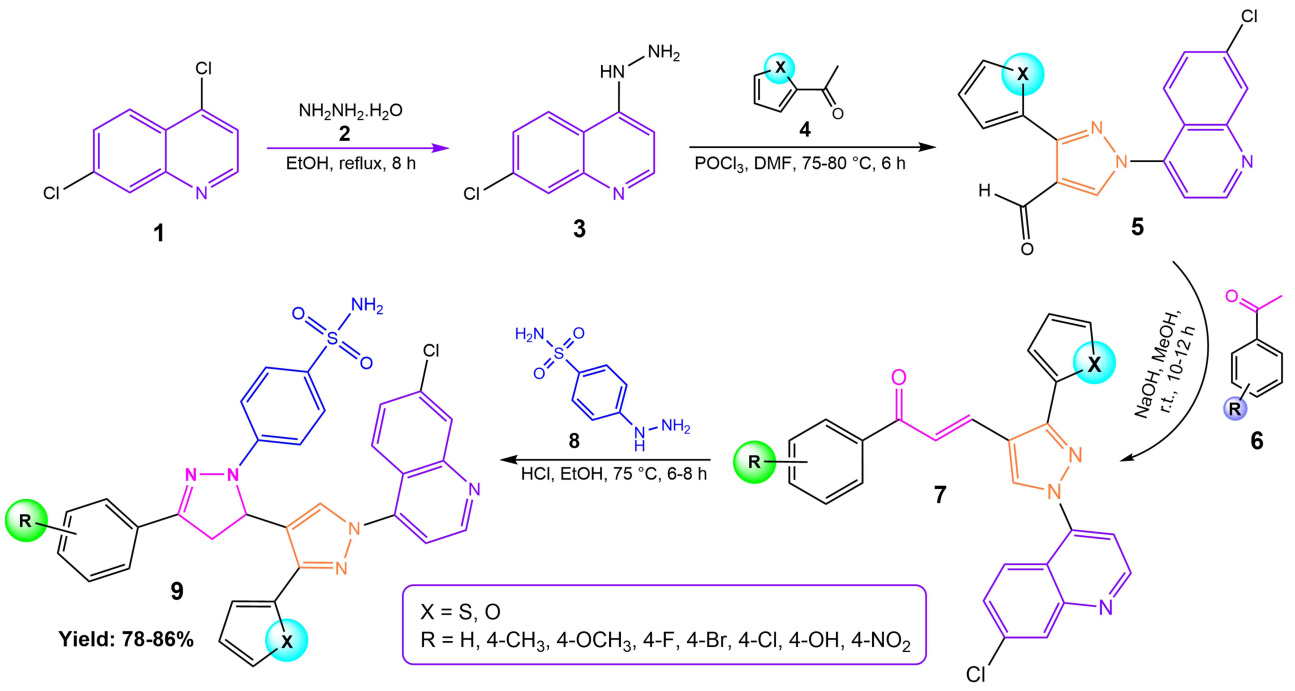

Figure 23 Synthesis of pyrazoline benzenesulfonamide derivatives bearing pyrazole–quinoline scaffold substituted with either a furan or thiophene side chain. 4,7-Dichloroquinoline (1) was reacted with hydrazine hydrate (2) to form 7-chloro-4-hydrazinylquinoline (3), then underwent the Vilsmeier–Haack reaction with a suitable furan or thiophene acetyl (4) to afford pyrazole-4-carbaldehyde intermediates (5), then condensed with substituted acetophenones (6) to prepare chalcone intermediates (7), which then reacted with 4-hydrazinylbenzenesulfonamide (8) to produce pyrazoline benzenesulfonamide derivatives bearing pyrazole–quinoline scaffold substituted with either a furan or thiophene side chain (9).

in ethanol using thionyl chloride to obtain the corresponding 4-(4-chlorophenyl)-2-oxo-but-3-enoic acid ethyl ester (1). This ester was then reacted with 4-hydrazinylbenzenesulfonamide in ethanol and acetic acid under reflux, yielding the 5-(4-chlorophenyl)-1-(4-sulfamoylphenyl)-4,5-dihydro-1H-pyrazole-3-carboxylic acid ethyl ester (2). These esters were converted to carbohydrazides (3) by treating with hydrazine hydrate in ethanol under reflux conditions. Reaction of esters (2) with aqueous ammonia in tetrahydrofuran (THF) at 50–55°C to give amide derivatives (4), then upon dehydration with oxalyl chloride in dimethylformamide (DMF) at 0°C, provides the corresponding nitrile derivatives (5). These nitriles reacted with hydroxylamine hydrochloride in the presence of sodium carbonate (Na_2CO_3) in methanol at 25–30°C, yielding carboxamidines (6). Carbohydrazides (3) reacted with carbonyldiimidazole (CDI) in(THF) using triethylamine (Et_3N) to form 2-hydroxy-1,3,4-oxadiazoles (7), or with carbon disulfide (CS_2) in the presence of potassium hydroxide in methanol to yield 2-thiol-1,3,4-oxadiazoles (8). Reacting the carbohydrazides with cyanogen bromide (CNBr) and sodium bicarbonate ($NaHCO_3$) in a dioxane–water mixture affords 2-amino-1,3,4-oxadiazoles (9). For thiadiazole synthesis, carbohydrazides were reacted sequentially with CS_2/KOH, methyl iodide (MeI), then cyclized with *p*-toluenesulfonic acid in toluene, affording 2-thiomethyl-1,3,4-thiadiazoles (10). Carboxamidines (6) reacted with ethyl chloroformate in pyridine, then refluxed in xylene to yield 5-hydroxy-1,2,4-oxadiazole (11), or acylated with acetic anhydride in the presence of Et_3N and converted with sodium hydride (NaH) and CS_2 to yield 2-thiol-1,2,4-oxadiazoles (12). Meanwhile, nitriles (5) are transformed into tetrazoles (13) via a [3+2] cycloaddition with trimethylsilyl azide ($TMSN_3$) in toluene, using dibutyltin oxide (DBTO) as a catalyst under reflux conditions. These tetrazole can be further modified by N-methylation by methyl iodide (MeI) in the presence of cesium carbonate (Cs_2CO_3) in DMF to yield N-methyltetrazole derivatives (14).

The Biological Activity of Pyrazoline Benzenesulfonamide Derivatives

Pyrazoline benzenesulfonamide derivatives constitute an important class of heterocyclic compounds that have received substantial attention within medicinal chemistry due to their wide-ranging and potent biological activities. The structural integration a pyrazoline ring with a benzenesulfonamide group offers a versatile and robust pharmacophore, facilitating

https://doi.org/10.2147/DDDT.S562109

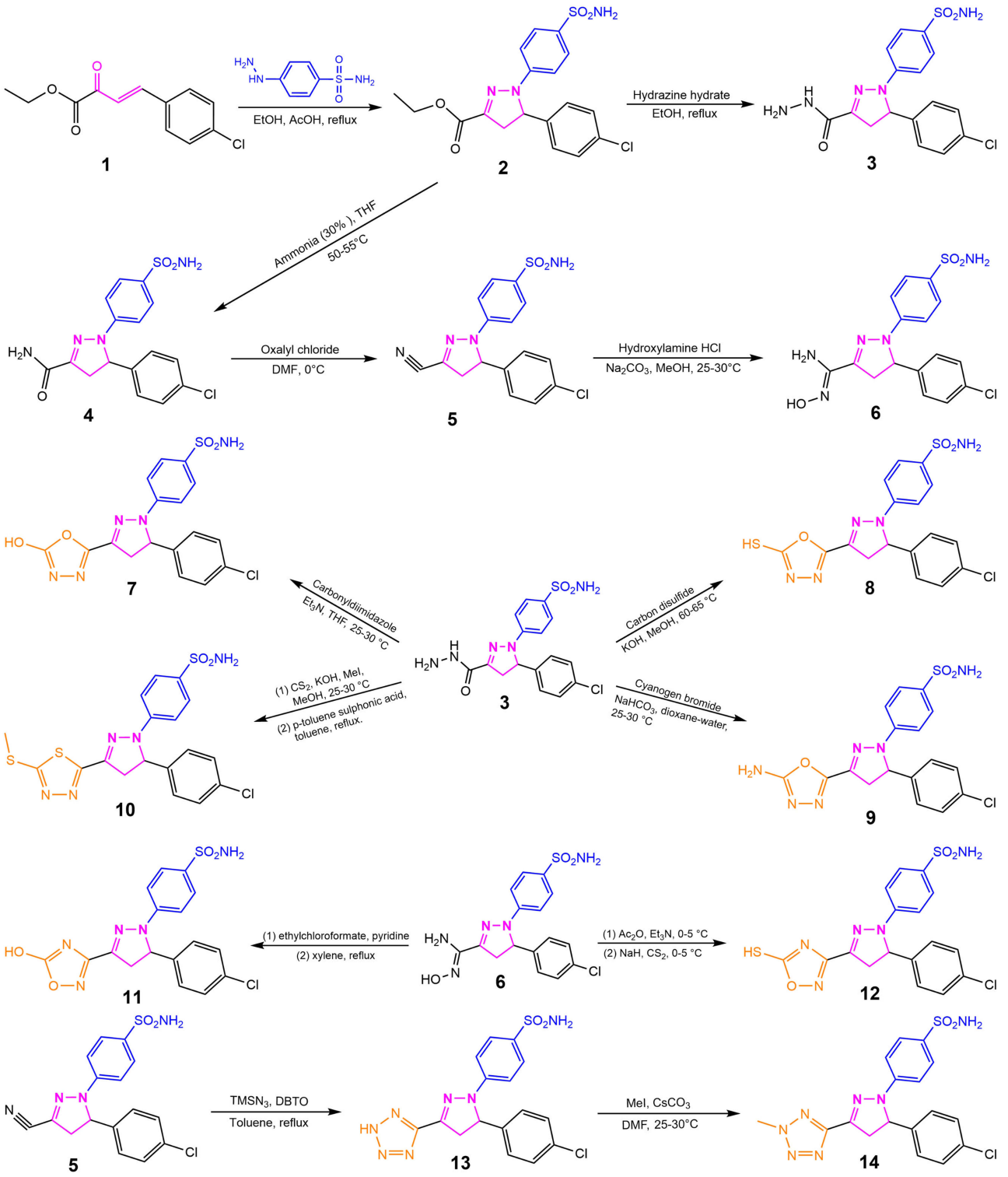

Figure 24 Synthesis of pyrazoline benzenesulfonamide derivatives bearing 1,3,4-oxadiazoles, 1,2,4-oxadiazoles, 1,3,4-thiadiazoles, and tetrazoles rings. 4-(4-chlorophenyl)-2-oxo-but-3-enoic acid ethyl ester (1) reacted with 4-hydrazinylbenzenesulfonamide to form 5-(4-chlorophenyl)-1-(4-sulfamoylphenyl)-4,5-dihydro-1H-pyrazole-3-carboxylic acid ethyl ester (2), then converted to carbohydrazides (3). Esters (2) also converted to give amide derivatives (4), which then converted to form nitrile derivatives (5), then reacted with hydroxylamine hydrochloride to form carboxamidines (6). Carbohydrazides (3) reacted with carbonyldiimidazole to form 2-hydroxy-1,3,4-oxadiazoles (7), or with carbon disulfide to yield 2-thiol-1,3,4-oxadiazoles (8), or with cyanogen bromide to afford 2-amino-1,3,4-oxadiazoles (9), or reacted sequentially with CS2/KOH, methyl iodide, then cyclized to afford 2-thiomethyl-1,3,4-thiadiazoles (10). Carboxamidines (6) reacted with ethyl chloroformate, then refluxed in xylene to yield 5-hydroxy-1,2,4-oxadiazoles (11), or acylated and converted to yield 5-thiol-1,2,4-oxadiazoles (12). Nitriles (5) are transformed into tetrazoles (13), then modified by N-methylation with methyl iodide to yield N-methyltetrazole derivatives (14).

the rational design and discovery of new therapeutic agents. These derivatives have demonstrated diverse pharmacological profiles, exhibiting antimicrobial,[117,122,151,154,155] antiviral,[132] antimalarial,[147,156] antioxidant,[157] antihyperglycemic,[140] and antitubercular[15] activities. Furthermore, significant analgesic, anti-inflammatory, and neuroprotective effects have been reported,[124,126,128,135,143,152,153,158] broadening their therapeutic utility. In addition to these properties, pyrazoline benzenesulfonamide derivatives show noteworthy enzyme inhibitory activities, including the inhibition tyrosinase,[118] matrix metalloproteinases (MMPs),[123,158] acetylcholinesterase (AChE),[159–161] and carbonic anhydrase.[137,139,156,162] The broad spectrum of bioactivity is shown in Figure 25, reflecting their potential as multi-target drug candidates. Importantly, the anticancer efficacy of certain pyrazoline benzenesulfonamide derivatives has been substantiated in recent studies,[163,164] with these compounds demonstrating tumor selectivity and potent cytotoxicity against specific cancer cell lines. This review highlights recent progress in the development of pyrazoline benzenesulfonamide derivatives, with a particular focus on their advancement as anticancer agents in drug design and discovery.

The Anticancer Activity of Pyrazoline Benzenesulfonamide Derivatives

The anticancer activity of pyrazoline benzenesulfonamide derivatives represents a promising area of research in the pursuit of novel anticancer drug candidates. Numerous studies have demonstrated that pyrazoline benzenesulfonamide derivatives possess significant anticancer potential and are among the most promising candidates.[165] These compounds exhibit their activity through diverse mechanisms, including the induction of apoptosis, cell cycle arrest, inhibition of angiogenesis, and modulation of key signaling pathways associated with tumor growth and metastasis. Structural

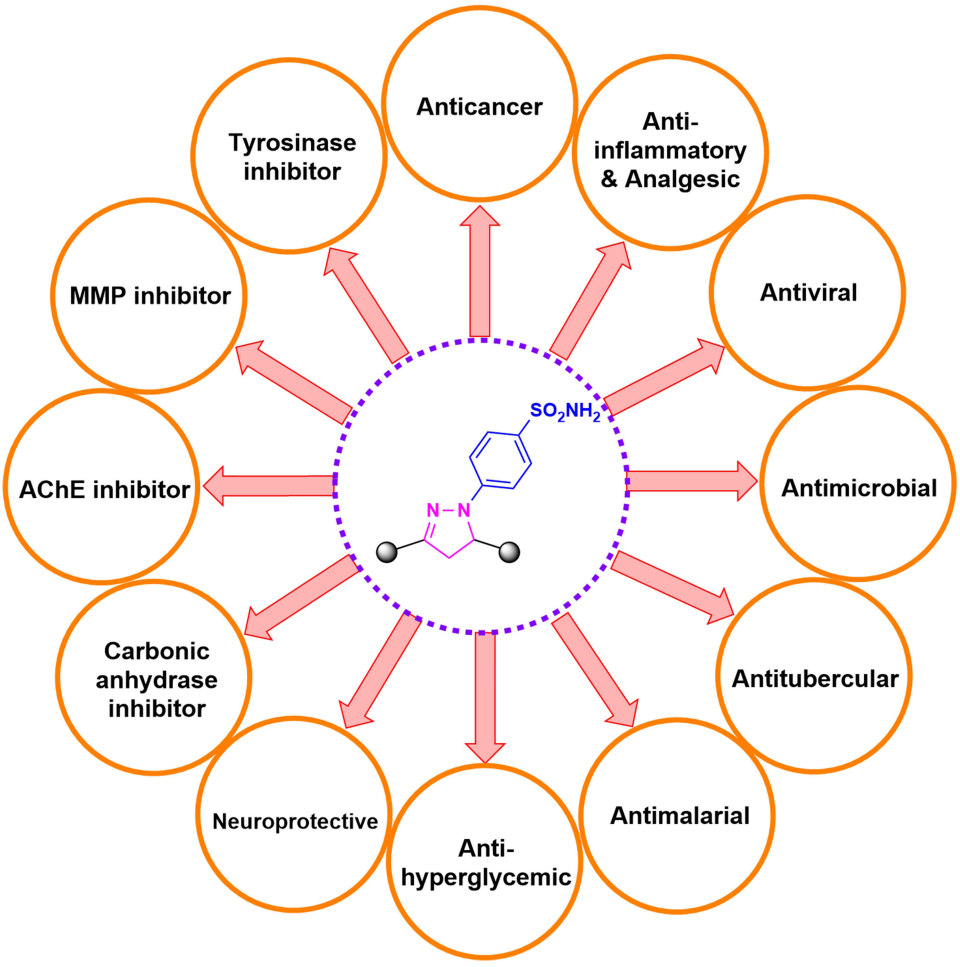

Figure 25 Representative biological activities exhibited by pyrazoline benzenesulfonamide derivatives.

https://doi.org/10.2147/DDDT.S562109

modifications on the pyrazoline ring and sulfonamide moiety have been shown to markedly influence cytotoxic potency and selectivity toward specific cancer cell lines, offering valuable insights into structure–activity relationships (SAR).

In 2011, Bano et al[166] successfully synthesized and conducted comprehensive in vitro evaluations of eight novel pyrazoline benzenesulfonamide derivatives across a diverse panel of 60 human tumor cell lines representing leukemia, lung, colon, central nervous system (CNS), ovarian, renal, prostate, breast, and melanoma malignancies, as shown in Figure 26. The screened compounds (1a–h) varied in terms of the substituent R groups attached to the phenyl ring, exhibiting notable differences in biological activity due to their structural modifications. Remarkably, derivatives 1c (4-Cl) and 1f (4-N(CH_3)$_2$) demonstrated significant antiproliferative properties. Compound 1f, in particular, exhibited exceptional growth inhibitory potency, achieving GI_{50} values below 2 μM in specific cell lines such as MOLT-4 (1.94 μM) and SR (1.28 μM) for leukemia, EKVX (1.88 μM) for non-small cell lung cancer, and COLO 205 (1.69 μM) for colon cancer. Additionally, compound 1c also showed substantial activity, with GI_{50} values such as 9.21 μM in prostate carcinoma (PC-3) and 13.3 μM in ovarian carcinoma (OVCAR-4). These empirical results substantiate the strong potential of pyrazoline benzenesulfonamide scaffolds, particularly 1f and 1c, as promising lead compounds for the development of new anticancer agents targeting leukemia, lung, and colon tumor cell lines.

The structure–activity relationship (SAR) analysis reveals that the presence and nature of substituents on the aromatic rings significantly influence the biological activity of pyrazoline benzenesulfonamide derivatives. Compounds bearing electron-withdrawing groups (such as chloro, as seen in 1c and 1f) and electron-donating groups (such as hydroxy or methoxy) on the aryl substituents at the 5-position of the pyrazoline core were found to affect anticancer potency. Notably, compound 1f, which features a 4-(N,N-dimethylamino)phenyl substituent, demonstrated the most potent and broad-spectrum antiproliferative effect across multiple cancer cell lines. In summary, the introduction of polar or electron-rich groups appears to enhance the anticancer activity of pyrazoline benzenesulfonamide derivatives, likely by promoting stronger interactions with biological targets critical for cancer cell survival.

In 2013, Amin et al[148] synthesized a series of pyrazoline benzenesulfonamide derivatives incorporating a coumarin moiety as part of a strategy to develop new antitumor agents, as shown in Figure 27. These hybrid molecules integrate

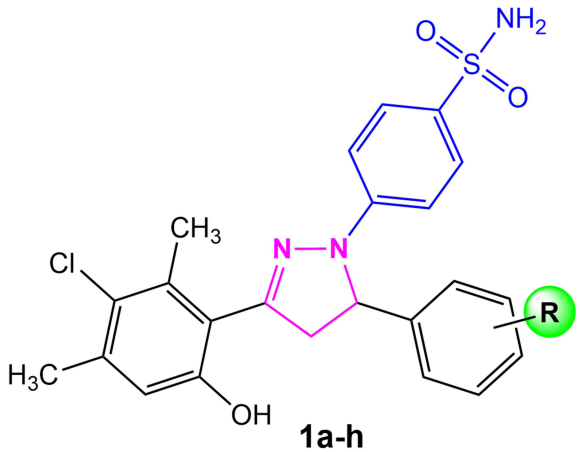

1a-h

	R
a.	H
b.	4-OCH_3
c.	4-Cl
d.	2-Cl
e.	2-OH
f.	4-N(CH_3)$_2$
g.	3,4-di-OCH_3
h.	3,4,5-tri-OCH_3

Cell Line	1c GI_{50}	1f GI_{50}	Cell Line	1c GI_{50}	1f GI_{50}
CCRF-CEM	15.1 μM	3.64 μM	IGROV1	18.3 μM	6.19 μM
HL-60(TB)	20.3 μM	7.84 μM	OVCAR-3	17.8 μM	4.21 μM
K-562	14.0 μM	2.24 μM	OVCAR-4	13.3 μM	7.68 μM
MOLT-4	12.7 μM	1.94 μM	OVCAR-5	19.4 μM	12.3 μM
SR	14.1 μM	1.28 μM	OVCAR-8	27.3 μM	5.75 μM
RPMI-8226	72.5 μM	3.99 μM	NCI/ADR-RES	19.3 μM	4.63 μM
A549/ATCC	14.7 μM	5.91 μM	SK-OV-3	27.4 μM	7.75 μM
EKVX	13.3 μM	1.88 μM	786-0	16.8 μM	4.97 μM
HOP-62	18.6 μM	10.4 μM	A498	26.7 μM	6.97 μM
HOP-92	10.3 μM	3.74 μM	ACHN	14.9 μM	3.70 μM
NCI-H226	13.4 μM	10.5 μM	CAKI-1	23.3 μM	4.38 μM
NCI-H23	17.7 μM	5.82 μM	RXF 393	24.5 μM	5.83 μM
NCI-H322M	18.0 μM	5.01 μM	SN12C	9.62 μM	5.71 μM
NCI-H460	12.2 μM	2.53 μM	TK-10	22.1 μM	4.48 μM
NCI-H522	18.6 μM	6.24 μM	UO-31	12.7 μM	3.78 μM
COLO 205	12.3 μM	1.69 μM	MCF7	6.55 μM	2.01 μM
HCC-2998	14.8 μM	6.48 μM	MDA-MB-231	11.0 μM	2.34 μM
HCT-116	76.0 μM	3.47 μM	HS 578T	23.0 μM	3.45 μM
HCT-15	14.2 μM	5.48 μM	BT-549	15.4 μM	1.31 μM
HT29	10.9 μM	3.30 μM	T-47D	5.72 μM	2.93 μM
KM12	13.3 μM	2.80 μM	MDA-MB-468	17.1 μM	10.7 μM
SW-620	18.4 μM	3.72 μM	LOX IMVI	14.8 μM	2.34 μM
SF-268	18.7 μM	5.76 μM	MALME-3M	14.8 μM	14.8 μM
SF-295	19.2 μM	16.0 μM	M14	14.0 μM	2.62 μM
SF-539	15.7 μM	12.3 μM	MDA-MB-435	13.4 μM	3.57 μM
SNB-19	22.2 μM	12.4 μM	SK-MEL-2	21.4 μM	11.9 μM
SNB-75	17.0 μM	10.9 μM	SK-MEL-28	19.4 μM	11.7 μM
U251	11.8 μM	3.34 μM	SK-MEL-5	14.5 μM	9.59 μM
PC-3	9.21 μM	4.44 μM	UACC-257	26.3 μM	11.9 μM
DU-145	19.2 μM	5.60 μM	UACC-62	9.92 μM	3.49 μM

Figure 26 Chemical structures of pyrazoline benzenesulfonamide derivatives (1a–h) and GI_{50} values of compounds 1c and 1f against 60 human cancer cell lines.

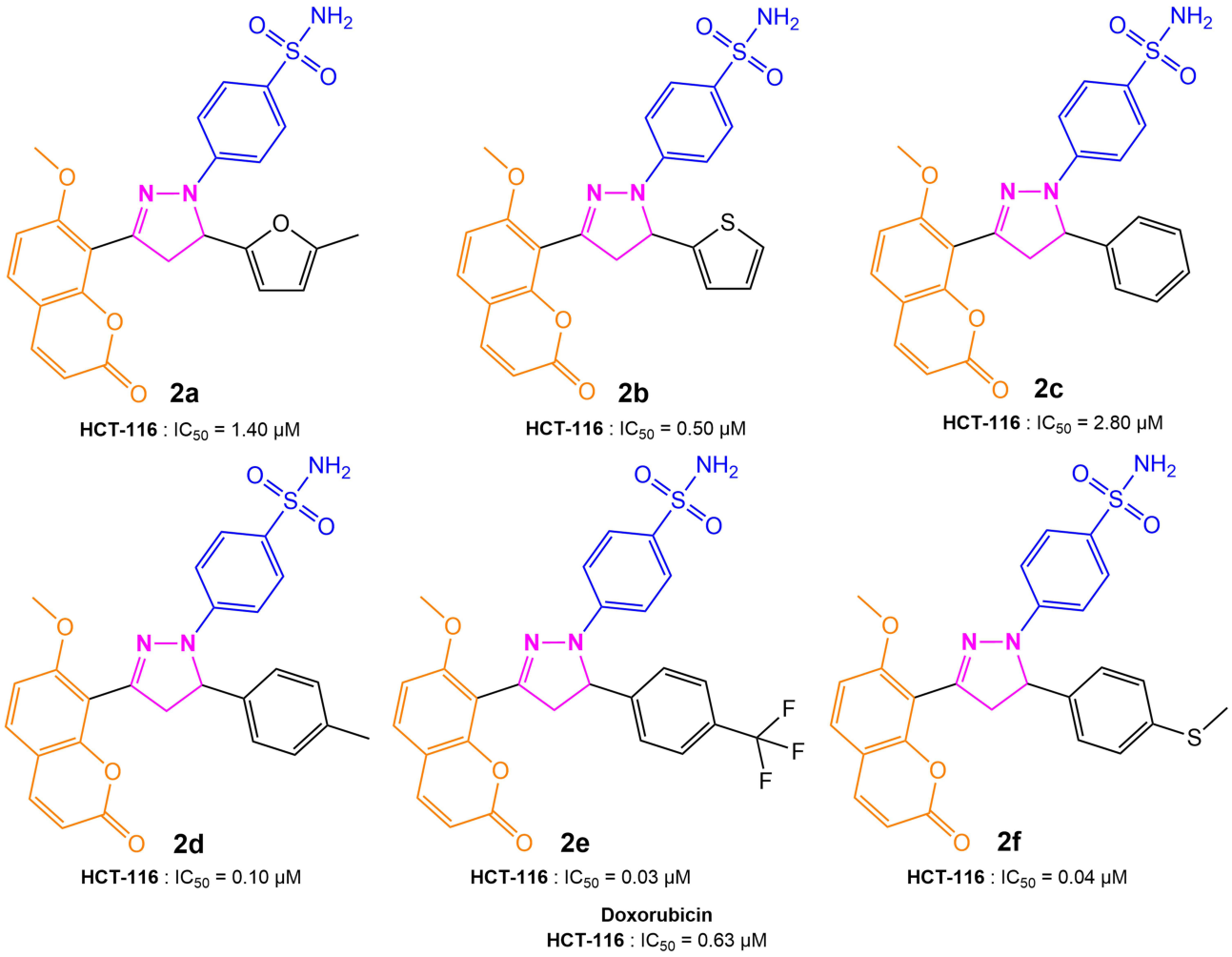

Figure 27 Chemical structures of pyrazoline benzenesulfonamide derivatives (2a–f) and their cytotoxic activity (IC_{50}) against HCT-116 human colorectal cancer cells. Doxorubicin was used as a reference drug.

three pharmacologically active components: a coumarin scaffold, a pyrazoline ring, and a benzenesulfonamide group. The rationale behind this hybridization approach is to enhance anticancer potency by combining multiple bioactive motifs within a single molecular framework. When evaluated for antiproliferative activity, particularly against HCT-116 human colon cancer cells, several derivatives demonstrated remarkable cytotoxicity, surpassing that of the standard chemotherapeutic drug Doxorubicin. Notably, compounds 2e and 2f bearing electron-withdrawing 4-trifluoromethyl and 4-methylthio substituents on the aryl ring displayed IC_{50} values of 0.03 μM and 0.04 μM, respectively, which are substantially lower than that of Doxorubicin (IC_{50} = 0.63 μM). These findings highlight the potential of coumarin-conjugated pyrazoline benzenesulfonamides as promising lead structures for the development of anticancer drugs.

The structure–activity relationship (SAR) analysis reveals that the presence of strong electron-withdrawing substituents (eg, -CF_3 or CH_3S-) at the para position of the 5-aryl ring significantly enhances cytotoxic potency. This finding is particularly evident in derivatives 2e and 2f, which display the lowest IC_{50} values in the series. In contrast, analogues lacking these substituents or bearing neutral/aromatic rings (such as 2a and 2c) exhibit markedly reduced antiproliferative activity. The coumarin moiety may further contribute to improved cellular uptake and biological target affinity, while the sulfonamide group is recognized to enhance drug-likeness and binding interactions. These observations suggest that rational structural modification, particularly the introduction of electron-withdrawing groups and retention of the coumarin core, is essential for optimizing antitumor activity within this compound class.

https://doi.org/10.2147/DDDT.S562109

In 2015, pyrazoline benzenesulfonamide derivatives garnered significant attention as potential anticancer agents due to their potent inhibitory effects on matrix metalloproteinase-2 (MMP-2), an enzyme that facilitates tumor progression and metastasis. Wang et al[159] reported a series of such derivatives that demonstrated notable cytotoxicity across several cancer cell lines, including A549 (lung), MCF-7 (breast), HeLa (cervical), and HepG2 (liver), with IC_{50} values ranging from 1.93 to 36.8 μM for A549 cells, 1.62 to 22.92 μM for MCF-7 cells, 1.70 to 16.52 μM for HeLa cells, and 1.01 to 11.51 μM for HepG2 cells, as shown in Figure 28. Meanwhile, the reference drug Gefitinib has IC_{50} values of 2.83 μM for A549 cells, 6.76 μM for MCF-7 cells, and 1.43 μM for HeLa cells, and Celecoxib has IC_{50} values of 2.26 μM for A549 cells, 6.89 μM for MCF-7 cells, 7.61 μM for HeLa cells, and 0.73 μM for HepG2 cells. Among these, compound 3c was identified as the most potent, showing outstanding antiproliferative activity against A549, MCF-7, HeLa, and HepG2 cell lines. Specifically, compound 3c achieved superior MMP-2 inhibition (IC_{50} = 0.33 μM) relative to the standard control CMT-1 (IC_{50} = 1.13 μM) and significantly induced apoptosis in HeLa cells in a dose-dependent manner. These data highlight the critical impact of structural modifications within the benzenesulfonamide scaffold, which can modulate both potency and selectivity. Consequently, such derivatives are promising candidates for further optimization and advancement as targeted anticancer therapies.

The structure–activity relationship (SAR) analysis revealed that substitutions on the benzene ring of acetophenone notably influenced bioactivity, whereas variations in the salicylaldehyde substituent had minimal effects. Compounds possessing electron-donating groups such as methyl (CH_3) and methoxy (OCH_3) at the para-position displayed significantly enhanced inhibitory potency against MMP-2 and antiproliferative effects on multiple tumor cell lines compared to those with electron-withdrawing or bulky groups. For example, compound 3c, with an ethoxy group (OCH_2CH_3) substituent, exhibited the strongest MMP-2 inhibition (IC_{50} = 0.33 μM) and potent anticancer activity, while compounds with electron-withdrawing groups like fluorine had lower activity. This pattern underscores that electron-donating substituents on the benzene ring are more favorable for improving pharmaceutical potency in this compound class.

Molecular docking studies were performed using the crystal structure of MMP-2 (PDB ID: 1QIB) to elucidate the binding mode of the most active compound 3c. The docking model revealed key interactions of compound 3c within the enzyme's active site, highlighting the roles of amino acid residues Tyr155, Phe157, and Phe180 in stabilizing ligand binding. Two hydrogen bonds and two π-π interactions were identified in the 2D interaction model, complemented by two coordination bonds between the zinc ion in the catalytic site and the sulfonamide moiety of the compound in the 3D

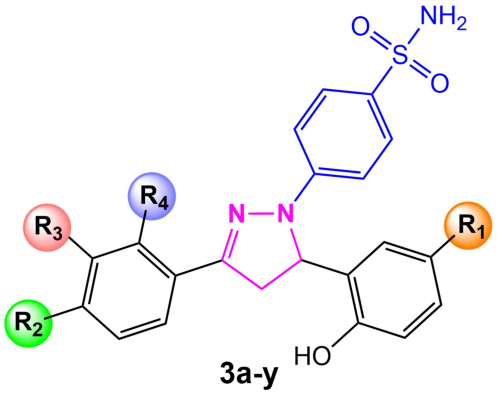

	R_1	R_2	R_3	R_4	A549 IC_{50}	MCF-7 IC_{50}	HeLa IC_{50}	HepG2 IC_{50}	293T CC_{50}
a.	H	H	H	H	3.97 μM	2.68 μM	1.70 μM	4.56 μM	62.19 μM
b.	H	H	H	Cl	12.00 μM	5.96 μM	7.45 μM	2.31 μM	58.10 μM
c.	H	OCH_2CH_3	H	H	1.93 μM	4.37 μM	3.17 μM	4.21 μM	48.95 μM
d.	H	Br	H	H	2.88 μM	6.31 μM	4.68 μM	7.05 μM	47.74 μM
e.	H	H	OCH_3	H	5.24 μM	4.27 μM	6.63 μM	5.51 μM	53.29 μM
f.	H	CH_3	CH_3	H	6.18 μM	5.30 μM	8.64 μM	9.54 μM	50.20 μM
g.	H	Cl	Cl	H	13.32 μM	5.69 μM	12.15 μM	10.02 μM	48.53 μM
h.	Cl	F	H	H	6.49 μM	3.14 μM	4.51 μM	7.21 μM	48.41 μM
i.	Cl	H	H	Cl	7.35 μM	1.67 μM	8.13 μM	4.21 μM	50.22 μM
j.	Cl	H	H	H	19.40 μM	1.85 μM	16.52 μM	9.64 μM	54.60 μM
k.	Cl	Cl	H	H	5.87 μM	3.35 μM	5.99 μM	4.45 μM	45.27 μM
l.	Cl	OCH_3	H	H	7.39 μM	1.87 μM	8.53 μM	8.73 μM	46.14 μM
m.	Cl	Br	H	H	14.03 μM	1.62 μM	9.87 μM	6.77 μM	49.84 μM
n.	Cl	Cl	Cl	H	24.67 μM	2.45 μM	11.74 μM	5.20 μM	44.41 μM
o.	Cl	OCH_2CH_3	H	H	9.52 μM	22.94 μM	10.05 μM	11.38 μM	45.40 μM
p.	Cl	H	OCH_3	H	4.12 μM	6.95 μM	5.13 μM	6.78 μM	45.28 μM
q.	Br	H	H	H	14.03 μM	2.39 μM	7.21 μM	10.03 μM	47.59 μM
r.	Br	H	OCH_3	H	7.39 μM	2.40 μM	6.09 μM	8.59 μM	42.64 μM
s.	Br	F	H	H	24.67 μM	3.73 μM	3.54 μM	7.66 μM	45.20 μM
t.	Br	H	H	Cl	9.51 μM	2.40 μM	6.89 μM	4.13 μM	41.90 μM
u.	Br	Cl	H	H	2.25 μM	3.73 μM	1.74 μM	1.01 μM	43.14 μM
v.	Br	Br	H	H	4.12 μM	2.40 μM	4.95 μM	5.69 μM	41.97 μM
w.	Br	Cl	Cl	H	5.24 μM	13.96 μM	14.98 μM	4.51 μM	44.56 μM
x.	H	F	H	H	36.80 μM	18.50 μM	7.61 μM	7.05 μM	51.98 μM
y.	H	OCH_3	H	H	8.93 μM	12.60 μM	7.85 μM	11.51 μM	53.97 μM
Gefitinib					2.83 μM	6.76 μM	1.43 μM	–	–
Celecoxib					2.26 μM	6.89 μM	7.61 μM	0.73 μM	54.99 μM

Figure 28 Chemical structures of pyrazoline benzenesulfonamide derivatives (3a–y) and their cytotoxic activities (IC_{50}) against A549, MCF-7, HeLa, and HepG2 human cancer cell lines, as well as cytotoxicity (CC_{50}) in 293T normal cells. Gefitinib and celecoxib were used as reference drugs.

structure. These interactions fostered robust steric stabilization of the ligand. The sulfonamide and salicylaldehyde backbones were deemed critical for zinc chelation and hydrogen bonding, respectively, supporting the observed biological activity. The acetophenone portion provided additional steric bulk, which enhanced the binding affinity. The docking results were consistent with biological assay data, confirming the potential of compound 3c as a selective and potent MMP-2 inhibitor for antitumor therapy.

Pyrazoline benzenesulfonamide derivatives have shown promising anticancer activity, particularly as inhibitors of matrix metalloproteinases MMP-2 and MMP-9, which are essential in tumor progression and metastasis. In the work of Yan et al,[123] a series of 25 novel derivatives was synthesized and systematically screened for antiproliferative effects against four cancer cell lines, namely MCF-7 (breast), HeLa (cervical), A549 (lung), and HepG2 (liver), as shown in Figure 29. The majority of compounds demonstrated significant cytotoxicity, with IC_{50} values ranging from 8.63 to 50.61 μM for MCF-7 cells, 6.37 to 36.49 μM for HeLa cells, 1.90 to 17.82 μM for A549 cells, and 5.38 to 36.42 μM for HepG2 cells. Notably, compound 4i demonstrated the highest potency, particularly against A549 lung cancer cells, with an IC_{50} value of 1.90 μM, outperforming standard agents such as Gefitinib (IC_{50} = 2.86 μM) and Celecoxib (IC_{50} = 2.15 μM). Furthermore, these derivatives exhibited potent inhibitory activity against MMP-2 and MMP-9, with compound 4i achieving IC_{50} values of 0.21 μM for MMP-2 and 1.87 μM for MMP-9, both of which are lower than those of the reference inhibitor CMT-1 (IC_{50} = 1.26 μM for MMP-2, IC_{50} = 2.52 μM for MMP-9). Importantly, tested compounds displayed relatively low cytotoxicity against normal human kidney epithelial cells (293T), reflected by high CC_{50} values, suggesting an encouraging therapeutic window for further development.

The structure–activity relationship (SAR) analysis revealed that the presence and position of functional groups significantly influenced both anticancer potency and selectivity. Derivatives bearing strong electron-donating groups (such as methoxy or ethoxy) at the para-position of the benzene ring generally exhibited enhanced MMP-2 inhibitory activity compared to analogs with electron-withdrawing groups (such as chloro or bromo). Additionally, compounds containing an

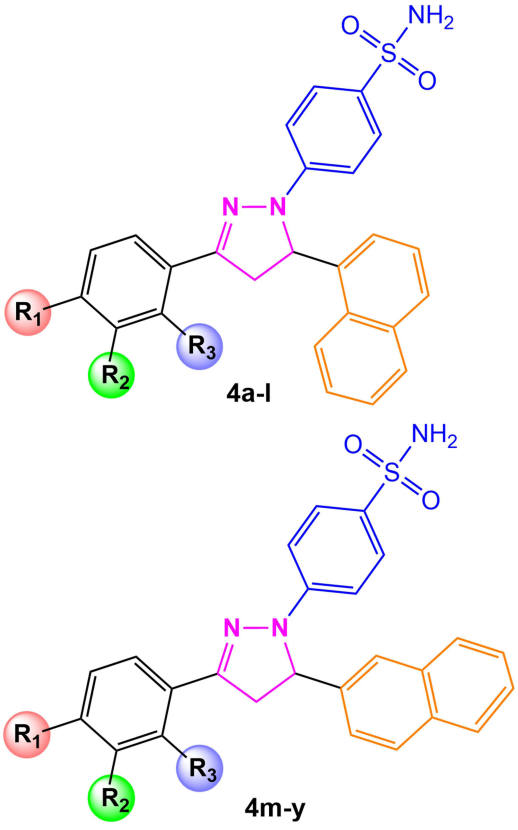

	R_1	R_2	R_3	MCF-7 IC_{50}	HeLa IC_{50}	A549 IC_{50}	HepG2 IC_{50}	293T CC_{50}
a.	H	H	H	22.62 μM	20.16 μM	12.91 μM	19.08 μM	51.35 μM
b.	H	H	CH_3	10.03 μM	6.37 μM	2.84 μM	5.38 μM	51.23 μM
c.	H	H	Cl	23.61 μM	29.07 μM	7.38 μM	10.03 μM	53.14 μM
d.	H	CH_3	H	8.63 μM	9.87 μM	3.14 μM	5.83 μM	48.24 μM
e.	H	OCH_3	H	26.14 μM	30.60 μM	5.82 μM	36.42 μM	45.32 μM
f.	H	Br	H	28.83 μM	28.75 μM	8.19 μM	14.92 μM	42.21 μM
g.	H	I	H	18.06 μM	26.04 μM	6.83 μM	8.06 μM	46.88 μM
h.	CH_3	H	H	9.89 μM	8.61 μM	7.77 μM	7.04 μM	51.26 μM
i.	CH_3	H	CH_3	18.06 μM	12.13 μM	1.90 μM	6.99 μM	52.45 μM
j.	OCH_3	H	H	26.37 μM	30.12 μM	6.51 μM	27.76 μM	47.06 μM
k.	OCH_2CH_3	H	H	35.05 μM	18.52 μM	3.33 μM	8.66 μM	59.50 μM
l.	Cl	H	H	18.02 μM	11.51 μM	2.98 μM	16.45 μM	49.22 μM
m.	H	H	H	21.63 μM	13.04 μM	8.42 μM	17.85 μM	50.54 μM
n.	H	H	CH_3	16.34 μM	15.63 μM	6.84 μM	6.88 μM	51.68 μM
o.	H	H	Cl	8.64 μM	16.44 μM	2.16 μM	31.08 μM	49.88 μM
p.	H	CH_3	H	11.08 μM	26.43 μM	7.64 μM	7.68 μM	52.41 μM
q.	H	OCH_3	H	13.56 μM	36.49 μM	8.67 μM	26.04 μM	49.38 μM
r.	H	F	H	13.08 μM	21.05 μM	7.83 μM	24.83 μM	48.96 μM
s.	H	Br	H	9.15 μM	23.67 μM	10.32 μM	28.98 μM	47.04 μM
t.	H	I	H	11.06 μM	32.04 μM	12.04 μM	18.06 μM	55.86 μM
u.	CH_3	H	H	18.17 μM	17.56 μM	6.90 μM	8.32 μM	53.13 μM
v.	OCH_3	H	H	50.61 μM	35.35 μM	9.31 μM	22.32 μM	45.40 μM
w.	OCH_2CH_3	H	H	38.23 μM	35.35 μM	17.82 μM	9.17 μM	53.77 μM
x.	F	H	H	12.28 μM	26.11 μM	6.95 μM	20.66 μM	49.53 μM
y.	Cl	H	H	12.41 μM	19.21 μM	2.76 μM	25.03 μM	54.76 μM
Gefitinib				6.71 μM	1.52 μM	2.86 μM	–	–
Celecoxib				6.88 μM	7.55 μM	2.15 μM	0.76 μM	54.38 μM

Figure 29 Chemical structures of pyrazoline benzenesulfonamide derivatives (4a–y) and their cytotoxic activities (IC_{50}) against MCF-7, HeLa, A549, and HepG2 human cancer cell lines, as well as cytotoxicity (CC_{50}) in 293T normal cells. Gefitinib and celecoxib were used as reference drugs.

https://doi.org/10.2147/DDDT.S562109

α-naphthyl moiety displayed greater anticancer activity and stronger MMP inhibition than those with a β-naphthyl group. SAR findings also indicated that the modifications at the R1, R2, and R3 positions significantly impacted both enzymatic inhibition and cytotoxicity profiles. Optimal activity was observed when a methyl group was introduced at the R1 position. These SAR findings were further supported by molecular docking studies, which demonstrated that compound 4i established strong binding interactions within the MMP active site, facilitated by hydrogen bonds, π-cation interactions, and coordinate bonding with the catalytic zinc ion. Overall, these insights suggest that strategic structural modifications can be employed to fine-tune both the potency and selectivity of pyrazoline benzenesulfonamide derivatives as effective anticancer agents.

Molecular docking simulations positioned compound 4i within the active site of MMP-2 (PDB ID: 1QIB) and MMP-9 (PDB ID: 2OVX), elucidating its probable binding modalities. For MMP-2, the binding configuration involved a critical hydrogen bond with the backbone NH of Phe146, a π-cation interaction with Phe157, and a coordinate bond between the zinc ion and an oxygen atom of the ligand. These specific interactions significantly enhanced binding affinity and inhibition. Similarly, docking with MMP-9 revealed multiple hydrogen bonds with Leu397 and Leu418, a π-interaction with His401, and a coordinate bond between the zinc cation and the ligand's nitrogen atom, contributing to robust inhibition. The estimated binding free energies for compound 4i were −53.29 kcal/mol (MMP-2) and −48.37 kcal/mol (MMP-9), indicating very strong binding. These in silico findings corroborated the biological assay data, supporting the conclusion that compound 4i is a highly effective inhibitor of both MMP-2 and MMP-9, with strong potential as an anticancer agent.

In 2016, Qiu et al[144] reported the rational design and synthesis of a series of pyrazoline benzenesulfonamide derivatives, aimed at selectively inhibiting cyclooxygenase-2 (COX-2) and exploring their cytotoxic potential against human cancer cell lines. The synthesized compounds (5a–t) were systematically evaluated for their antiproliferative effects against A549 (lung carcinoma), HeLa (cervical carcinoma), and HepG2 (hepatocellular carcinoma) cell lines, along with an assessment of cytotoxicity in the non-cancerous 293T cell line as shown in Figure 30. The screening results indicated that these pyrazoline derivatives demonstrated a broad range of anticancer activities, with IC_{50} values ranging from 1.63 ± 0.97 to 20.84 ± 0.13 μM for A549 cells, 6.12 ± 0.84 to 22.70 ± 2.09 μM for HeLa cells, and 9.54 ± 1.24 to 38.53 ± 0.67 μM for HepG2 cells. Notably, compound 5d (bearing 2,4-difluoro substitution) showed superior potency, achieving an IC_{50} value of 1.63 ± 0.97 μM against A549 cells, which exceeds the efficacy of the reference COX-2 inhibitor Celecoxib (IC_{50} = 2.21 ± 1.31 μM) under identical conditions. Furthermore, compound 5d exhibited good selectivity, as evidenced by its low cytotoxicity profile toward 293T cells (CC_{50} > 100 μM). Further biological assays revealed that compound 5d induces apoptosis and causes cell cycle arrest at the G2/M phase in a dose–dependent manner. Mechanistic investigations further established that compound 5d is capable of permeating cancer cell membranes, reduce

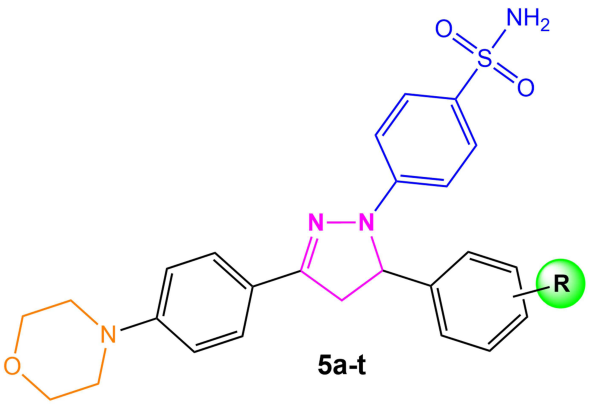

	R	A549 IC_{50} ± SD (μM)	HeLa IC_{50} ± SD (μM)	HepG2 IC_{50} ± SD (μM)	293T CC_{50} ± SD (μM)
a.	4-F	4.43 ± 0.31	10.37 ± 0.49	14.88 ± 0.87	>100
b.	3-F	6.29 ± 0.43	11.44 ± 0.34	20.51 ± 0.66	>100
c.	2-F	9.87 ± 1.01	22.70 ± 1.15	27.38 ± 1.34	>100
d.	2,4-di-F	1.63 ± 0.97	6.12 ± 0.84	10.21 ± 0.45	>100
e.	3,5-di-F	1.80 ± 0.25	6.98 ± 0.21	18.92 ± 0.67	>100
f.	4-Cl	5.18 ± 0.37	13.51 ± 0.33	20.92 ± 0.34	>100
g.	3-Cl	11.51 ± 1.05	15.88 ± 0.65	19.99 ± 0.85	>100
h.	2-Cl	13.65 ± 1.30	18.47 ± 0.53	23.75 ± 0.44	>100
i.	3,4-di-Cl	4.21 ± 0.32	13.43 ± 0.21	15.91 ± 0.98	>100
j.	3,4,5-tri-Cl	3.25 ± 0.19	10.30 ± 0.34	14.26 ± 0.25	>100
k.	4-Br	6.38 ± 0.54	8.69 ± 0.88	9.54 ± 1.24	>100
l.	3-Br	6.80 ± 0.29	9.06 ± 1.54	11.38 ± 2.08	>100
m.	2-Br	10.22 ± 0.14	15.82 ± 0.58	13.28 ± 0.71	>100
n.	4-I	10.47 ± 0.91	14.24 ± 0.82	11.54 ± 1.90	>100
o.	3-I	11.61 ± 0.28	12.55 ± 0.35	11.93 ± 1.36	>100
p.	2-I	15.11 ± 0.47	17.30 ± 0.51	22.96 ± 0.98	>100
q.	4-CH_3	20.84 ± 0.13	15.35 ± 0.32	38.53 ± 0.67	>100
r.	4-CF_3	4.43 ± 0.45	11.44 ± 0.69	14.50 ± 2.71	>100
s.	3-OCH_3	8.29 ± 0.19	22.70 ± 2.09	31.39 ± 2.28	>100
t.	3-NO_2	6.87 ± 0.12	10.37 ± 0.21	13.11 ± 0.82	>100
Celecoxib		2.21 ± 1.31	7.51 ± 1.28	0.68 ± 3.14	65.34 ± 0.18

Figure 30 Chemical structures of pyrazoline benzenesulfonamide derivatives (5a–t) and their cytotoxic activities (IC_{50}) against A549, HeLa, and HepG2 human cancer cell lines, as well as cytotoxicity (CC_{50}) in 293T normal cells. Celecoxib was used as a reference drug.

cell adhesion (for a key factor in metastasis), and decrease COX-2 protein expression, suggesting that its anticancer effects are closely associated with COX-2 inhibition.

The structure–activity relationship (SAR) study centered on the dihydropyrazole scaffold substituted with a sulfonamide moiety at the para position of one aryl ring, a known pharmacophore crucial for selective COX-2 inhibition. Modifications focused on substitutions at the 3-position of the dihydropyrazole core and the aryl rings. The library of compounds synthesized demonstrated varying degrees of COX-2 inhibitory potency and selectivity, with compound 5d displaying the highest selectivity index (SI = 451), surpassing that of Celecoxib (SI = 415). The high selectivity aligns with the molecule's specific structural attributes, including optimal binding interactions and physicochemical properties, notably a moderate AlogP value, which facilitates drug-likeness.

Molecular docking simulations against the COX-2 enzyme (PDB ID: 3LN1) elucidated the binding interactions of the derivatives, with compound 5d showing the most favorable binding affinity (interaction energy of −63.11 kcal/mol), exceeding that of celecoxib (−56.13 kcal/mol). The docking model revealed that 5d forms five key hydrogen bonds with COX-2 active site residues Gln178, Leu338, Ser339, Arg499, and Phe504. Additionally, a Pi-Sigma interaction with Ser339 and various van der Waals contacts were observed, explaining the compound's high potency and selectivity. These interactions are consistent with the bioactivity profile, confirming compound 5d as a promising selective COX-2 inhibitor with anticancer properties.

In the same year, Kucukoglu et al[138] reported the synthesis and biological evaluation of pyrazoline benzenesulfonamide derivatives as potential anticancer agents, focusing on their dual roles as carbonic anhydrase (CA) inhibitors and cytotoxic agents. This investigation, a series of polymethoxylated-pyrazoline benzenesulfonamides (6a–f), was synthesized and subjected to cytotoxicity assays against human oral squamous carcinoma cell lines (Ca9-22, HSC-2, HSC-3, HSC-4) as well as human normal oral cells (HGF, HPLF, HPC), with 5-Fluorouracil and Melphalan as standard controls, as shown in Figure 31. All tested compounds (except compound 6a) exhibited cytotoxic activity, with CC_{50} values ranging from 7.7 to 200 μM across cancer cell lines. Trimethoxy derivatives (6d, 6e, and 6f) demonstrated markedly

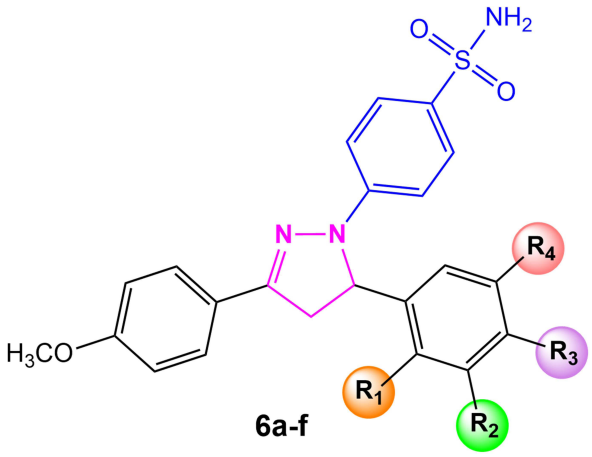

	R_1	R_2	R_3	R_4	**Ca9-22** CC_{50} (μM)	**HSC-2** CC_{50} (μM)	**HSC-3** CC_{50} (μM)	**HSC-4** CC_{50} (μM)	Mean CC_{50} (μM)	SD CC_{50} (μM)	**HGF** CC_{50} (μM)	**HPLF** CC_{50} (μM)	**HPC** CC_{50} (μM)	Mean CC_{50} (μM)	SD CC_{50} (μM)	TS1	TS2
a.	OCH_3	H	H	OCH_3	*Not Tested*												
b.	OCH_3	H	OCH_3	H	22	200	200	200	155.5	89.0	22	119	46	62.3	50.5	0.4	1.0
c.	H	OCH_3	OCH_3	H	200	200	200	200	200.0	0.0	63	120	181	121.3	59.0	0.6	0.3
d.	OCH_3	OCH_3	OCH_3	H	22	200	200	200	155.5	89.0	75	135	115	108.3	30.6	0.7	3.4
e.	OCH_3	H	OCH_3	OCH_3	7.7	41	31	20	24.9	14.3	11	12	12	11.7	0.6	0.5	1.4
f.	H	OCH_3	OCH_3	OCH_3	10	11	14	22	14.3	5.4	20	21	23	21.3	1.5	1.5	2.0
5-Fluorouracil					55.1	24.4	72.7	38.9	47.8	–	>200	>200	>200	>200	–	>4.2	>3.6
Melphalan					40.3	13.6	11	10.3	18.80	–	>200	151.0	175.5	175.2	–	>9.3	>4.9

Figure 31 Chemical structures of pyrazoline benzenesulfonamide derivatives (6a–f) and their cytotoxicity (CC_{50}) against human oral squamous carcinoma cell lines (Ca9-22, HSC-2, HSC-3, HSC-4) and normal oral cells (HGF, HPLF, HPC). 5-Fluorouracil and melphalan were used as reference drugs.

https://doi.org/10.2147/DDDT.S562109

enhanced cytotoxic profiles compared to their dimethoxy analogs (6b and 6c), suggesting that increased methoxylation in the phenyl moieties improves anticancer efficacy. The most potent compound, 6f, displayed CC_{50} values of 10 μM, 11 μM, 14 μM, and 22 μM against Ca9-22, HSC-2, HSC-3, and HSC-4 cell lines, respectively, outperforming 5-Fluorouracil (CC_{50} = 24.4–72.7 μM) on several cell lines. Compound 6f also showed superior tumor selectivity (TS1 = 1.5, TS2 = 2.0) compared to other analogs and control agents, indicating favorable selectivity towards malignant cells over normal cells. Additionally, all synthesized pyrazoline derivatives exhibited potent inhibitory activity against human carbonic anhydrase isoforms I and II, with inhibition constants (Ki) values ranging from 26.5 ± 4.6 to 55.5 ± 19.4 nM for hCA I and 18.9 ± 9.0 to 28.8 ± 6.5 nM for hCA II. These values were significantly lower, and thus more potent, than those observed for the reference inhibitor Acetazolamide (Ki = 276.3 ± 98.1 nM for hCA I and 117.8 ± 14.1 nM for hCA II). Collectively, these findings highlight the promising potential of methoxylated–pyrazoline benzenesulfonamides, particularly compound 6f, as selective and potent lead candidates for further development in anticancer therapy and carbonic anhydrase (CA) inhibition.

The structure–activity relationship (SAR) of these derivatives highlights the critical role of methoxy group substitution patterns on the aromatic rings attached to the pyrazoline core. Trimethoxy-substituted compounds (6d, 6e, and 6f) exhibited enhanced cytotoxic activity and greater selectivity toward tumor cells compared to the dimethoxy analogues. This SAR indicates that increasing the number of methoxy groups may enhance the ability of the molecules to form hydrogen bonds and interact more efficiently with biological targets, such as CA isoenzymes, thereby contributing to both anticancer potency and selectivity. Additionally, the modifications on the methoxy position (such as shifting from 2,5-dimethoxy to 3,4,5-trimethoxy) significantly influence inhibitory activities against CA I and II enzymes, with specific substitution patterns favoring CA I inhibition more than CA II. These findings highlight how subtle structural modifications can finely tune the biological profile of these compounds.

In 2017, Gul et al[167] reported the synthesis and biological evaluation of pyrazoline benzenesulfonamide derivatives as anticancer agents, investigating their dual functionality as carbonic anhydrase (CA) inhibitors and cytotoxic compounds. Building on this framework, a series of analogous compounds (7a–i) bearing varied aryl (Ar) substituents was synthesized and evaluated for their cytotoxic activities against human oral squamous carcinoma cell lines (Ca9-22, HSC-2, HSC-3, and HSC-4) as well as human normal oral cells (HGF, HPLF, and HPC), with the reference drug 5-Fluorouracil, as shown in Figure 32. The cytotoxic concentration (CC_{50}) values for these derivatives generally ranged from 39.3 to 99.3 μM, indicating moderate cytotoxicity toward cancer cells when compared to the reference drug 5-Fluorouracil (CC_{50} = 13–29 μM) under similar conditions. Among the studied compounds, the 4-chlorophenyl-substituted derivative (7d) exhibited the strongest tumor selectivity (TS1 = 1.5 and TS2 = 2.2) and potency-selectivity expression (PSE = 2.6), indicating favorable discrimination between cancerous and normal oral cells. Additionally, this analog displayed improved selectivity indices compared to its analogs, underscoring its potential as a lead structure for further optimization. Other derivatives, such as those bearing 2,4-dichlorophenyl (7e), 4-fluorophenyl (7f), and 4-nitrophenyl (7h) groups, also demonstrated notable cytotoxic profiles and selectivity indices. All derivatives were evaluated for their inhibitory effects on the cancer-associated carbonic anhydrase isoenzymes hCA IX and hCA XII. Consistent with previous findings, the Ki values for hCA IX inhibition by this series ranged from 53.5 to 923 nM, whereas Ki values for hCA XII ranged from 6.2 to 68.9 nM. Most compounds exhibited pronounced selectivity for hCA XII over hCA IX, indicating a preferential impact on tumor pH regulation through the inhibition of hCA XII. Compound 7i (thiophen-2-yl derivative) emerged as the most potent dual CA inhibitor, with Ki values of 53.5 nM (hCA IX) and 6.2 nM (hCA XII), further validating its promise for targeted cancer therapy interventions.

The structure–activity relationship (SAR) analysis revealed that the substitution pattern on the aryl group at the 5-position of the pyrazoline scaffold has a pronounced impact on both cytotoxic activity and carbonic anhydrase (CA) inhibition. Incorporation of strong electron-withdrawing substituents, such as nitro (7h) or halogens such as chloro (7d), dichloro (7e), fluoro (7f), and bromo (7g), generally led to enhanced cytotoxic activity and improved selectivity against tumor cells when compared to unsubstituted or electron-donating derivatives. Nitro- and halogen-substituted analogs yielded the most significant enhancement in CA IX and XII inhibition, with compound 7h (bearing a nitro group) possessing the lowest Ki values for both isoenzymes in the series, indicating superior inhibitory potency. Furthermore, the replacement of the phenyl ring with a thiophene moiety (7i) significantly increased CA inhibition compared to the

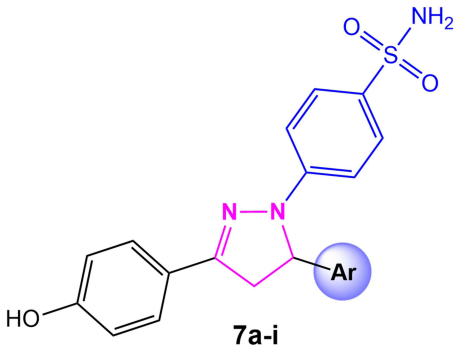

7a-i

	Ar	Ca9-22 CC_{50} (μM)	SI	HSC-2 CC_{50} (μM)	SI	HSC-3 CC_{50} (μM)	SI	HSC-4 CC_{50} (μM)	SI	Mean CC_{50} (μM)	SD CC_{50} (μM)	Mean SI	HGF CC_{50} (μM)	HPLF CC_{50} (μM)	HPC CC_{50} (μM)	Mean CC_{50} (μM)	SD CC_{50} (μM)	TS1	TS2	PSE
a.	phenyl	82.0	1.4	94.7	1.2	81.0	1.5	83.7	1.4	85.3	6.3	1.4	133.3	59.7	161.0	118.0	52.4	1.4	1.6	1.6
b.	4-CH_3-phenyl	57.0	1.7	95.3	1.0	67.3	1.4	70.3	1.4	72.5	16.3	1.4	99.3	42.3	150.0	97.2	53.9	1.3	1.7	1.9
c.	4-OCH_3-phenyl	53.3	2.0	95.3	1.1	71.0	1.5	88.3	1.2	77.0	18.8	1.4	107.7	39.3	167.3	104.8	64.0	1.4	2.0	1.9
d.	4-Cl-phenyl	39.7	2.2	81.7	1.1	57.0	1.5	61.0	1.4	59.8	17.3	1.6	89.0	29.3	144.3	87.6	57.5	1.5	2.2	2.6
e.	2,4-di-Cl-phenyl	44.3	1.7	82.3	0.9	76.0	1.0	54.0	1.4	64.2	18.0	1.3	63.0	34.7	131.0	76.2	49.5	1.2	1.4	2.0
f.	4-F-phenyl	61.7	1.4	84.7	1.0	78.0	1.1	62.3	1.4	71.7	11.5	1.2	64.7	33.0	155.0	84.2	63.3	1.2	1.0	1.7
g.	4-Br-phenyl	55.7	1.4	85.0	0.9	70.3	1.1	61.7	1.3	68.2	12.7	1.2	52.0	34.3	149.3	78.6	61.9	1.2	0.9	1.7
h.	4-NO_2-phenyl	39.3	1.7	76.0	0.9	63.3	1.0	63.7	1.0	60.6	15.3	1.2	42.0	30.0	126.7	66.2	52.7	1.1	1.1	1.9
i.	thiophen-2-yl	99.3	1.2	67.0	1.8	87.3	1.4	93.7	1.3	86.8	14.1	1.4	165.7	26.7	173.3	121.9	82.6	1.4	1.7	1.7
5-Fluorouracil		29.0	>34.5	13.0	>76.9	16.0	>62.5	13.0	>76.9	17.8	7.6	>62.7	>1000	>1000	>1000	>1000	>1000	>56.2	>34.5	>352.2

Figure 32 Chemical structures of pyrazoline benzenesulfonamide derivatives (7a–i) and their cytotoxicity (CC_{50}) against human oral squamous carcinoma cell lines (Ca9-22, HSC-2, HSC-3, HSC-4) and normal oral cells (HGF, HPLF, HPC). 5-Fluorouracil was used as a reference drug.

parent compound, underscoring the positive effect of bioisosteric substitution on biological activity. These SAR findings collectively demonstrate that both cytotoxicity and selectivity toward tumor-associated CA isoenzymes can be efficiently modulated through strategic aryl substitution, emphasizing the significance of electron-withdrawing groups and heterocyclic replacements for the design of potent and selective antitumor agents.

In the same year, Gul et al[121] synthesized and evaluated a series of novel pyrazoline benzenesulfonamide derivatives (8a–g) for cytotoxic activity against human oral squamous carcinoma cell lines (Ca9–22, HSC-2, HSC-3, HSC-4) as well as normal oral cells (HGF, HPLF, HPC), with the reference drug 5-Fluorouracil (5-FU), as shown in Figure 33. All compounds demonstrated cytotoxicity within the micromolar concentration range toward carcinoma cells, and certain analogs, specifically 8f (4-bromophenyl), 8e (4-chlorophenyl), and 8b (4-methylphenyl), exhibited markedly enhanced potency and selectivity, as reflected in their higher potency selectivity expression (PSE) values, compared to other analogs and 5-FU in Ca9–22 assays. The selectivity indices (TS1, TS2) and PSE values emphasize their dual functionality in achieving potent tumor cell toxicity while maintaining favorable selectivity over normal oral cell lines. Additionally, these compounds were reported to act as effective inhibitors for human carbonic anhydrase (hCA) isoenzymes, hCA I and hCA II, with IC_{50} values in the low nanomolar range, outperforming the standard inhibitor Acetazolamide. This dual inhibitory profile suggests that the anticancer activity of these pyrazoline benzenesulfonamide derivatives may partly stem from the perturbation of intracellular pH regulation, a crucial element in tumor cell proliferation and survival.

The structure–activity relationship (SAR) analysis indicates that the electronic nature and position of the substituents on the aromatic ring at the 3-position of the pyrazoline core critically influence both cytotoxic and enzyme-inhibitory activities. Derivatives bearing electron-withdrawing groups (such as halogens like Cl, Br, and F) or groups capable of participating in hydrogen bonding (such as methoxy and methyl) generally exhibit enhanced cytotoxic potency and tumor selectivity compared to non-substituted analogues. Notably, the introduction of bromine (8f) or chlorine (8e) resulted in the highest selectivity and potency values. Replacing the phenyl ring with a bioisosteric thiophene moiety (8g) further increased both cytotoxicity and selectivity parameters. A positive correlation was also found between the lipophilicity (logP) and the potency-selectivity expression (PSE) of the derivatives, suggesting that increased hydrophobic character

https://doi.org/10.2147/DDDT.S562109

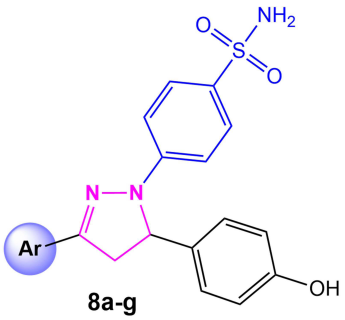

8a-g

	Ar	Ca9-22 CC_{50} (μM)	SD CC_{50} (μM)	SI	HSC-2 CC_{50} (μM)	SD CC_{50} (μM)	SI	HSC-3 CC_{50} (μM)	SD CC_{50} (μM)	SI	HSC-4 CC_{50} (μM)	SD CC_{50} (μM)	SI	Mean CC_{50} (μM)	SD CC_{50} (μM)	HGF CC_{50} (μM)	SD CC_{50} (μM)	HPLF CC_{50} (μM)	SD CC_{50} (μM)	HPC CC_{50} (μM)	SD CC_{50} (μM)	Mean CC_{50} (μM)	SD CC_{50} (μM)	TS1	TS2	PSE
a.	phenyl	42.0	5.0	1.8	67.0	12.2	1.1	66.3	11.9	1.1	50.3	7.1	1.5	56.4	12.3	85.0	13.5	54.3	5.0	88.3	6.8	75.9	18.7	1.3	2.0	2.3
b.	4-CH_3-phenyl	25.7	4.2	1.7	33.3	2.1	1.3	39.7	0.6	1.1	31.7	2.1	1.4	32.6	5.8	43.7	4.0	39.3	4.2	49.7	3.8	44.2	5.2	1.4	1.7	4.2
c.	4-OCH_3-phenyl	37.7	1.5	1.3	65.3	5.7	0.8	47.0	8.7	1.1	40.7	2.1	1.2	47.7	12.4	47.3	1.5	44.0	2.0	61.0	12.5	50.8	9.0	1.1	1.3	2.2
d.	4-F-phenyl	36.3	2.5	1.6	46.3	10.1	1.3	43.3	5.9	1.4	39.3	4.7	1.5	41.3	4.4	66.7	3.5	43.0	4.6	67.7	0.6	59.1	14.0	1.4	1.8	3.5
e.	4-Cl-phenyl	22.3	1.5	2.0	39.0	2.6	1.1	38.3	2.5	1.2	31.3	4.5	1.4	32.8	7.8	44.0	3.6	38.3	3.8	50.7	7.4	44.3	6.2	1.4	2.0	4.1
f.	4-Br-phenyl	20.7	0.6	1.7	37.7	11.6	0.9	34.7	2.9	1.0	25.7	6.1	1.4	29.7	7.9	34.7	4.2	29.7	0.6	39.7	8.1	34.7	5.0	1.2	1.7	3.9
g.	thiophen-2-yl	45.7	3.1	1.8	55.0	18.5	1.5	61.3	3.1	1.4	55.3	4.9	1.5	54.3	6.5	88.3	6.8	73.0	30.3	87.3	6.7	82.9	8.6	1.5	1.9	2.8
5-Fluorouracil		100	4.4	>167.3	45.7	19.6	>16.1	27.3	10.3	>71.5	17.3	12.2	>60.3	47.6	36.9	>1000	0.0	208.3	72.2	>1000	0.0	>736	457.1	>15.5	>10	>32.6

Figure 33 Chemical structures of pyrazoline benzenesulfonamide derivatives (8a–g) and their cytotoxicity (CC_{50}) against human oral squamous carcinoma cell lines (Ca9-22, HSC-2, HSC-3, HSC-4) and normal oral cells (HGF, HPLF, HPC). 5-Fluorouracil was used as a reference drug.

may enhance tumor selectivity and efficacy. These findings underscore that strategic modification of aromatic substituents can effectively fine-tune both the anticancer and carbonic anhydrase inhibitory activities of this compound class.

In 2018, Gul et al [169] reported that pyrazoline benzenesulfonamide derivatives possess significant potential as anticancer agents, particularly through the selective inhibition of cancer-associated carbonic anhydrases (CAs), with marked activity against hCA IX and hCA XII. In this research, a series of derivatives was synthesized and evaluated for cytotoxicity against oral squamous cell carcinoma lines (Ca9-22, HSC-2), as well as normal human oral cells (HGF, HPLF), employing 5-Fluorouracil as a standard reference, as shown in Figure 34. All compounds demonstrated notable anticancer effectiveness, with CC_{50} values ranging from 6.3 to 24.7 μM for Ca9-22 cells and 7.3 to 42.6 μM for HSC-2 cells. Notably, compounds 9p and 9r, featuring a thiophene group and trimethoxyphenyl substituent, exhibited the most promising cytotoxic profiles, displaying pronounced activity against carcinoma cells and substantial selectivity. Compound 9p achieved tumor selectivity (TS) values of 9.5 (TS1) and 10.5 (TS2), while compound 9r showed TS values of 8.9 (TS1) and 10.0 (TS2). Furthermore, their potency-selectivity expression (PSE) values were the highest among the tested molecules, with PSE values of 141 for compound 9p and 54.5 for compound 9r, significantly surpassing those of 5-Fluorouracil. These findings underscore the promise of these pyrazoline benzenesulfonamide derivatives as selective, potent anticancer agents, underscoring the relevance of targeting Cas, especially hCA IX and XII, which are frequently overexpressed in malignancies and are crucial for regulating tumor microenvironment pH and supporting tumor survival and progression.

The structure–activity relationship (SAR) analysis demonstrates that both the nature and the spatial arrangement of substituents on the aromatic ring significantly influence the cytotoxic activity and selectivity of the synthesized pyrazoline benzenesulfonamide derivatives. Notably, derivatives incorporating thiophene bioisosteres as replacements for phenyl moieties tend to exhibit superior cytotoxic effects and elevated tumor selectivity indices, as reflected by their lower CC_{50} values against cancer cell lines and higher selectivity ratios (TS1, TS2, PSE). Furthermore, compounds bearing either 2,3,4-trimethoxy or 3,4,5-trimethoxy substitutions on the aromatic ring adjacent to the pyrazoline core display enhanced potency, as indicated by improved CC_{50} data across Ca9-22 and HSC-2 cell lines. The introduction of electron-withdrawing (halogen) substituents, such as fluoro, chloro, and bromo groups, also appears to enhance selectivity toward malignant cells, as observed in the increased TS and PSE metrics. Most notably, compound 9r, featuring both thiophene moiety and 3,4,5-trimethoxyphenyl substituent, stood out due to its prominent selectivity and

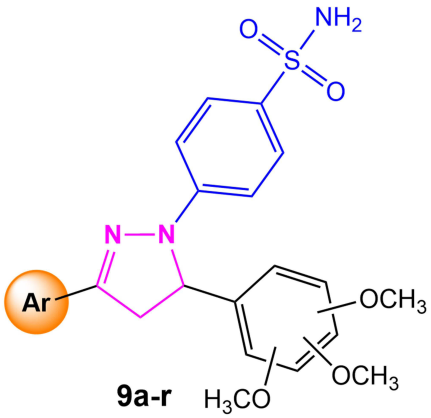

9a-r

	Ar	Positions of the methoxy groups	**Ca9-22** CC_{50} (μM)	SD CC_{50} (μM)	SI	**HSC-2** CC_{50} (μM)	SD CC_{50} (μM)	SI	Mean CC_{50} (μM)	Mean SI	**HGF** CC_{50} (μM)	SD CC_{50} (μM)	**HPLF** CC_{50} (μM)	SD CC_{50} (μM)	Mean CC_{50} (μM)	TS1	TS2	PSE
a.	phenyl	2,3,4-tri-OCH_3	11.9	1.5	1.9	19.5	1.9	1.1	15.7	1.5	27.3	12.4	17.4	1.0	22.4	1.4	2.3	9.5
b.	phenyl	2,4,5-tri-OCH_3	24.7	3.4	0.6	25.0	11.1	0.6	24.9	0.6	17.3	10.4	13.0	2.4	15.1	0.6	0.7	2.4
c.	phenyl	3,4,5-tri-OCH_3	13.7	1.5	2.5	18.1	1.8	1.9	15.9	2.2	38.9	2.1	29.8	6.3	34.4	2.2	2.8	13.8
d.	4-F-phenyl	2,3,4-tri-OCH_3	12.6	0.7	2.0	19.2	1.3	1.3	15.9	1.6	33.2	7.4	16.1	0.8	24.6	1.6	2.6	10.1
e.	4-F-phenyl	2,4,5-tri-OCH_3	19.5	1.5	1.5	42.6	10.7	0.7	31.0	1.1	17.9	4.1	41.3	23.8	29.6	1.0	0.9	3.5
f.	4-F-phenyl	3,4,5-tri-OCH_3	12.0	1.6	1.5	20.4	1.6	0.9	16.2	1.2	17.6	2.3	18.6	1.9	18.1	1.1	1.5	7.4
g.	4-Cl-phenyl	2,3,4-tri-OCH_3	8.0	0.4	1.4	15.2	0.9	0.8	11.6	1.1	10.2	2.2	12.7	1.3	11.5	1.0	1.3	9.5
h.	4-Cl-phenyl	2,4,5-tri-OCH_3	10.3	0.6	1.0	25.4	5.9	0.4	17.9	0.7	9.5	0.7	10.0	0.4	9.8	0.5	0.9	3.9
i.	4-Cl-phenyl	3,4,5-tri-OCH_3	8.3	0.6	1.4	18.1	3.1	0.6	13.2	1.0	12.0	4.3	10.8	0.9	11.4	0.9	1.5	7.6
j.	4-Br-phenyl	2,3,4-tri-OCH_3	8.2	0.7	1.5	15.9	2.5	0.8	12.0	1.1	9.2	1.4	14.9	0.9	12.1	1.0	1.1	9.2
k.	4-Br-phenyl	2,4,5-tri-OCH_3	10.3	0.8	1.0	21.6	1.0	0.5	16.0	0.7	9.2	1.5	11.2	0.4	10.2	0.6	0.9	4.4
l.	4-Br-phenyl	3,4,5-tri-OCH_3	9.0	0.5	1.5	23.6	2.0	0.6	16.3	1.0	14.0	2.5	12.8	1.4	13.4	0.8	1.6	6.1
m.	4-CF_3-phenyl	2,3,4-tri-OCH_3	9.3	0.4	1.5	16.4	1.1	0.8	12.8	1.2	16.0	1.0	11.8	1.5	13.9	1.1	1.7	9.4
n.	4-CF_3-phenyl	2,4,5-tri-OCH_3	6.3	0.8	2.1	15.4	2.9	0.9	10.8	1.5	16.6	5.3	10.2	0.5	13.4	1.2	2.6	13.9
o.	4-CF_3-phenyl	3,4,5-tri-OCH_3	8.3	0.5	2.1	17.6	2.1	1.0	12.9	1.5	20.9	1.9	13.9	3.3	17.4	1.3	2.5	11.6
p.	thiophen-2-yl	2,3,4-tri-OCH_3	6.3	1.0	10.3	7.3	2.2	8.8	6.8	9.6	66.2	41.0	63.1	70.9	64.7	9.5	10.5	141
q.	thiophen-2-yl	2,4,5-tri-OCH_3	9.3	2.6	1.9	23.1	4.5	0.8	16.2	1.3	18.3	5.7	16.8	3.8	17.5	1.1	2.0	8
r.	thiophen-2-yl	3,4,5-tri-OCH_3	14.3	1.6	10.2	18.7	1.6	7.8	16.5	9.0	143.7	12.2	149.0	18.1	146.3	8.9	10.0	54.5
5-Fluorouracil			8.7	2.3	62.7	4.8	2.4	114.1	6.8	88.4	1000	0.0	95.0	17.5	547.5	80.9	114.5	1300

Figure 34 Chemical structures of pyrazoline benzenesulfonamide derivatives (9a–r) and their cytotoxicity (CC_{50}) against human oral squamous carcinoma cell lines (Ca9-22, HSC-2) and normal oral cells (HGF, HPLF). 5-Fluorouracil was used as a reference drug.

cytotoxic activity against cancer cell lines, underscoring its potential as a lead candidate for further development targeting cancer-associated human carbonic anhydrase isoenzymes, particularly hCA XII.

Three pyrazoline benzenesulfonamide derivatives (10a–c) were synthesized and evaluated for cytotoxic activity against both cancer and normal cell lines, as shown in Figure 35. Gul et al[149] reported that compounds 10a and 10b exhibited significant cytotoxic effects toward HCC1937 breast cancer cells, with IC_{50} values of 22.39 ± 1.76 μM and 16.9 ± 1.53 μM, respectively. Notably, compound 10b also demonstrated enhanced cytotoxicity against MCF-7 breast and A549 lung cancer cell lines, as indicated with IC_{50} values of 17.65 ± 2.13 μM and 23.1 ± 2.43 μM, respectively, while maintaining low toxicity to normal cells (MRC5 and Vero). In contrast, compound 10c did not exhibit measurable cytotoxic effects at the tested concentrations in any of the cell lines. Mechanistically, these compounds induce apoptosis and autophagy in cancer cells, as evidenced by the cleavage of PARP, activation of caspases, increased LC3 levels, and reduced p62 protein levels. These pathways are crucial for the efficient clearance of cancer cells. Furthermore, these derivatives display potent inhibitory activity against tumor-associated human carbonic anhydrase isoforms IX and XII, with inhibition constants (Ki) values in the nanomolar range (hCA I: 47.9–170.4 nM, hCA II: 4.3–6.4 nM, hCA IX: 20.7–28.1 nM, hCA XII: 4.5–9.3 nM). For reference, Acetazolamide exhibited Ki values of 250 nM (hCA I), 12.1 nM (hCA II), 25.8 nM (hCA IX), and 5.7 nM (hCA XII), highlighting the superior potency of these compounds for CA inhibition.

The structure–activity relationship (SAR) analysis reveals that variations in the methoxy substitution pattern on the aromatic ring, specifically the number and positions of methoxy groups, have a significant impact on both cytotoxic and enzyme inhibitory effects. Notably, compound 10b, containing a 2,4-dimethoxyphenyl moiety, displayed greater cytotoxicity (eg, toward HCC1937 and MCF-7 cells) and hCA I inhibition compared to the monosubstituted 4-methoxy

https://doi.org/10.2147/DDDT.S562109

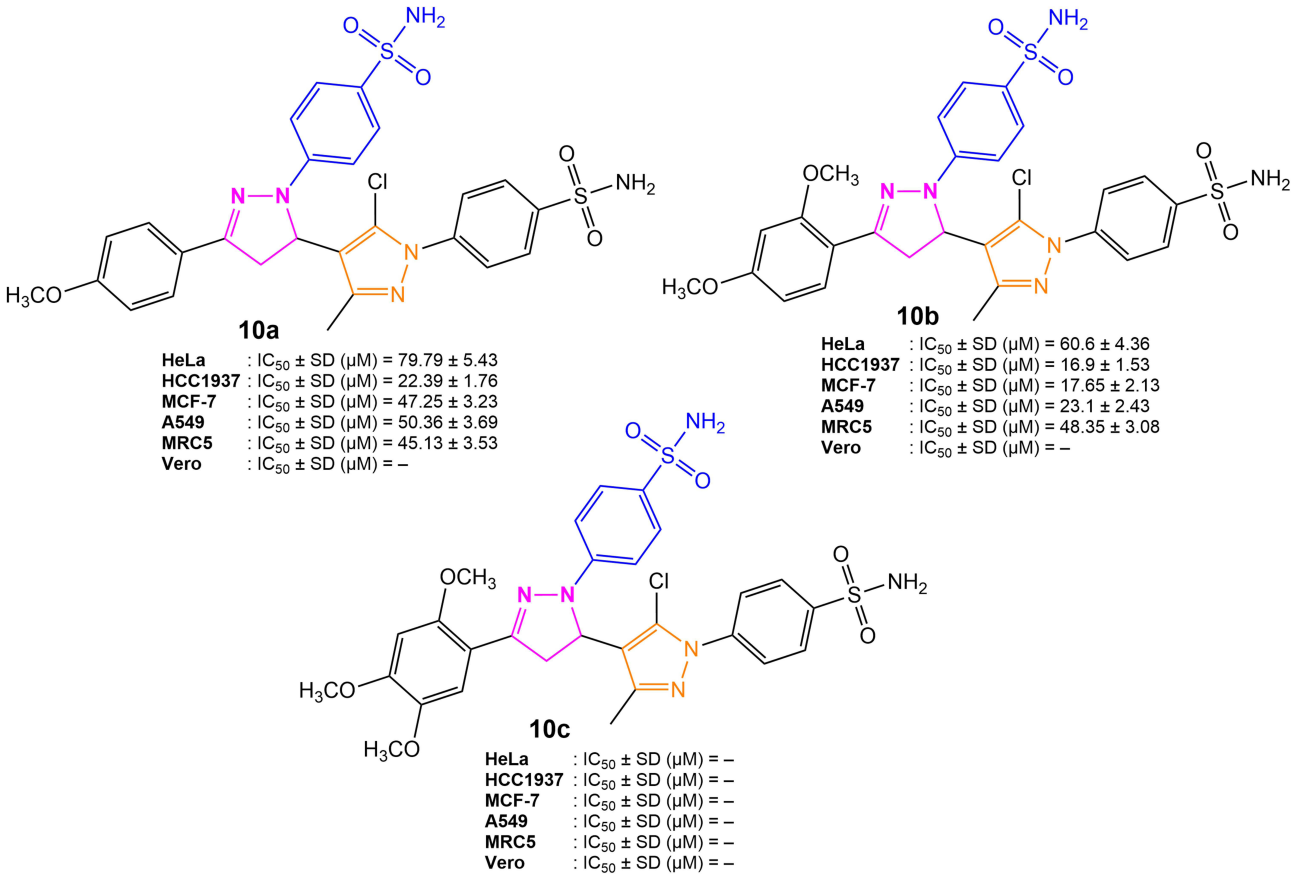

Figure 35 Chemical structures of pyrazoline benzenesulfonamide derivatives (10a–c) and their cytotoxic activities (IC_{50}) against human cancer cell lines (HeLa, HCC1937, MCF-7, A549) and normal cell lines (MRC5, Vero).

analog (10a). The dual presence of sulfonamide functionalities within these molecules was essential for achieving robust inhibition of hCA II, as well as for pronounced activity against the tumor-associated hCA IX and XII isoforms. In terms of selectivity, both 10a and 10b exhibited a favorable cytotoxic profile against cancer cells compared to normal cells (MRC5 and Vero), suggesting that their intermediate lipophilicity (logP, approximately 3.1–3.2) facilitates effective membrane permeability while minimizing toxicity in non-cancerous tissues. In contrast, the introduction of an additional methoxy group (trimethoxyphenyl, compound 10c) did not yield further cytotoxic benefit, underscoring that both the quantity and spatial arrangement of substituents are pivotal in fine-tuning the biological activities observed for this class of compounds.

In 2019, Yan et al[142] reported the synthesis of novel pyrazoline benzenesulfonamide derivatives as potential anticancer agents, attributed to their selective inhibitory potency against cyclooxygenase-2 (COX-2). This enzyme is markedly elevated in various malignancies. Specifically, two structural series were generated, incorporating either a benzodioxole (11a–j) or a benzodioxane scaffold (11k–z), as shown in Figure 36. These compounds were evaluated for both COX-2 enzyme inhibition and antiproliferative activity against a panel of human cancer cell lines, namely SW620 (colorectal), MCF-7 (breast), HeLa (cervical), A549 (lung), and HepG2 (liver), along with cytotoxicity assessments in normal colon cells (NCM460). The derivatives demonstrated substantial anticancer activity, with IC_{50} values ranging from 0.86 ± 0.02 to 7.99 ± 0.56 μM for SW620 cells, 2.99 ± 0.13 to 12.68 ± 0.89 μM for MCF-7 cells, 2.98 ± 0.17 to 14.61 ± 0.96 μM for HeLa cells, 1.94 ± 0.06 to 9.42 ± 0.74 μM for A549 cells and 2.96 ± 0.14 to 18.22 ± 1.15 μM for HepG2 cells. Notably, compound 11b exhibited the most pronounced cytotoxicity against SW620 cells (IC_{50} = 0.86 ± 0.02 μM), with minimal toxicity to NCM460 cells (CC_{50} = 134.33 ± 7.85 μM), thereby highlighting its selectivity towards cancer cells versus normal cells. Moreover, compound 11b was shown to surpass celecoxib in both COX-2 inhibition and tumor suppression in SW620 xenograft models, attributed mechanistically to induction of apoptosis,

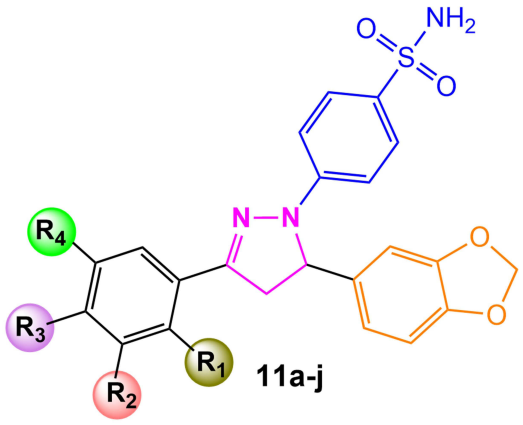

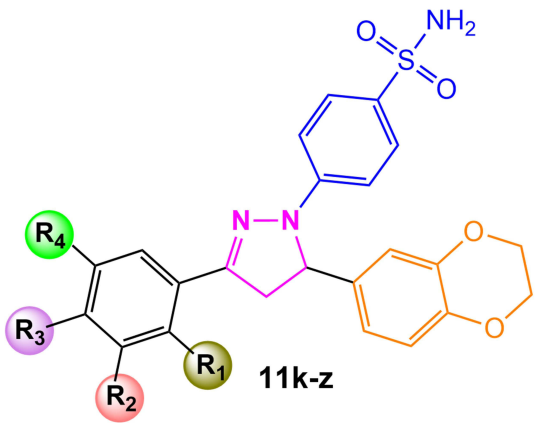

	R_1	R_2	R_3	R_4	SW620 IC_{50} ± SD (μM)	MCF-7 IC_{50} ± SD (μM)	HeLa IC_{50} ± SD (μM)	A549 IC_{50} ± SD (μM)	HepG2 IC_{50} ± SD (μM)	NCM460 CC_{50} ± SD (μM)
a.	H	H	H	H	3.38 ± 0.27	5.77 ± 0.39	6.32 ± 0.55	3.54 ± 0.19	7.64 ± 0.57	88.62 ± 3.96
b.	H	H	CH_3	H	0.86 ± 0.02	2.99 ± 0.13	2.98 ± 0.17	1.94 ± 0.06	2.96 ± 0.14	134.33 ± 7.85
c.	H	H	OCH_2CH_3	H	5.07 ± 0.26	8.31 ± 0.67	9.37 ± 0.90	6.93 ± 0.17	13.74 ± 0.93	159.38 ± 11.36
d.	H	H	I	H	3.04 ± 0.17	5.26 ± 0.42	5.71 ± 0.47	2.86 ± 0.06	6.42 ± 0.25	74.47 ± 5.23
e.	H	CH_3	H	H	3.88 ± 0.36	6.52 ± 0.46	7.22 ± 0.65	4.54 ± 0.18	9.44 ± 0.74	109.54 ± 7.71
f.	H	CH_3	CH_3	H	4.34 ± 0.33	7.21 ± 0.62	8.05 ± 0.77	5.49 ± 0.44	11.15 ± 1.03	129.34 ± 8.96
g.	H	OCH_3	H	H	7.99 ± 0.56	12.68 ± 0.89	14.61 ± 0.96	9.42 ± 0.74	18.22 ± 1.15	211.35 ± 18.15
h.	H	F	H	H	3.24 ± 0.18	5.56 ± 0.38	6.07 ± 0.41	3.26 ± 0.29	7.14 ± 0.66	82.82 ± 7.59
i.	CH_3	H	CH_3	H	4.96 ± 0.38	8.14 ± 0.69	9.16 ± 0.37	6.71 ± 0.57	13.32 ± 0.89	154.51 ± 12.66
j.	F	H	H	H	4.54 ± 0.29	7.51 ± 0.57	8.41 ± 0.29	5.86 ± 0.36	11.82 ± 0.96	137.11 ± 12.74
k.	H	H	H	H	4.56 ± 0.14	7.54 ± 0.42	8.44 ± 0.48	5.92 ± 0.31	11.88 ± 0.91	137.88 ± 10.96
l.	H	H	CH_3	H	2.35 ± 0.11	4.22 ± 0.16	4.46 ± 0.36	2.58 ± 0.18	5.92 ± 0.39	68.67 ± 5.28
m.	H	H	OCH_3	H	3.88 ± 0.37	6.52 ± 0.33	7.22 ± 0.19	4.54 ± 0.29	9.44 ± 0.77	109.54 ± 7.42
n.	H	H	OCH_2CH_3	H	6.12 ± 0.49	9.88 ± 0.86	11.25 ± 0.86	6.81 ± 0.55	13.52 ± 0.59	156.83 ± 9.98
o.	H	H	F	H	3.83 ± 0.27	6.44 ± 0.37	7.12 ± 0.69	4.43 ± 0.33	9.24 ± 0.74	107.18 ± 9.21
p.	H	H	Cl	H	3.53 ± 0.16	5.99 ± 0.38	6.58 ± 0.49	3.83 ± 0.26	8.16 ± 0.63	94.65 ± 3.65
q.	H	H	Br	H	3.18 ± 0.19	5.47 ± 0.29	5.96 ± 0.39	3.14 ± 0.25	6.92 ± 0.28	80.27 ± 8.01
r.	H	H	I	H	2.17 ± 0.05	3.95 ± 0.18	4.14 ± 0.21	3.12 ± 0.08	3.28 ± 0.17	38.04 ± 1.19
s.	H	CH_3	CH_3	H	4.54 ± 0.31	7.51 ± 0.47	8.41 ± 0.17	5.86 ± 0.47	11.82 ± 0.59	137.11 ± 3.98
t.	H	CH_3	F	H	3.74 ± 0.12	6.31 ± 0.39	6.97 ± 0.51	4.26 ± 0.19	8.94 ± 0.67	103.74 ± 4.74
u.	H	OCH_3	H	H	6.63 ± 0.42	10.64 ± 0.67	12.16 ± 0.85	7.81 ± 0.37	15.32 ± 1.09	177.71 ± 10.69
v.	H	F	H	H	4.84 ± 0.27	7.96 ± 0.55	8.95 ± 0.39	6.47 ± 0.29	12.92 ± 0.99	149.87 ± 6.94
w.	H	F	H	F	3.78 ± 0.22	6.37 ± 0.39	7.04 ± 0.47	4.34 ± 0.28	9.08 ± 0.71	105.32 ± 8.87
x.	H	Cl	Cl	H	4.46 ± 0.19	7.39 ± 0.55	8.26 ± 0.65	5.75 ± 0.44	11.52 ± 0.92	133.63 ± 9.48
y.	F	H	H	H	5.51 ± 0.37	8.96 ± 0.74	10.15 ± 0.72	7.83 ± 0.58	15.37 ± 0.84	178.29 ± 12.69
z.	F	H	F	H	4.48 ± 0.24	7.42 ± 0.63	8.34 ± 0.69	5.78 ± 0.16	11.68 ± 0.86	135.48 ± 9.63
Celecoxib					1.29 ± 0.04	2.63 ± 0.09	2.56 ± 0.15	1.93 ± 0.09	3.12 ± 0.27	136.19 ± 9.86

Figure 36 Chemical structures of pyrazoline benzenesulfonamide derivatives (11a–z) and their cytotoxic activities (IC_{50}) against SW620, MCF-7, HeLa, A549, and HepG2 human cancer cell lines, as well as cytotoxicity (CC_{50}) in NCM460 normal colon cell lines. Celecoxib was used as a reference drug.

suppression of cell adhesion, and reduced metastasis potential. Collectively, these findings position pyrazoline benzenesulfonamide hybrids, particularly 11b, as a promising scaffold for further development of safe and effective COX-2-targeted anticancer therapies.

The structure–activity relationship (SAR) analysis revealed that multiple structural elements are crucial for optimizing both COX-2 selectivity and anticancer efficacy among pyrazoline benzenesulfonamide derivatives. Specifically, the integration of a benzo–oxygen heterocycle with the pyrazoline scaffold, as well as the para-sulfonamide group on the phenyl ring, proved essential for robust COX-2 inhibition. Derivatives bearing a benzodioxole moiety (compounds 11a–j) consistently showed more potent inhibition and antiproliferative effects compared to their benzodioxane analogues (11k–z), underscoring the superior target affinity afforded by the former motif. Substitution at the pyrazoline aryl position further modulated biological activity; the p-tolyl group, exemplified by compound 11b, markedly enhanced both potency and selectivity. Similarly, the incorporation of a 4-iodophenyl group (compound 11d) also resulted in improved COX-2 inhibition and cytotoxicity against SW620 cells. These findings suggest that strategic modification of the pyrazoline and aryl substituents is crucial for optimizing the therapeutic index in this chemotype.

https://doi.org/10.2147/DDDT.S562109

Molecular docking simulations were performed using the crystal structure of COX-2 (PDB ID: 3LN1) to explore the binding modes and affinities between the synthesized dihydropyrazole derivatives and the COX-2 active site. The calculated CDOCKER interaction energies ranged from –45.96 to –33.41 kcal/mol, with compound 11b displaying the most favorable binding score (–45.96 kcal/mol), surpassing that of celecoxib (–42.57 kcal/mol). Docking visualizations revealed that 11b formed nine hydrogen bonds and fourteen π-π interactions with key residues within the COX-2 active site, including Arg106, Ser339, Arg499, Gln178, and Leu338; additionally, it established strong contacts via His75, Phe504, and Val102, which interact with the sulfonamide and benzodioxole fragments. A linear correlation was observed between binding energies and experimental COX-2 inhibition, validating the design rationale. Collectively, these findings position compound 11b as a promising COX-2-targeted anticancer candidate, with both robust in vitro efficacy and strong computational support for its mechanism of action.

Another series of pyrazoline benzenesulfonamide derivatives (12a–h) has been investigated for their biological properties, particularly as enzyme inhibitors and potential anticancer agents. Ozgun et al[160] reported that a series of compounds was synthesized and evaluated for cytotoxic effects against human oral squamous cell carcinoma lines (Ca9-22, HSC-2, HSC-3, HSC-4) and human normal oral cells (HGF, HPLF, HPC), with the standard drugs 5-Fluorouracil and Melphalan, as shown in Figure 37. Most derivatives exhibited moderate cytotoxicity against cancer cell lines, with CC_{50} values ranging from 15 to 200 μM, indicating low to moderate anticancer potency compared to standard drugs such as 5-Fluorouracil (CC_{50} = 24.4–72.7 μM) and Melphalan (CC_{50} = 10.3–40.3 μM). Selectivity toward malignant cells was limited; only derivatives bearing a 3,4-dimethoxyphenyl group, notably compounds 12f and 12b, showed slightly improved tumor selectivity (TS1 = 1.3–1.4). Overall, the cytotoxic profiles suggested that these compounds may not be optimal for direct anticancer applications. However, the derivatives demonstrated potent enzyme inhibition at nanomolar concentrations against human carbonic anhydrase isoforms (hCA I and II) with inhibition constants (Ki)

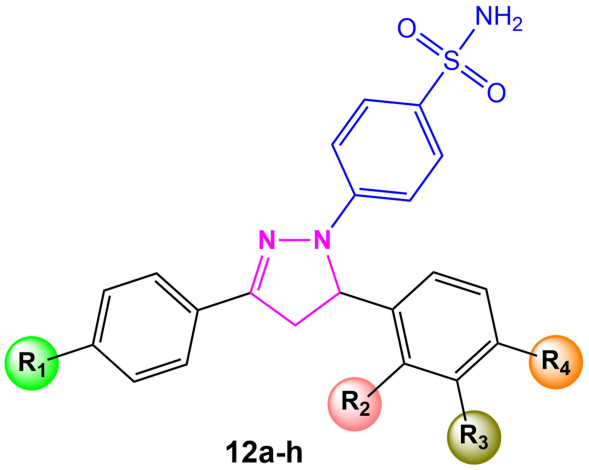

12a-h

	R_1	R_2	R_3	R_4	**Ca9-22** CC_{50} (μM)	**HSC-2** CC_{50} (μM)	**HSC-3** CC_{50} (μM)	**HSC-4** CC_{50} (μM)	Mean CC_{50} (μM)	SD CC_{50} (μM)	**HGF** CC_{50} (μM)	**HPLF** CC_{50} (μM)	**HPC** CC_{50} (μM)	Mean CC_{50} (μM)	SD CC_{50} (μM)	TS1	TS2
a.	H	OCH_3	H	OCH_3	27	41	41	35	36.0	6.6	21	41	29	33.7	6.4	0.9	1.1
b.	H	H	OCH_3	OCH_3	21	200	200	44	116.3	97.2	29	112	28	56.3	48.2	0.5	1.4
c.	F	OCH_3	H	OCH_3	65	42	41	35	45.8	13.2	37	37	35	36.3	1.2	0.8	0.6
d.	F	H	OCH_3	OCH_3	24	152	177	33	96.5	79.3	25	139	80	81.3	57.0	0.8	1.0
e.	Cl	OCH_3	H	OCH_3	19	22	23	23	21.8	1.9	19	23	21	21.0	2.0	1.0	1.0
f.	Cl	H	OCH_3	OCH_3	16	21	25	18	20.0	3.9	22	41	17	26.7	12.7	1.3	1.4
g.	Br	OCH_3	H	OCH_3	18	20	20	15	18.3	2.4	18	21	19	19.3	1.5	1.1	1.0
h.	Br	H	OCH_3	OCH_3	17	39	24	17	24.3	10.4	18	20	19	19.0	1.0	0.8	1.1
5-Fluorouracil					55.1	24.4	72.7	38.9	47.8	–	>200	>200	>200	>200	–	>4.2	>3.6
Melphalan					40.3	13.6	11	10.3	18.8	–	>200	151.0	>175.5	>175.2	–	>9.3	>4.9

Figure 37 Chemical structures of pyrazoline benzenesulfonamide derivatives (12a–h) and their cytotoxicity (CC_{50}) against human oral squamous carcinoma cell lines (Ca9-22, HSC-2, HSC-3, HSC-4) and normal oral cells (HGF, HPLF, HPC). 5-Fluorouracil and melphalan were used as reference drugs.

values ranging from 27.9 ± 3.2 to 74.3 ± 28.9 nM for hCA I and 27.4 ± 1.4 to 54.5 ± 11.6 nM for hCA II. In comparison, the reference drug Acetazolamide exhibited Ki values of 164.7 ± 14.1 nM (hCA I) and 132.6 ± 13.1 nM (hCA II). Additionally, the compounds showed strong inhibition of acetylcholinesterase with Ki values ranging from 37.7 ± 14.4 to 89.2 ± 30.2 nM, compared to the reference drug Tacrine (Ki = 282.5 ± 55.4 nM). These findings support the potential of these derivatives as enzyme-targeted agents, with possible value in adjunctive cancer therapy or the development of enzyme inhibitors with added bioactive properties.

The structure–activity relationship (SAR) analysis revealed that both the electronic properties and positional orientation of the substituents on the aromatic rings were pivotal determinants of bioactivity among the compounds 12a–h. The incorporation of halogen atoms, such as fluorine, chlorine, or bromine at the R_1 position typically resulted in enhanced inhibitory potency against both carbonic anhydrase and acetylcholinesterase, with a trend also observed for the placement of a methoxy group. Notably, derivatives containing a 3,4-dimethoxyphenyl substitution, particularly those also bearing halogen atoms (eg, compounds 12f and 12g), recorded the lowest CC_{50} values and strongest enzyme inhibition, underscoring the additive effects of electron-donating and electron-withdrawing groups. The brominated analogue (12g) exhibited the highest acetylcholinesterase inhibition among the series, indicating a favorable synergy between bromine and the methoxy substituents. Despite these enhancements in enzyme inhibition, neither halogenation nor increased methoxylation substantially improved cytotoxic potency or selectivity towards tumor cells, as TS indices remained low throughout the group. Overall, these data underscore the significance of both electronic and steric influences imposed by aromatic substituents, demonstrating that strategic modification of these groups can be leveraged to optimize enzyme inhibition, albeit with only modest impact on anticancer selectivity within this chemotype.

In 2021, Thach et al[120] reported the synthesis and anticancer evaluation of a series of pyrazoline benzenesulfonamide derivatives containing substituted-diphenyl (13a–s) and styryl (13t–z) moieties. These compounds were screened for their cytotoxic effects against human cervical carcinoma (Hep-2C) and human lung carcinoma (A549) cell lines, with additional assessment of selectivity using the non-cancerous Vero cell line and the reference drug Ellipticine, as shown in Figure 38. The cytotoxicity and selectivity profiles were quantified by percentage cell survival (CS%) and half-maximal inhibitory concentration (IC_{50}) values. Notably, several compounds demonstrated pronounced antiproliferative activity. Specifically, derivatives such as 13f, 13j, 13L, 13m, and 13p exhibited potent cytotoxicity towards Hep-2C cells, with IC_{50} values ranging from 16.03 ± 1.63 to 22.75 ± 0.19 μM. Furthermore, these compounds also exhibited strong cytotoxic effects against A549 cells, with IC_{50} values ranging from 18.64 ± 1.02 to 20.66 ± 2.09 μM. Crucially, these active analogues maintained relatively low cytotoxicity against Vero cells, with several analogues exhibiting IC_{50} values above 10 μM, indicating a degree of selectivity for cancer cells over normal cells. This selectivity profile highlights their potential as lead compounds for further development as chemotherapeutic agents with a favorable therapeutic index, meriting additional investigation for translational relevance and safety optimization.

The structure–activity relationship (SAR) analysis reveals that the nature and position of substituents on the aromatic rings significantly influence the anticancer activity of these pyrazoline benzenesulfonamide derivatives. As shown in Figure 38, the incorporation of electron-donating groups such as methyl (–CH_3), methoxy (–OCH_3), and hydroxyl (–OH) in the para or meta positions tends to enhance cytotoxic potency against both Hep-2C and A549 cancer cell lines. For example, compound 13f (4-CH_3, 3-OH) and 13p (4-Cl, 3-OH) exhibited superior activity, while compounds 13j (4-OCH_3, 4-CH_3), 13L (4-OCH_3, 2,3-di-OCH_3), and 13m (4-OCH_3, 2-Cl) bearing methoxy and/or chloro substituents also displayed pronounced cytotoxic effects against Hep-2C cell lines. The enhanced activity associated with these substituents may be attributed to their ability to alter the electronic distribution and steric configuration of the molecules, thereby promoting more effective interactions with biological targets. Conversely, derivatives featuring bulky styryl groups (13t–z) consistently lacked significant cytotoxicity, suggesting that increased steric hindrance at this position attenuates antiproliferative efficacy. Collectively, these SAR findings underscore the importance of judiciously tailoring aromatic substituents within the scaffold to optimize both anticancer potency and selectivity for potential chemotherapeutic development.

In the same year, Tuğrak et al[127] reported the synthesis of a series of novel pyrazoline benzenesulfonamide derivatives, incorporating a benzodioxole moiety (14a–j) and diverse methoxy group substitutions on the aromatic ring. They evaluated their cytotoxic effects against human oral squamous cell carcinoma cell lines (Ca9-22, HSC-2,

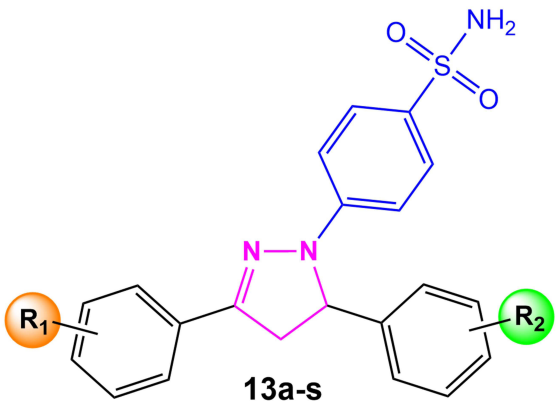

13a-s

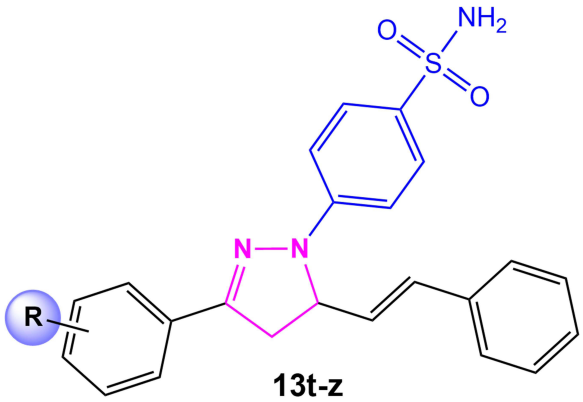

13t-z

	R_1	R_2	R	Hep-2C CS ± SD (%)	A549 CS ± SD (%)	Vero CS ± SD (%)	Hep-2C IC_{50} ± SD (μM)	A549 IC_{50} ± SD (μM)	Vero IC_{50} ± SD (μM)
a.	H	3-OH	–	79.08 ± 2.16	83.54 ± 3.07	–	–	–	–
b.	H	2-OCH_3	–	0	0	6.99 ± 0.97	17.42 ± 2.95	18.16 ± 0.83	5.99 ± 0.17
c.	H	2-Cl	–	99.86 ± 0.09	99.57 ± 0.41	–	–	–	–
d.	H	3-NO_2	–	99.08 ± 0.68	99.89 ± 0.07	–	–	–	–
e.	4-CH_3	H	–	96.78 ± 1.51	97.19 ± 0.22	–	–	–	–
f.	4-CH_3	3-OH	–	23.62 ± 2.80	11.54 ± 3.23	99.78 ± 0.68	22.75 ± 0.19	20.32 ± 2.31	–
g.	4-CH_3	2-OCH_3	–	98.17 ± 0.48	98.74 ± 1.60	–	–	–	–
h.	4-CH_3	4-Cl	–	0	0	2.44 ± 1.20	16.56 ± 0.89	18.47 ± 2.31	19.22 ± 0.25
i.	4-CH_3	3-NO_2	–	0	3.25 ± 2.75	20.14 ± 0.86	16.26 ± 1.49	20.87 ± 2.38	12.59 ± 0.46
j.	4-OCH_3	4-CH_3	–	3.23 ± 0.43	26.31 ± 2.26	70.24 ± 0.89	17.10 ± 1.42	20.66 ± 2.09	–
k.	4-OCH_3	4-OCH_3	–	98.23 ± 1.67	96.64 ± 1.26	–	–	–	–
l.	4-OCH_3	2,3-di-OCH_3	–	19.30 ± 2.16	41.85 ± 1.97	78.57 ± 0.66	17.23 ± 2.38	19.82 ± 1.75	–
m.	4-OCH_3	2-Cl	–	0	0	94.28 ± 0.32	16.03 ± 1.63	18.64 ± 1.02	–
n.	4-OCH_3	3-NO_2	–	46.90 ± 2.21	66.65 ± 2.33	87.62 ± 0.73	20.69 ± 0.56	–	–
o.	4-Cl	H	–	0	0	43.88 ± 0.86	17.20 ± 2.11	18.44 ± 0.92	23.96 ± 1.02
p.	4-Cl	3-OH	–	0	0	71.19 ± 1.63	16.62 ± 1.38	20.02 ± 2.71	–
q.	4-Cl	2-OCH_3	–	0	0	0	16.26 ± 2.17	16.19 ± 0.99	4.42 ± 0.06
r.	4-Cl	3-NO_2	–	94.93 ± 0.84	96.38 ± 0.90	–	–	–	–
s.	4-F	3-NO_2	–	99.07 ± 0.53	99.36 ± 0.44	–	–	–	–
t.	–	–	H	99.07 ± 1.45	97.32 ± 0.77	–	–	–	–
u.	–	–	4-CH_3	98,70 ± 0.25	97,66 ± 1,02	–	–	–	–
v.	–	–	4-OCH_3	98.53 ± 0.77	98.91 ± 1.24	–	–	–	–
w.	–	–	2,5-di-OCH_3	59.75 ± 3.25	60.69 ± 1.83	–	–	–	–
x.	–	–	4-Cl	96.99 ± 1.03	95.25 ± 1.73	–	–	–	–
y.	–	–	4-F	89.91 ± 2.57	94.18 ± 2.05	–	–	–	–
z.	–	–	3-NO_2	98.52 ± 0.24	96.31 ± 2.17	–	–	–	–
Ellipticine				1.34 ± 0.52	2.82 ± 1.69	20.66 ± 1.54	0.89 ± 0.28	1.34 ± 0.61	14.34 ± 0.16

Figure 38 Chemical structures of pyrazoline benzenesulfonamide derivatives (13a–z) and their cytotoxic activities, expressed as percent cell survival (CS) and IC_{50} values, in human cancer cell lines (Hep-2C and A549) and normal cells (Vero). Ellipticine was used as a reference drug.

HSC-3, HSC-4), as well as human normal oral cells (HGF, HPLF, HPC), with 5-Fluorouracil as the reference drug, as shown in Figure 39. The tested compounds exhibited a broad range of cytotoxic activity, with CC_{50} values ranging from 6.7 to 400 μM. Several analogues demonstrated marked selectivity toward tumor cell lines relative to normal cells. In particular, mono- and polymethoxy-substituted derivatives, including 14b (4-methoxy), 14f (2,5-dimethoxy), 14g (2,4-dimethoxy), and 14i (3,4,5-trimethoxy), demonstrated the lowest CC_{50} values and the most significant tumor selectivity, as indicated by high potency-selectivity expression (PSE2) scores, often exceeding those of 5-Fluorouracil (PSE2 = 206). These data highlight their promise as lead structures for further development of anticancer drugs. Furthermore, the pharmacological profiling of these derivatives revealed potent inhibitory activity against human carbonic anhydrase isoenzymes I and II (hCA I, hCA II), with Ki values ranging from 12.7 ± 1.7 to 59.8 ± 3.0 μM for hCA I and 6.9 ± 1.5 to 24.1 ± 7.1 μM for hCA II. By comparison, the reference drug Acetazolamide exhibited Ki values of 30.2 ± 7.8 μM (hCA I) and 4.4 ± 0.6 μM (hCA II). Notably, compound 14g (2,4-dimethoxy) emerged as the most effective hCA I inhibitor, while compound 14c (3-methoxy) showed superior potency against hCA II. Inhibition of carbonic anhydrase isoforms is therapeutically relevant as these enzymes are commonly upregulated within the tumor microenvironment, facilitating cancer cell survival, proliferation, and contributing to an acidic extracellular milieu.

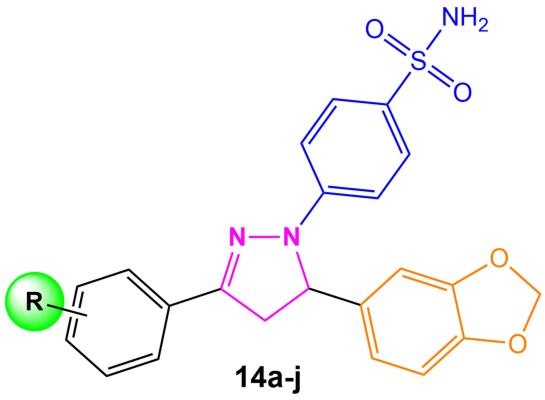

14a-j

	R	Ca9-22 CC_{50} (μM)	SI	HSC-2 CC_{50} (μM)	SI	HSC-3 CC_{50} (μM)	SI	HSC-4 CC_{50} (μM)	SI	Mean CC_{50} (μM)	SD CC_{50} (μM)	HGF CC_{50} (μM)	HPLF CC_{50} (μM)	HPC CC_{50} (μM)	Mean CC_{50} (μM)	SD CC_{50} (μM)	TS1	TS2	PSE1	PSE2
a.	H	17.1	3.1	26.1	2.0	20.8	2.5	26.1	2	22.5	4.4	56.3	37.6	63.2	52.4	13.3	2.3	3.3	10.3	19.3
b.	4-OCH_3	14.0	21.4	18.0	16.7	16.2	18.5	18.2	16.5	16.6	2.0	400	400	98.7	299.6	174.0	18	28.6	108.6	205.1
c.	3-OCH_3	19.5	6.1	18.3	6.5	13.9	8.6	18.0	6.6	17.4	2.4	38.2	178	140	118.7	72.3	6.8	2.0	39.1	10.1
d.	2-OCH_3	13.8	2.7	17.1	2.2	12.4	3.0	14.9	2.5	14.6	2.0	36.9	39.7	37	37.8	1.6	2.6	2.7	17.9	19.5
e.	3,4-di-OCH_3	47.2	8.5	400	1.0	61.0	6.6	400	1.0	227	199.8	400	400	400	400	0.0	1.8	8.5	0.8	17.9
f.	2,5-di-OCH_3	9.7	28.2	15.7	17.4	11.5	23.8	12.0	22.8	12.2	2.5	400	276.3	147	274.4	126.5	22.4	41.2	183.6	425.1
g.	2,4-di-OCH_3	9.9	25.8	13.5	18.9	9.8	26.0	12.7	20.1	11.5	1.9	400	234.3	131	255.1	135.7	22.2	40.3	193.2	405.4
h.	2,4,5-tri-OCH_3	400	1.0	400	1.0	21.3	18.8	21.8	18.3	211	218.5	400	400	400	400	0.0	1.9	1.0	0.9	0.3
i.	3,4,5-tri-OCH_3	9.3	30.6	30.9	9.2	11.3	25.2	6.7	42.5	14.6	11.0	400	83.7	371.3	285	174.9	19.6	43	134.6	461.5
j.	4-OH-3-OCH_3	17	3.8	26.7	2.4	26.3	2.5	16.8	3.9	21.7	5.6	76.7	64.7	54.3	65.2	11.2	3.0	4.5	13.8	26.4
5-Fluorouracil		22	44.8	261	3.8	7.8	126.4	12.5	78.9	75.8	123.6	1000	1000	958.3	986.1	24.1	13.0	45.4	17.1	206

Figure 39 Chemical structures of pyrazoline benzenesulfonamide derivatives (14a–j) and their cytotoxicity (CC_{50}) against human oral squamous carcinoma cell lines (Ca9-22, HSC-2, HSC-3, HSC-4) and normal oral cells (HGF, HPLF, HPC). 5-Fluorouracil was used as a reference drug.

Collectively, these findings substantiate the dual anticancer and carbonic anhydrase inhibitory activities of pyrazoline benzenesulfonamide derivatives as promising candidates for further investigation.

The structure–activity relationship (SAR) analysis highlighted the significant impact of both the number and position of methoxy substituents on the phenyl ring in modulating the cytotoxicity and selectivity of this series. Polymethoxylated derivatives, such as 14i (3,4,5-trimethoxy), 14f (2,5-dimethoxy), and 14g (2,4-dimethoxy), consistently demonstrated superior anticancer activity across multiple oral squamous cell carcinoma cell lines, as reflected by their low CC_{50} values and high potency-selectivity expression (PSE2) scores relative to both mono-methoxylated or unsubstituted analogues. In particular, specific arrangements of methoxy groups, namely 2,4-dimethoxy (14g), 2,5-dimethoxy (14f), and 3,4,5-trimethoxy (14i), notably enhanced both potency and selectivity towards tumor cells, suggesting that these substitution patterns facilitate optimized molecular interactions, possibly through improved binding affinity or cell permeability. Conversely, specific substitution motifs, such as the 2,4,5-trimethoxy group in compound 14h, were associated with a pronounced reduction in cytotoxic activity, underscoring the importance of regioselectivity in pharmacophore optimization. Collectively, these SAR observations highlight that not only the presence but also the precise topological arrangement of methoxy substituents is critical for attaining potent and tumor-selective anticancer effects within this compound class.

In 2022, Bilginer et al[119] reported the synthesis and anticancer evaluation of a new series of pyrazoline benzenesulfonamide derivatives featuring phenol or polyphenol moieties. The compounds (15a–n) exhibited notable in vitro anticancer activity, demonstrated through their cytotoxic effects against human lung carcinoma (A549), colorectal adenocarcinoma (Caco2), and breast adenocarcinoma (MCF7) cell lines, as shown in Figure 40. The derivatives exhibited half-maximal inhibitory concentration (IC_{50}) values in the low micromolar range, ranging from 24.52 to 138.10 μM against A549 cells, 7.78 to 56.18 μM against Caco2 cells, and 6.49 to 40.28 μM against MCF-7 cells. Particularly, compounds 15c, 15e, and 15k were identified as lead candidates, demonstrating both high cytotoxicity (low IC_{50} values) and superior selectivity indices (SI), indicating enhanced selectivity towards cancer cells relative to normal

https://doi.org/10.2147/DDDT.S562109

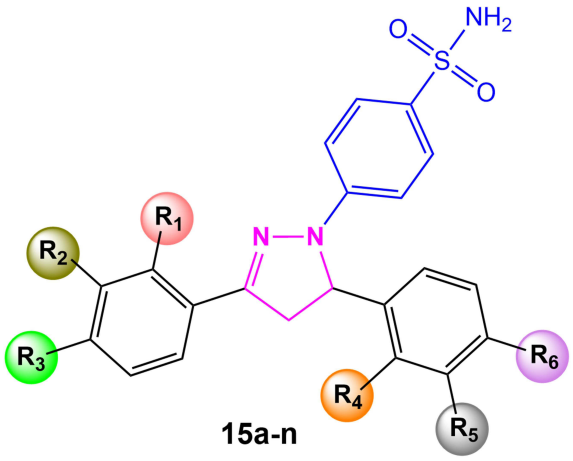

	R_1	R_2	R_3	R_4	R_5	R_6	**A549** IC_{50}	SI	**Caco2** IC_{50}	SI	**MCF-7** IC_{50}	SI	**Fibroblasts normal cells**, IC_{50}
a.	H	H	OH	H	H	OH	33.88 µM	3.2	35.95 µM	3.0	9.09 µM	11.7	106.29 µM
b.	OH	H	H	H	H	OH	49.42 µM	1.4	8.29 µM	8.4	10.27 µM	6.8	69.89 µM
c.	H	H	OH	H	H	OH	45.50 µM	1.8	7.78 µM	10.4	7.31 µM	11.1	81.20 µM
d.	H	OCH_3	OH	H	H	OH	61.18 µM	1.5	10.63 µM	8.7	11.03 µM	8.4	92.17 µM
e.	H	OCH_3	OH	H	OH	H	69.80 µM	1.3	12.40 µM	7.6	6.49 µM	14.4	93.68 µM
f.	H	H	OH	H	OH	H	46.51 µM	2.2	54.95 µM	1.9	18.13 µM	5.7	103.48 µM
g.	H	OH	H	H	OH	H	42.48 µM	2.8	48.89 µM	2.5	22.48 µM	5.3	119.99 µM
h.	H	OH	H	OH	H	H	25.20 µM	5.7	53.72 µM	2.7	34.72 µM	4.1	142.65 µM
i.	H	H	H	H	OH	OH	62.19 µM	2.2	56.18 µM	2.5	40.28 µM	3.5	139.20 µM
j.	H	OH	H	H	OCH_3	OH	48.15 µM	2.8	40.14 µM	3.3	35.61 µM	3.7	132.70 µM
k.	H	H	OH	H	OCH_3	OH	24.52 µM	4.3	22.47 µM	4.7	19.69 µM	5.3	104.58 µM
l.	H	OCH_3	OH	H	OCH_3	OH	50.89 µM	2.2	20.46 µM	5.4	17.11 µM	6.4	109.71 µM
m.	H	H	H	H	H	OH	46.38 µM	2.1	15.25 µM	6.5	16.03 µM	6.2	99.39 µM
n.	H	H	OH	H	H	H	138.10 µM	0.9	39.40 µM	3.1	33.87 µM	3.6	122.10 µM
Cisplatin							18.40 µM	11.0	–	–	–	–	112.10 µM
Doxorubicin							–	–	8.4 µM	21.41	1.4 µM	128.45	179.83 µM

Figure 40 Chemical structures of pyrazoline benzenesulfonamide derivatives (15a–n) and their cytotoxic activities (IC_{50}) against human cancer cell lines (A549, Caco2, MCF-7) and normal fibroblast cell lines. Cisplatin and doxorubicin were used as reference drugs.

fibroblasts. Notably, compound 15c displayed greater cytotoxic efficacy than the reference drug Doxorubicin (IC_{50} = 8.4 µM) against Caco-2 cells, whereas compounds 15e and 15c exhibited pronounced potency against MCF-7 cells. Beyond their anticancer potential, the series also showed remarkable inhibitory effects on carbonic anhydrase (CA) isoenzymes hCA I and hCA II, which are implicated in tumor progression. All tested derivatives surpassed the inhibitory activity of the reference drug Acetazolamide, with inhibition constants (Ki) values ranging from 7.53 ± 0.91 to 58.26 ± 9.61 nM for hCA I and 8.49 ± 1.45 to 33.35 ± 3.22 nM for hCA II, compared to Acetazolamide Ki values of 68.13 ± 9.11 nM (hCA I) and 48.13 ± 8.28 nM (hCA II). Compound 15a exhibited the most potent inhibition against hCA I (Ki = 7.53 nM), while compound 15d showed the strongest hCA II inhibition (Ki = 8.49 nM). These dual-acting profiles underscore the potential of this compound series as promising therapeutic agents combining anticancer efficacy with enzyme inhibition, meriting further investigation.

The structure–activity relationship (SAR) analysis revealed that the substitution patterns on the aromatic rings play a pivotal role in modulating both cytotoxic effects and selectivity toward cancer cells. Compounds bearing 4-hydroxy-3-methoxy substituents on the phenyl ring at the 3-position of the pyrazoline scaffold (such as 15d and 15e) exhibited marked improvements in cytotoxic potency, especially against Caco2 and MCF-7 cell lines, relative to their unsubstituted or differently substituted analogs. The introducing of methoxy substituents at this position was associated with several-fold enhancements in anticancer activity, as exemplified by the substantially lower IC_{50} values of 15e (Caco2 IC_{50} = 6.19 µM, MCF-7 IC_{50} = 6.49 µM). In contrast, increasing the number of hydroxyl substituents, as seen in compound 15i, led to diminished cytotoxicity and selectivity indices, underscoring the importance of judiciously balancing

hydrophilicity and electron-donating effects for optimal activity. Moreover, the SAR analysis highlighted the critical influence of the phenyl ring at the 5-position of the pyrazoline core. The presence of at least one hydroxyl substituent on this ring proved essential for both potent activity and favorable selectivity, with compounds lacking such substituents (eg, 15n) displaying weak anticancer effects (A549 IC_{50} = 138.10 µM; SI = 0.9) and low selectivity indices across all tested cell lines. These observations collectively indicate that both the nature and spatial arrangement of substituents on the aromatic rings are decisive factors in optimizing the therapeutic profile of pyrazoline benzenesulfonamide derivatives for anticancer applications.

In the same year, Fadhil et al [170] reported the synthesis and anticancer evaluation of a series of novel pyrazoline benzenesulfonamide derivatives. The biological activity of these compounds was evaluated both in silico using molecular docking techniques and in vitro assays against human breast cancer cell lines, specifically estrogen receptor-positive (MCF-7) and triple-negative (MDA-MB-468) models, as shown in Figure 41. The in vitro results highlighted that several derivatives exhibited measurable antiproliferative effects, with their activity profiles varying according to structural modifications. Notably, compound 16e demonstrated prominent cytotoxicity against the MCF-7 cell line, with an IC_{50} value of 4.6 µM, indicating substantially greater potency compared to Tamoxifen (IC_{50} = 18.0 µM). Conversely, compound 16c was identified as the most active derivative against the MDA-MB-468 cell line, with an IC_{50} value of 7.70 µM, outperforming Tamoxifen (IC_{50} = 15.29 µM), by a considerable margin. Additional derivatives, such as 16a and 16d, also showed selective activity with IC_{50} values of 16.33 µM and 20.09 µM, respectively, against MDA-MB-468 cells, but exhibited limited activity against MCF-7 cells (IC_{50} > 40 µM). Interestingly, compound 16b exhibited minimal cytotoxicity towards both cell lines (IC_{50} > 40 µM). These findings underscore the critical influence of substituent variation on anticancer activity and reinforce the hypothesis that hybridization of pyrazoline and benzenesulfonamide scaffolds yields promising candidates for further development as breast cancer therapeutics.

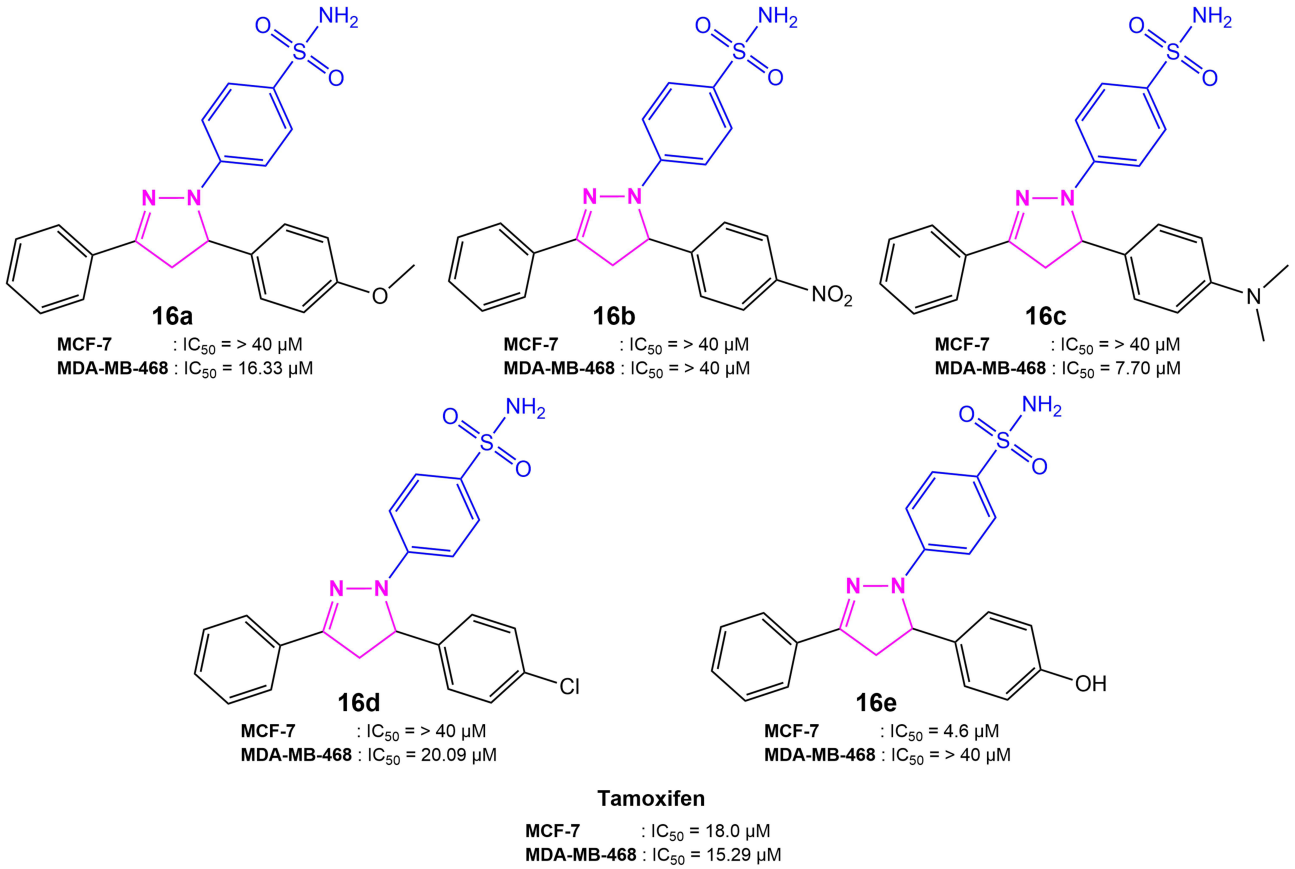

Figure 41 Chemical structures of pyrazoline benzenesulfonamide derivatives (16a–e) and their cytotoxic activities (IC_{50}) against MCF-7 and MDA-MB-468 human breast cancer cell lines. Tamoxifen was used as reference drug.

https://doi.org/10.2147/DDDT.S562109

The structure–activity relationship (SAR) analysis indicated that the nature and position of the substituent played a critical role in modulating cytotoxicity. Among the derivatives evaluated, the presence of a para-hydroxy group (compound 16e) markedly enhanced activity towards the MCF-7 cells, which was substantially lower than that of the reference drug Tamoxifen Conversely, derivatives with electron-donating or electron-withdrawing groups on other positions demonstrated moderate to weak activity, particularly against the triple-negative MDA-MB-468 cells. Notably, the para-dimethylamino derivative (compound 16c) exhibited improved activity against MDA-MB-468 cells, outperforming Tamoxifen. Derivatives bearing less optimal groups generally showed diminished cytotoxicity (>40 μM), underscoring the influence of substituent electronics and hydrogen bonding potential on bioactivity. Overall, the introduction of specific functional groups capable of forming key molecular interactions, such as hydrogen bonds, significantly increases antiproliferative potency on selected breast cancer phenotypes.

Molecular docking studies were conducted using the GOLD Suite platform, targeting both the human estrogen receptor (hER) (PDB ID: 1ERR) and PARP1 (PDB ID: 5HA9), to investigate the binding affinities and interaction landscapes of the synthesized compounds. The docking protocol measured Piecewise Linear Potential (PLP) fitness scores and mapped hydrogen bond and hydrophobic contacts. Compound 16e (para-hydroxy) exhibited the highest affinity towards the hER binding site, with a PLP fitness score of 98.46, forming key hydrogen bonds with Glu353 and Arg394, critical residues for ligand recognition and receptor modulation. Comparable interactions were observed for tamoxifen and its active metabolite, validating the relevance of the docking models. Meanwhile, compound 16c (para-dimethylamino) was notable for its favorable binding with PARP1, correlating with its selective efficacy against the triple-negative line. Docking results aligned well with in vitro antiproliferative data, demonstrating that a strong binding affinity, particularly facilitated by hydrogen bond donors and acceptors that overlap with the pharmacophoric features of known ligands, reliably translates to heightened biological activity. All lead compounds satisfied drug-likeness parameters (Lipinski's Rule of Five) and possessed high predicted bioavailability, supporting their therapeutic potential as anti-breast cancer candidates.

In 2024, Fadhil et al[125] reported the synthesis and biological evaluation of several novel pyrazoline benzenesulfonamide derivatives for their cytotoxic activities against breast cancer cell lines MCF-7 (estrogen receptor-positive) and MDA-MB-468 (triple-negative), as shown in Figure 42. The series demonstrated differential antiproliferative properties, which were strongly influenced by the nature of the substituents on the aromatic rings. Specifically, compound 17d exhibited the highest cytotoxic potency toward MDA-MB-468 cells, with an IC_{50} value of 2.79 μM, markedly outperforming Tamoxifen (IC_{50} = 15.29 μM) in this context. Meanwhile, compounds 17c and 17e showed selective activity against MCF-7 cells, with IC_{50} values of 7.4 μM and 17.96 μM, respectively, which are nearly similar to those of Tamoxifen (IC_{50} = 18.0 μM). In contrast, other analogs (17a, 17b) were less effective (IC_{50} > 50 μM for both cell lines). These results articulated the significance of rational structural modifications within the pyrazoline benzenesulfonamide scaffold, guiding the development of derivatives with target-specific cytotoxicity against breast cancer subtypes.

The structure–activity relationship (SAR) analysis of the newly synthesized pyrazoline benzenesulfonamide derivatives indicates that the substituent patterns on both the phenyl and pyridine rings greatly influence biological activity against breast cancer cell lines. Derivatives featuring electron-withdrawing substituents, such as chlorine (compound 17d), significantly enhance cytotoxic potency against the MDA-MB-468 (triple-negative) cell lines. Meanwhile, compounds bearing electron-donating groups such as dimethylamino (compound 17c) and hydroxy (compound 17e) showed selective activity against the MCF-7 (ER-positive) cell lines. In contrast, derivatives without such substituents generally exhibited weak or negligible antiproliferative effects (IC_{50} > 50 μM). These findings demonstrate that minor structural modifications on the aromatic rings critically modulate both potency and selectivity towards different breast cancer subtypes, likely by altering the binding efficacy and interaction profiles with target proteins.

Molecular docking studies evaluated the binding affinities of pyrazoline benzenesulfonamide derivatives against two key breast cancer protein targets, the human estrogen receptor alpha (hER) (PDB ID: 1ERR) and poly(ADP-ribose) polymerase 1 (PARP1) (PDB ID: 5HA9). Using the GOLD Suite docking software, all tested compounds showed favorable binding interactions with both protein targets, as reflected by piecewise linear potential (PLP) fitness scores ranging from 78.24 to 89.37 for hER and 81.62 to 93.24 for PARP1. Docking results indicated that these compounds formed multiple hydrogen bonds and short contacts, such as van der Waals and π-π stacking interactions, with key active-

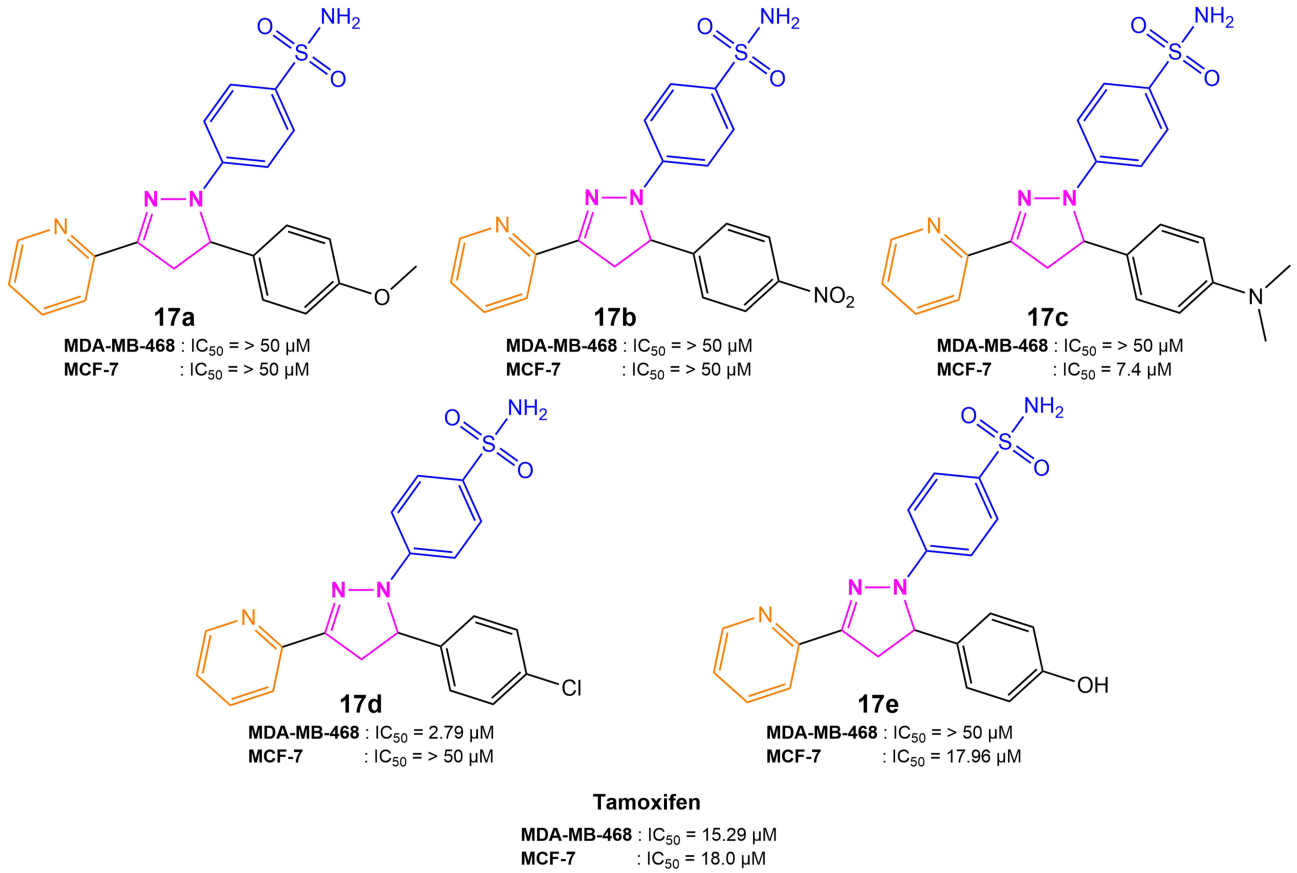

Figure 42 Chemical structures of pyrazoline benzenesulfonamide derivatives (17a–e) and their cytotoxic activity (IC_{50}) against MDA-MB-468 and MCF-7 human breast cancer cell lines. Tamoxifen was used as reference drug.

site residues (eg, Ala350, Asp351, Trp383, Met388, Arg394, Phe404, Met421, Ile424, Leu428) in the estrogen receptor and important residues (eg, Tyr246, Asn106, Ser203, Arg204) in PARP1. Among the tested derivatives, the compound 17d exhibited the highest PLP fitness and excellent binding at the PARP1 active site, which aligns with its potent cytotoxicity towards triple-negative MDA-MB-468 cells (IC_{50} = 2.79 µM). Compounds 17c and 17e presented strong docking scores and binding modes at the ER target, consistent with their in vitro selectivity for ER-positive MCF-7 cells (IC_{50} values of 7.4 µM and 17.96 µM, respectively). Comparative analysis with tamoxifen and 4-hydroxytamoxifen revealed that these reference drugs scored slightly higher in PLP fitness, yet the novel derivatives showed significant and therapeutically relevant interactions. Overall, the molecular docking studies substantiate that rational modifications of the pyrazoline-benzenesulfonamide framework can yield compounds with high and selective binding affinity towards breast cancer therapeutic targets, supporting their potential as anticancer agents.

Future Perspectives

The ongoing exploration of pyrazoline benzenesulfonamide derivatives as anticancer agents continues to show exceptional promise, greatly supported by advances in synthetic methodologies and a deeper understanding of their mechanistic profiles. Recent innovations, including one-pot, multi-step reactions, as well as microwave and ultrasound-assisted protocols, have enabled the efficient generation of structurally diverse derivatives that integrate a wide array of heterocyclic and aromatic substituents, such as morpholine, tetrazole, benzodioxole, pyrazole, thiazole, and ferrocene, as illustrated in Figure 43. Such chemical diversity not only expands the pharmacological spectrum but also allows for tailored bioactivity targeting. Empirical cytotoxicity assays and enzyme inhibitory studies have validated the potent anticancer effects of these compounds, particularly their strong inhibition of key cancer-related enzymes including matrix metalloproteinases (MMP-2 MMP-9), carbonic anhydrase isoforms (hCA IX, hCA XII), and cyclooxygenase-2 (COX-2),

 https://doi.org/10.2147/DDDT.S562109

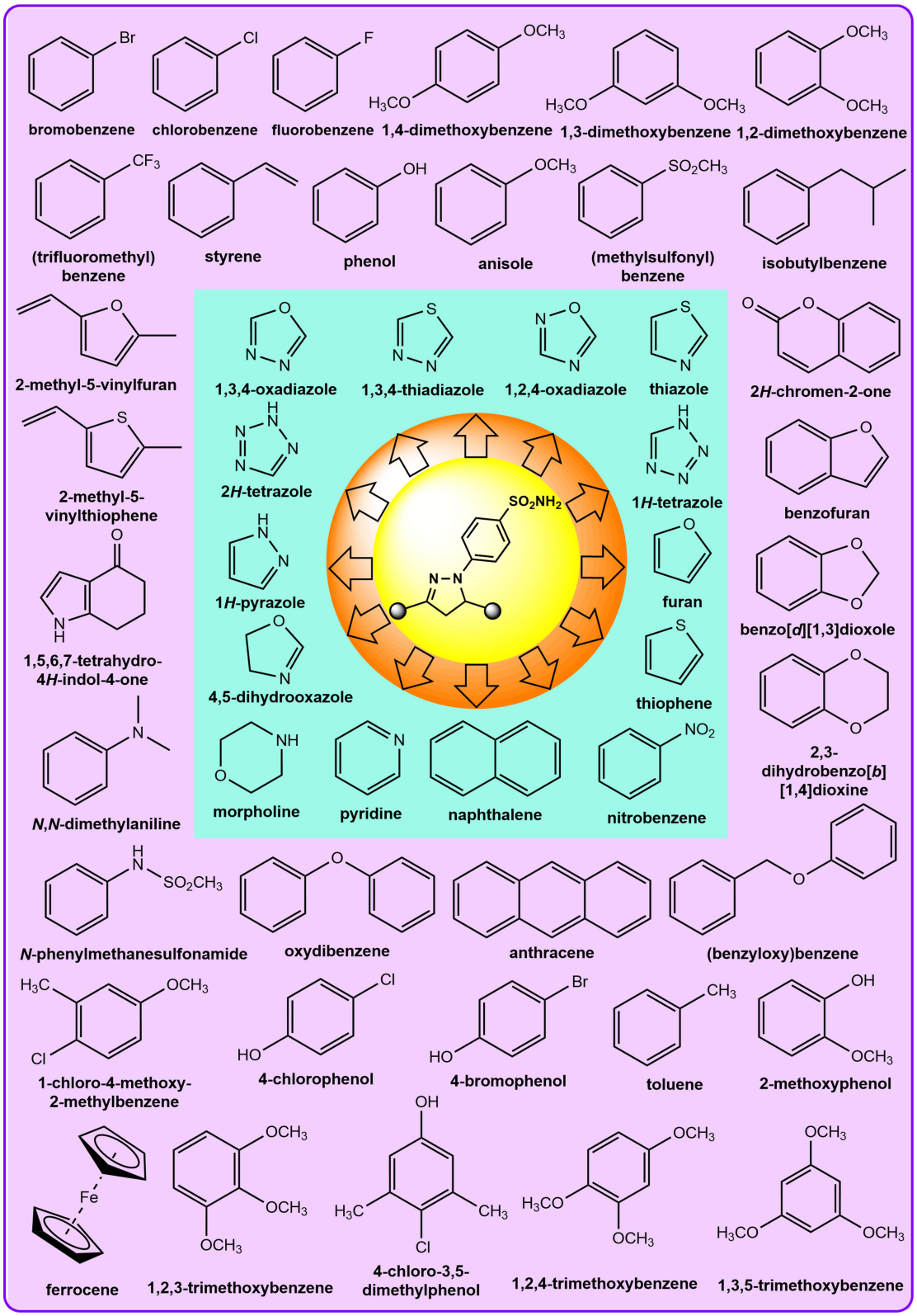

Figure 43 Diverse substituents and hybrid structures of pyrazoline benzenesulfonamide, including aliphatic heterocyclics (eg, morpholine, 4,5-dihydrooxazole, 1,5,6,7-tetrahydro-4H-indol-4-one), aromatic heterocyclics (eg, furan, thiophene, pyrazole, tetrazole, thiazole, 1,2,4-oxadiazole, 1,3,4-oxadiazole, 1,3,4-thiadiazole, 2*H*-chromen-2-one, pyridine, benzofuran, benzo[*d*][1,3]dioxole, and 2,3-dihydrobenzo[*b*][1,4]dioxine), aromatic polycyclics (eg, naphthalene and anthracene), organometallic (ferrocene), and various benzene derivatives (eg, phenyl, toluene, aniline).

each of which plays a central role in tumor progression, metastasis, and the regulation of the tumor microenvironment. Structure-activity relationship investigations further highlight that electron-donating substituents such as methoxy and methyl groups positioned on aromatic rings consistently increase anticancer potency and selectivity. Importantly, these compounds exhibit dual-targeting capabilities, enhancing therapeutic action against both enzymatic and cellular pathways, and demonstrate the ability to induce apoptosis and autophagy in a range of cancer cell lines (breast, lung, cervical, colon, and oral squamous carcinoma), while sparing normal cells. Computational molecular docking analyses have become invaluable by elucidating binding interactions and supporting the rational design of new analogues with enhanced affinity for relevant cancer targets, such as estrogen receptor and PARP1. Docking studies demonstrate how key derivatives selectively form multiple hydrogen bonds and hydrophobic contacts within the active sites of target proteins, thus reinforcing experimental findings and guiding structure-based lead optimization.

Moreover, antimicrobial investigations have identified certain pyrazoline benzenesulfonamide derivatives as potent antibacterial and antifungal agents. Selected analogues exhibit significant inhibitory activity against both Gram-positive and Gram-negative bacteria, as well as several pathogenic fungi, thereby expanding their clinical relevance for cancer patients at risk of infectious complications. The inclusion of antimicrobial testing in future screening paradigms is anticipated to facilitate the development of multifunctional agents that can address both malignancy and secondary infections. To advance these promising molecules toward clinical utility, future research should strive to optimize eco-friendly and scalable synthetic approaches, deepen mechanistic studies incorporating both experimental and computational perspectives, and conduct comprehensive in vivo pharmacological and toxicological evaluations. Interdisciplinary collaborations spanning medicinal chemistry, molecular biology, pharmacology, computational modeling, and microbiology will be essential for the successful identification and translation of lead compounds with superior efficacy, pharmacokinetics, and safety. Such integrated approaches are critical for the realization of pyrazoline benzenesulfonamide derivatives as next-generation agents in cancer therapy and infectious disease management.

Conclusion

Pyrazoline benzenesulfonamide derivatives have emerged as a highly promising scaffold in anticancer drug discovery, demonstrated by their versatile synthetic accessibility and broad spectrum of potent bioactivities against various cancer types, including lung, breast, cervical, colon, and oral squamous carcinoma. Diverse synthetic methodologies, ranging from classical Claisen–Schmidt condensation to innovative ultrasound- and microwave-assisted protocols, enable the efficient generation of structurally diverse derivatives incorporating multiple pharmacophores such as morpholine, pyrazole, benzodioxole, tetrazole, and organometallic ferrocene moieties, which enhance therapeutic profiles. Biological evaluations reveal these derivatives exhibit multifaceted mechanisms of action, prominently including strong inhibitory effects on matrix metalloproteinases (MMP-2 and MMP-9), cyclooxygenase-2 (COX-2), and cancer-associated carbonic anhydrase isoforms (hCA IX and XII), leading to suppression of tumor proliferation, metastasis, as well as induction of apoptosis and autophagy with favorable selectivity indices. Structure-activity relationship analyses highlight the crucial role of electron-donating and electron-withdrawing substituents, as well as their positions on aromatic rings, in influencing efficacy and selectivity. Integrative in vitro, in vivo, and in silico studies, particularly molecular docking studies, have further substantiated the potential of these derivatives as lead compounds, revealing the molecular basis for their potent inhibition and binding affinity to cancer-relevant enzymes, such as MMPs, COX-2, and carbonic anhydrases. These approaches illuminate key interactions, including hydrogen bonds, hydrophobic contacts, and metal coordination, that underpin both potency and selectivity, thus guiding rational design toward improved pharmacokinetic and safety profiles. Looking ahead, the clinical translation of pyrazoline benzenesulfonamide derivatives will be accelerated by optimizing sustainable synthetic strategies and elucidating deeper mechanistic insights. Importantly, emerging evidence of their antibacterial and antifungal activity suggests a further expanded scope for these compounds. Future studies focusing on systematic antimicrobial screening and rational pharmacophore integration may provide novel dual-action agents, particularly relevant for immunocompromised cancer patients or settings with oncologic comorbidity. Continued interdisciplinary research will be vital for advancing these derivatives as safe, selective, and multifunctional therapeutics capable of addressing existing challenges, such as drug resistance, toxicity, and secondary infections, within cancer treatment regimens.

Acknowledgments

This study was funded by Universitas Padjadjaran through the Indonesian Endowment Fund for Education (LPDP) on behalf of the Indonesian Ministry of Higher Education, Science and Technology and managed under the EQUITY Program (Contract No. 4303/B3/DT.03.08/2025) and 3927/UN6.RKT/HK.07.00/2025).

Disclosure

The author(s) report no conflicts of interest in this work.

References

1. Brown JS, Amend SR, Austin RH, Gatenby RA, Hammarlund EU, Pienta KJ. Updating the definition of cancer. *Mol Cancer Res*. 2023;21(11):1142–1147. doi:10.1158/1541-7786.MCR-23-0411
2. Alvarado AS. Cellular hyperproliferation and cancer as evolutionary variables. *Curr Biol*. 2012;22(17):R772–R778. doi:10.1016/j.cub.2012.08.008
3. Block KI, Gyllenhaal C, Lowe L, et al. Designing a broad-spectrum integrative approach for cancer prevention and treatment. *Semin Cancer Biol*. 2015;35(Suppl):S276–S304. doi:10.1016/j.semcancer.2015.09.007
4. Liu B, Zhou H, Tan L, Siu KTH, Guan XY. Exploring treatment options in cancer: tumor treatment strategies. *Signal Transduct Target Ther*. 2024;9(1):175. doi:10.1038/s41392-024-01856-7
5. Anand U, Dey A, Chandel AKS, et al. Cancer chemotherapy and beyond: current status, drug candidates, associated risks and progress in targeted therapeutics. *Genes Dis*. 2023;10(4):1367–1401. doi:10.1016/j.gendis.2022.02.007
6. Apetoh L, Ladoire S, Coukos G, Ghiringhelli F. Combining immunotherapy and anticancer agents: the right path to achieve cancer cure? *Ann Oncol*. 2015;26(9):1813–1823. doi:10.1093/annonc/mdv209
7. Gomtsyan A. Heterocycles in drugs and drug discovery. *Chem Heterocycl Compd*. 2012;48(1):7–10. doi:10.1007/s10593-012-0960-z
8. Haider K, Shafeeque M, Yahya S, Yar MS. A comprehensive review on pyrazoline based heterocyclic hybrids as potent anticancer agents. *Eur J Med Chem Rep*. 2022;5:100042. doi:10.1016/j.ejmcr.2022.100042
9. Rasal NK, Sonawane RB, Jagtap SV. Synthesis, characterization, and biological study of 3-trifluoromethylpyrazole tethered chalcone-pyrrole and pyrazoline-pyrrole derivatives. *Chem Biodivers*. 2021;18(10):e2100504. doi:10.1002/cbdv.202100504
10. Rana M, Arif R, Khan FI, et al. Pyrazoline analogs as potential anticancer agents and their apoptosis, molecular docking, MD simulation, DNA binding and antioxidant studies. *Bioorg Chem*. 2021;108:104665. doi:10.1016/j.bioorg.2021.104665
11. Tok F, Irem Abas B, Ö Ç, Koçyiğit-Kaymakçıoğlu B. Design, synthesis and biological evaluation of some new 2-pyrazoline derivatives as potential anticancer agents. *Bioorg Chem*. 2020;102:104063. doi:10.1016/j.bioorg.2020.104063
12. Machado V, Cenci AR, Teixeira KF, et al. Pyrazolines as potential anti-Alzheimer's agents: DFT, molecular docking, enzyme inhibition and pharmacokinetic studies. *RSC Med Chem*. 2022;13(12):1644–1656. doi:10.1039/D2MD00262K
13. Unsal-Tan O, Tüylü Küçükkılınç T, Ayazgök B, Balkan A, Ozadali-Sari K. Synthesis, molecular docking, and biological evaluation of novel 2-pyrazoline derivatives as multifunctional agents for the treatment of Alzheimer's disease. *Med Chem Commun*. 2019;10(6):1018–1026. doi:10.1039/C9MD00030E
14. Ahmad A, Husain A, Khan SA, Mohd M, Bhandari A. Synthesis, antimicrobial and antitubercular activities of some novel pyrazoline derivatives. *J Saudi Chem Soc*. 2016;20(5):577–584. doi:10.1016/j.jscs.2014.12.004
15. Zala M, Vora JJ, Khedkar VM, Almalki AH, Tivari S, Jatvada R. Development of novel sulfonamide-based pyrazole-clubbed pyrazoline derivatives: synthesis, biological evaluation, and molecular docking study. *ACS Omega*. 2025;10(7):7120–7130. doi:10.1021/acsomega.4c10198
16. Ahsan MJ, Khalilullah H, Stables JP, Govindasamy J. Synthesis and anticonvulsant activity of 3a,4-dihydro-3H-indeno[1,2-c]pyrazole-2-carboxamide/carbothioamide analogues. *J Enzyme Inhib Med Chem*. 2013;28(3):644–650. doi:10.3109/14756366.2012.663364
17. Beyhan N, Kocyigit-Kaymakcioglu B, Gümrü S, Aricioglu F. Synthesis and anticonvulsant activity of some 2-pyrazolines derived from chalcones. *Arab J Chem*. 2017;10(Suppl. 2):S2073–S2081. doi:10.1016/j.arabjc.2013.07.037
18. Abdel-Sayed MA, Bayomi SM, El-Sherbeny MA, et al. Synthesis, anti-inflammatory, analgesic, COX-1/2 inhibition activities and molecular docking study of pyrazoline derivatives. *Bioorg Med Chem*. 2016;24(9):2032–2042. doi:10.1016/j.bmc.2016.03.032
19. Akhtar W, Marella A, Alam MM, et al. Design and synthesis of pyrazole–pyrazoline hybrids as cancer-associated selective COX-2 inhibitors. *Arch Pharm*. 2021;354(1):2000116. doi:10.1002/ardp.202000116
20. Mantzanidou M, Pontiki E, Hadjipavlou-Litina D. Pyrazoles and pyrazolines as anti-inflammatory agents. *Molecules*. 2021;26(11):3439. doi:10.3390/molecules26113439
21. Tripathi AC, Upadhyay S, Paliwal S, Saraf SK. N1-benzenesulfonyl-2-pyrazoline hybrids in neurological disorders: synthesis, biological screening and computational studies. *EXCLI J*. 2018;17:126–148. doi:10.17179/excli2017-871
22. Asad M, Arshad MN, Oves M, et al. N-Trifluoroacetylated pyrazolines: synthesis, characterization and antimicrobial studies. *Bioorg Chem*. 2020;99:103842. doi:10.1016/j.bioorg.2020.103842
23. Payne M, Bottomley AL, Och A, Asmara AP, Harry EJ, Ung AT. Synthesis and biological evaluation of 3,5-substituted pyrazoles as possible antibacterial agents. *Bioorg Med Chem*. 2021;48:116401. doi:10.1016/j.bmc.2021.116401
24. Yadav CS, Krishna A, Singh SP, et al. Synthesis, characterization and bio-evaluation of novel series of pyrazoline derivatives as potential antifungal agents. *Sci Rep* 2025;15(1):14752. doi:10.1038/s41598-025-98645-1
25. Ahsan MJ, Govindasamy J, Khalilullah H, et al. POMA analyses as new efficient bioinformatics' platform to predict and optimise bioactivity of synthesized 3a,4-dihydro-3H-indeno[1,2-c]pyrazole-2-carboxamide/carbothioamide analogues. *Bioorg Med Chem Lett*. 2012;22(23):7029–7035. doi:10.1016/j.bmcl.2012.09.108
26. Al-Masoudi WA, Al-Masoudi NA, Saeed BA, Winter R, Pannecouque C. Synthesis, in vitro anti-HIV activity, cytotoxicity, and computational studies of some new steroids and their pyrazoline and oxime analogues. *Russ J Bioorg Chem*. 2020;46(5):822–836. doi:10.1134/S1068162020050039

27. Rizvi SUF, Siddiqui HL, Johns M, Detorio M, Schinazi RF. Anti-HIV-1 and cytotoxicity studies of piperidyl-thienyl chalcones and their 2-pyrazoline derivatives. *Med Chem Res*. 2012;21(11):3741–3749. doi:10.1007/s00044-011-9912-x
28. Akolkar HN, Dengale SG, Deshmukh KK, et al. Design, synthesis and biological evaluation of novel furan & thiophene containing pyrazolyl pyrazolines as antimalarial agents. *Polycycl Aromat Compd*. 2022;42(5):1959–1971. doi:10.1080/10406638.2020.1821231
29. Ahsan MJ, Ali A, Ali A, et al. Pyrazoline containing compounds as therapeutic targets for neurodegenerative disorders. *ACS Omega*. 2022;7 (43):38207–38245. doi:10.1021/acsomega.2c05339
30. Singh R, Thota S, Bansal R. Studies on 16,17-pyrazoline substituted heterosteroids as anti-Alzheimer and anti-parkinsonian agents using LPS induced neuroinflammation models of mice and rats. *ACS Chem Neurosci*. 2018;9(2):272–283. doi:10.1021/acschemneuro.7b00303
31. Kumar A, Varadaraj BG, Singla RK. Synthesis and evaluation of antioxidant activity of novel 3,5-disubstituted-2-pyrazolines. *Bull Fac Pharm Cairo Univ*. 2013;51(2):167–173. doi:10.1016/j.bfopcu.2013.04.002
32. Mohammed N, Mulugeta E, Garg A, Tadesse A. Synthesis, molecular docking studies, and evaluation of antibacterial and antioxidant activities of pyrazoline derivatives. *Results Chem*. 2024;8:101570. doi:10.1016/j.rechem.2024.101570
33. El-Sabbagh OI, Baraka MM, Ibrahim SM, et al. Synthesis and antiviral activity of new pyrazole and thiazole derivatives. *Eur J Med Chem*. 2009;44(9):3746–3753. doi:10.1016/j.ejmech.2009.03.038
34. Hayat F, Salahuddin A, Umar S, Azam A. Synthesis, characterization, antiamoebic activity and cytotoxicity of novel series of pyrazoline derivatives bearing quinoline tail. *Eur J Med Chem*. 2010;45(10):4669–4675. doi:10.1016/j.ejmech.2010.07.028
35. Parveen H, Mukhtar S, Azam A. Novel ferrocenyl linked pyrazoline analogs as potent antiamoebic agents. *J Heterocycl Chem*. 2016;53 (2):473–478. doi:10.1002/jhet.2427
36. Uğraş Z, Tok F, Çakir C, et al. Exploring 2-pyrazoline derivatives as potent antidiabetic agents and cholinesterase inhibitors: their synthesis and molecular docking studies. *J Mol Struct*. 2024;1315:138978. doi:10.1016/j.molstruc.2024.138978
37. Zhao C, Rakesh KP, Ravidar L, Fang WY, Qin HL. Pharmaceutical and medicinal significance of sulfur (SVI)-containing motifs for drug discovery: a critical review. *Eur J Med Chem*. 2019;162:679–734. doi:10.1016/j.ejmech.2018.11.017
38. Ahmed RF, Mahmoud WR, Abdelgawad NM, Fouad MA, Said MF. Exploring novel anticancer pyrazole benzenesulfonamides featuring tail approach strategy as carbonic anhydrase inhibitors. *Eur J Med Chem*. 2023;261:115805. doi:10.1016/j.ejmech.2023.115805
39. Mishra CB, Kumari S, Angeli A, Bua S, Tiwari M, Supuran CT. Discovery of benzenesulfonamide derivatives as carbonic anhydrase inhibitors with effective anticonvulsant action: design, synthesis, and pharmacological evaluation. *J Med Chem*. 2018;61(7):3151–3165. doi:10.1021/acs.jmedchem.8b00208
40. Ovung A, Bhattacharyya J. Sulfonamide drugs: structure, antibacterial property, toxicity, and biophysical interactions. *Biophys Rev*. 2021;13 (2):259–272. doi:10.1007/s12551-021-00795-9
41. Pippi B, Joaquim AR, Lopes W, et al. 8-Hydroxyquinoline-5-sulfonamides are promising antifungal candidates for the topical treatment of dermatomycosis. *J Appl Microbiol*. 2020;128(4):1038–1049. doi:10.1111/jam.14545
42. Gök N, Akıncıoğlu A, Erümit Binici E, Akıncıoğlu H, Kılınç N, Göksu S. Synthesis of novel sulfonamides with anti-Alzheimer and antioxidant capacities. *Arch Pharm*. 2021;354(7):2000496. doi:10.1002/ardp.202000496
43. Abdel-Aziz AAM, Angeli A, El-Azab AS, Hammouda MEA, El-Sherbeny MA, Supuran CT. Synthesis and anti-inflammatory activity of sulfonamides and carboxylates incorporating trimellitimides: dual cyclooxygenase/carbonic anhydrase inhibitory actions. *Bioorg Chem*. 2019;84:260–268. doi:10.1016/j.bioorg.2018.11.033
44. Ayoup MS, Khaled N, Abdel-Hamid H, et al. Novel sulfonamide derivatives as multitarget antidiabetic agents: design, synthesis, and biological evaluation. *RSC Adv*. 2024;14(11):7664–7675. doi:10.1039/D4RA01060D
45. Pastewska M, Żołnowska B, Kovačević S, et al. Modeling of anticancer sulfonamide derivatives lipophilicity by chemometric and quantitative structure-retention relationships approaches. *Molecules*. 2022;27(13):3965. doi:10.3390/molecules27133965
46. Wan Y, Fang G, Chen H, Deng X, Tang Z. Sulfonamide derivatives as potential anti-cancer agents and their SARs elucidation. *Eur J Med Chem*. 2021;226:113837. doi:10.1016/j.ejmech.2021.113837
47. Wani TA, Zargar S, Alkahtani HM, Altwaijry N, Al-Rasheed LS. Anticancer potential of sulfonamide moieties via in-vitro and in-silico approaches: comparative investigations for future drug development. *Int J Mol Sci*. 2023;24(9):7953. doi:10.3390/ijms24097953
48. Ismail MMF, El-Sayed NAM, Rateb HS, Ammar YA. New hybrids of sulfonamide/thiourea: synthesis, in silico study and antihypertensive evaluation. *Polycycl Aromat Compd*. 2022;42(6):3768–3779. doi:10.1080/10406638.2021.1872654
49. Kaya M, Demir E, Bekci H. Synthesis, characterization and antimicrobial activity of novel xanthene sulfonamide and carboxamide derivatives. *J Enzyme Inhib Med Chem*. 2013;28(5):885–893. doi:10.3109/14756366.2012.692087
50. Agertt VA, Marques LL, Bonez PC, Dalmolin TV, de Oliveira G N M, de Campos MMA. Evaluation of antimycobacterial activity of a sulphonamide derivative. *Tuberculosis*. 2013;93(3):318–321. doi:10.1016/j.tube.2013.02.003
51. Krátký M, Stolaříková J, Vinšová J. Novel sulfamethoxazole ureas and oxalamide as potential antimycobacterial agents. *Molecules*. 2017;22 (4):535. doi:10.3390/molecules22040535
52. Domínguez JN, León C, Rodrigues J, Gamboa de Domínguez N, Gut J, Rosenthal PJ. Synthesis and antimalarial activity of sulfonamide chalcone derivatives. *Il Farmaco*. 2005;60(4):307–311. doi:10.1016/j.farmac.2005.01.005
53. Chibale K, Haupt H, Kendrick H, et al. Antiprotozoal and cytotoxicity evaluation of sulfonamide and urea analogues of quinacrine. *Bioorg Med Chem Lett*. 2001;11(19):2655–2657. doi:10.1016/S0960-894X(01)00528-5
54. Bonardi A, Nocentini A, Bua S, et al. Sulfonamide inhibitors of human carbonic anhydrases designed through a three-tails approach: improving ligand/isoform matching and selectivity of action. *J Med Chem*. 2020;63(13):7422–7444. doi:10.1021/acs.jmedchem.0c00733
55. Scozzafava A, Briganti F, Ilies MA, Supuran CT. Carbonic anhydrase inhibitors: synthesis of membrane-impermeant low molecular weight sulfonamides possessing in vivo selectivity for the membrane-bound versus cytosolic isozymes. *J Med Chem*. 2000;43(2):292–300. doi:10.1021/jm990479
56. Battaglin WA, Furlong ET, Burkhardt MR, Peter CJ. Occurrence of sulfonylurea, sulfonamide, imidazolinone, and other herbicides in rivers, reservoirs and ground water in the Midwestern United States, 1998. *Sci Total Environ*. 2000;248(2):123–133. doi:10.1016/S0048-9697(99)00536-7
57. Chaudhari SB, Kumar A, Mankar VH, et al. Diverse role, structural trends, and applications of fluorinated sulphonamide compounds in agrochemical and pharmaceutical fields. *Heliyon*. 2024;10(12):e32434. doi:10.1016/j.heliyon.2024.e32434

58. Cheong MS, Seo KH, Chohra H, et al. Influence of sulfonamide contamination derived from veterinary antibiotics on plant growth and development. *Antibiotics*. 2020;9(8):456. doi:10.3390/antibiotics9080456
59. Crocetti L, Giovannoni MP, Cantini N, et al. Novel sulfonamide analogs of sivelestat as potent human neutrophil elastase inhibitors. *Front Chem*. 2020;8:795. doi:10.3389/fchem.2020.00795
60. Scozzafava A, Supuran CT. Protease inhibitors. Part 8: synthesis of potent Clostridium histolyticum collagenase inhibitors incorporating sulfonylated l-alanine hydroxamate moieties. *Bioorg Med Chem*. 2000;8(3):637–645. doi:10.1016/S0968-0896(99)00316-8
61. Karinen R, Høiseth G, Svendsen KO, Rogde S, Vindenes V. A fatal intoxication with phenazone (antipyrine). *Forensic Sci Int*. 2015;248:e13–e15. doi:10.1016/j.forsciint.2015.01.001
62. Sharma V, Bhatia P, Alam O, et al. Recent advancement in the discovery and development of COX-2 inhibitors: insight into biological activities and SAR studies (2008–2019). *Bioorg Chem*. 2019;89:103007. doi:10.1016/j.bioorg.2019.103007
63. Borges RS, Palheta IC, Ota SSB, et al. Toward of safer phenylbutazone derivatives by exploration of toxicity mechanism. *Molecules*. 2019;24 (1):143. doi:10.3390/molecules24010143
64. Lees P, Toutain PL. Pharmacokinetics, pharmacodynamics, metabolism, toxicology and residues of phenylbutazone in humans and horses. *Vet J*. 2013;196(3):294–303. doi:10.1016/j.tvjl.2013.04.019
65. Nehra B, Rulhania S, Jaswal S, Kumar B, Singh G, Monga V. Recent advancements in the development of bioactive pyrazoline derivatives. *Eur J Med Chem*. 2020;205:112666. doi:10.1016/j.ejmech.2020.112666
66. Rodriguez AT, Valtier S, Cody JT. Metabolic profile of famprofazone following multidose administration. *J Anal Toxicol*. 2004;28(6):432–438. doi:10.1093/jat/28.6.432
67. Tseng YL, Lin CT, Wang SM, Liu RH. Famprofazone as the source of methamphetamine and amphetamine in urine specimen collected during sport competition. *J Forensic Sci*. 2007;52(2):479–486. doi:10.1111/j.1556-4029.2006.00359.x
68. Lho D, Shin H, Park J. Simultaneous determination of morazone and phenmetrazine in rat plasma and urine using an on-column injection technique with fused-silica capillary column gas chromatography. *J Anal Toxicol*. 1990;14(2):113–115. doi:10.1093/jat/14.2.113
69. Gold B, Pingle M, Brickner SJ, et al. Nonsteroidal anti-inflammatory drug sensitizes Mycobacterium tuberculosis to endogenous and exogenous antimicrobials. *Proc Natl Acad Sci*. 2012;109(40):16004–16011. doi:10.1073/pnas.1214188109
70. Saleem S, Khan R, Afzal M, Kazmi I. Oxyphenbutazone promotes cytotoxicity in rats and Hep3B cellsvia suppression of PGE2 and deactivation of Wnt/β-catenin signaling pathway. *Mol Cell Biochem*. 2018;444(1):187–196. doi:10.1007/s11010-017-3243-2
71. Murtaza S, Akhtar MS, Kanwal F, Abbas A, Ashiq S, Shamim S. Synthesis and biological evaluation of schiff bases of 4-aminophenazone as an anti-inflammatory, analgesic and antipyretic agent. *J Saudi Chem Soc*. 2017;21:S359–S372. doi:10.1016/j.jscs.2014.04.003
72. Costa D, Vieira A, Fernandes E. Dipyrone and aminopyrine are effective scavengers of reactive nitrogen species. *Redox Rep*. 2006;11 (3):136–142. doi:10.1179/135100006X116637
73. Klose S, Pflock R, König IR, Linder R, Schwaninger M. Metamizole and the risk of drug-induced agranulocytosis and neutropenia in statutory health insurance data. *Naunyn-Schmiedeb Arch Pharmacol*. 2020;393(4):681–690. doi:10.1007/s00210-019-01774-4
74. Chen X, Sun Z, Wang J, et al. Predicting the pharmacokinetic characteristics of edaravone intravenous injection and sublingual tablet through modeling and simulation. *Clin Ther*. 2020;42(3):428–438. doi:10.1016/j.clinthera.2020.01.006
75. Watanabe K, Tanaka M, Yuki S, Hirai M, Yamamoto Y. How is edaravone effective against acute ischemic stroke and amyotrophic lateral sclerosis? *J Clin Biochem Nutr*. 2018;62(1):20–38. doi:10.3164/jcbn.17-62
76. Mikuls TR, Saag KG. Gout treatment: what is evidence-based and how do we determine and promote optimized clinical care? *Curr Rheumatol Rep*. 2005;7(3):242–249. doi:10.1007/s11926-996-0046-y
77. Yadav S, Bhosale M, Sattigeri B, Vimal S. Pharmacological overview for therapy of gout and hyperuricemia. *Int J Health Sci*. 2022;6 (S2):7772–7785. doi:10.53730/ijhs.v6nS2.6926
78. Grima M, Michel B, Barthelmebs M, Stephan D, Imbs JL. The effects of muzolimine and urine from muzolimine-treated rats on Na+K+Cl− cotransport in Madin-Darby canine kidney cells. *Eur J Pharmacol*. 1991;202(2):137–142. doi:10.1016/0014-2999(91)90287-Z
79. Dorigo P, Gaion RM, Bergamin M, Giacometti A, Valentini E, Maragno I. Comparison between the cardiac effects induced by muzolimine and furosemide in Guinea-pig atria. *Cardiovasc Drugs Ther*. 1990;4(6):1477–1485. doi:10.1007/BF02026495
80. Varughese T, Taur Y, Cohen N, et al. Serious infections in patients receiving ibrutinib for treatment of lymphoid cancer. *Clin Infect Dis*. 2018;67 (5):687–692. doi:10.1093/cid/ciy175
81. Rohrbach K, Thomas MA, Glick S, et al. Ibipinabant attenuates β-cell loss in male Zucker diabetic fatty rats independently of its effects on body weight. *Diabetes Obes Metab*. 2012;14(6):555–564. doi:10.1111/j.1463-1326.2012.01563.x
82. Tam J, Cinar R, Liu J, et al. Peripheral cannabinoid-1 receptor inverse agonism reduces obesity by reversing leptin resistance. *Cell Metab*. 2012;16(2):167–179. doi:10.1016/j.cmet.2012.07.002
83. Paik ES, Kim TH, Cho YJ, et al. Preclinical assessment of the VEGFR inhibitor axitinib as a therapeutic agent for epithelial ovarian cancer. *Sci Rep*. 2020;10(1):4904. doi:10.1038/s41598-020-61871-w
84. Cendrós JM, Salichs M, Encina G, Vela JM, Homedes JM. Pharmacology of enflicoxib, a new coxib drug: efficacy and dose determination by clinical and pharmacokinetic-guided approach for the treatment of osteoarthritis in dogs based on an acute arthritis induction model. *Vet Med Sci*. 2022;8(1):31–45. doi:10.1002/vms3.670
85. Homedes J, Salichs M, Guzman A. Long-term safety evaluation of Daxocox® tablets (enflicoxib) in dogs after weekly oral administrations for seven months. *BMC Vet Res*. 2021;17(1):205. doi:10.1186/s12917-021-02910-0
86. de Bruin NMWJ, Lange JHM, Kruse CG, et al. SLV330, a cannabinoid CB1 receptor antagonist, attenuates ethanol and nicotine seeking and improves inhibitory response control in rats. *Behav Brain Res*. 2011;217(2):408–415. doi:10.1016/j.bbr.2010.11.013
87. Chang LC, Lin HY, Tsai MT, et al. YC-1 inhibits proliferation of breast cancer cells by down-regulating EZH2 expression via activation of c-Cbl and ERK. *Br J Pharmacol*. 2014;171(17):4010–4025. doi:10.1111/bph.12708
88. Yeo EJ, Chun YS, Cho YS, et al. YC-1: a potential anticancer drug targeting hypoxia-inducible factor 1. *J Natl Cancer Inst*. 2003;95 (7):516–525. doi:10.1093/jnci/95.7.516
89. Ehrhardt M, Craveiro RB, Holst MI, Pietsch T, Dilloo D. The PI3K inhibitor GDC-0941 displays promising in vitro and in vivo efficacy for targeted medulloblastoma therapy. *Oncotarget*. 2015;6(2):802–813. doi:10.18632/oncotarget.2742

90. Reid JM, Walker DL, Miller JK, et al. The metabolism of pyrazoloacridine (NSC 366140) by cytochromes P450 and flavin monooxygenase in human liver microsomes. *Clin Cancer Res*. 2004;10(4):1471–1480. doi:10.1158/1078-0432.CCR-0557-03
91. Bendi A, Yadav P, Tiwari A, Bhathiwal AS, Afshari M, Rao GBD. One-pot strategic synthesis of 1,3,5-pyrazoline derivatives using NiFe2O4. Cu(OH)2 magnetic nanocomposite as heterogeneous catalyst and their theoretical studies as antifungal agents. *Iran J Catal*. 2024;14(2). doi:10.57647/j.ijc.2024.1402.10
92. Salih RHH, Hasan AH, Hussein AJ, et al. One-pot synthesis, molecular docking, ADMET, and DFT studies of novel pyrazolines as promising SARS-CoV-2 main protease inhibitors. *Res Chem Intermed*. 2022;48(11):4729–4751. doi:10.1007/s11164-022-04831-5
93. Seebacher W, Michl G, Belaj F, Brun R, Saf R, Weis R. One-pot syntheses of 2-pyrazoline derivatives. *Tetrahedron*. 2003;59(16):2811–2819. doi:10.1016/S0040-4020(03)00338-7
94. Farooq S, Ngaini Z. One-pot and two-pot synthesis of chalcone based mono and bis-pyrazolines. *Tetrahedron Lett*. 2020;61(4):151416. doi:10.1016/j.tetlet.2019.151416
95. Ur Rashid H, Khan S, Null I, et al. Direct synthesis, characterization, in vitro and in silico studies of simple chalcones as potential antimicrobial and antileishmanial agents. *R Soc Open Sci*. 2024;11(6):240410. doi:10.1098/rsos.240410
96. Azarifar D, Ghasemnejad H. Microwave-assisted synthesis of some 3,5-arylated 2-pyrazolines. *Molecules*. 2003;8(8):642–648. doi:10.3390/80800642
97. Vahedpour T, Hamzeh-Mivehroud M, Hemmati S, Dastmalchi S. Synthesis of 2-pyrazolines from hydrazines: mechanisms explained. *ChemistrySelect*. 2021;6(25):6483–6506. doi:10.1002/slct.202101467
98. Salum KA, Alidmat MM, Khairulddean M, Kamal NN, Muhammad M. Design, synthesis, characterization, and cytotoxicity activity evaluation of mono-chalcones and new pyrazolines derivatives. *J Appl Pharm Sci*. 2020;10(08):020–036. doi:10.7324/JAPS.2020.10803
99. Varghese B, Al-Busafi SN, Suliman FO, Al-Kindy SMZ. Unveiling a versatile heterocycle: pyrazoline – a review. *RSC Adv*. 2017;7(74):46999–47016. doi:10.1039/C7RA08939B
100. Zhang S, Neumann H, Beller M. Synthesis of α,β-unsaturated carbonyl compounds by carbonylation reactions. *Chem Soc Rev*. 2020;49(10):3187–3210. doi:10.1039/C9CS00615J
101. El-Naggar M, Rashdan HRM, Abdelmonsef AH. Cyclization of chalcone derivatives: design, synthesis, in silico docking study, and biological evaluation of new quinazolin-2,4-diones incorporating five-, six-, and seven-membered ring moieties as potent antibacterial inhibitors. *ACS Omega*. 2023;8(30):27216–27230. doi:10.1021/acsomega.3c02478
102. Xie C, Lu Z, Zhou W, Han J, Pan Y. A facile organocatalyzed Michael addition of pyrazolines to α,β-unsaturated carbonyl compounds. *Tetrahedron Lett*. 2012;53(49):6650–6653. doi:10.1016/j.tetlet.2012.09.096
103. Kharatmol MG, Jagdale DM. Eco-friendly synthesis of pyrazoline derivatives. *Int J Pharm Clin Res*. 2017;9(4):302–308. doi:10.25258/ijpcr.v9i04.8538
104. Safaei-Ghomi J, Masoomi R. An efficient comparison of methods involving conventional, grinding and ultrasound conditions for the synthesis of fulleroisoxazolines. *Ultrason Sonochem*. 2015;23:212–218. doi:10.1016/j.ultsonch.2014.08.004
105. Becerra D, Castillo JC. Recent advances in the synthesis of anticancer pyrazole derivatives using microwave, ultrasound, and mechanochemical techniques. *RSC Adv*. 2025;15(9):7018–7038. doi:10.1039/D4RA08866B
106. Lupacchini M, Mascitti A, Giachi G, et al. Sonochemistry in non-conventional, green solvents or solvent-free reactions. *Tetrahedron*. 2017;73(6):609–653. doi:10.1016/j.tet.2016.12.014
107. Dhonnar SL, Jagdale BS, Adole VA, Sadgir NV. PEG-mediated synthesis, antibacterial, antifungal and antioxidant studies of some new 1,3,5-trisubstituted 2-pyrazolines. *Mol Divers*. 2023;27(6):2441–2452. doi:10.1007/s11030-022-10562-x
108. Karabacak M, Altıntop MD, Ibrahim Çiftçi H, et al. Synthesis and evaluation of new pyrazoline derivatives as potential anticancer agents. *Molecules*. 2015;20(10):19066–19084. doi:10.3390/molecules201019066
109. Chovatia YS, Gandhi SP, Gorde PL, Bagade SB. Synthesis and antibacterial activity of some pyrazoline derivatives. *Orient J Chem*. 2010;26(1):275–278.
110. Sid A, Lamara K, Mokhtari M, Ziani N, Mosset P. Synthesis and characterization of 1-formyl-3-phenyl-5-aryl-2-pyrazolines. *Eur J Chem*. 2011;2(3):311–313. doi:10.5155/eurjchem.2.3.311-313.414
111. Singh P, Negi JS, Pant GJN, Rawat MSM. Synthesis and characterization of novel 1-chloroacetyl derivatives of 2-pyrazolines. *Heterocycl Commun*. 2011;17(1–2):61–63. doi:10.1515/hc.2011.013
112. Venugopal M, Choppala AD, Sundararajan R. A review on anti-inflammatory potential of substituted pyrazoline derivatives synthesised from chalcones. *Int J Pharm Pharm Sci*. 2018;10(2):9–14. doi:10.22159/ijpps.2018v10i2.23772
113. Mokle SS, Vibhute AY, Khansole SV, Zangade SB, Vibhute YB. Synthesis, characterization and antibacterial activity of some new 2-pyrazolines using triethanolamine as reaction solvent. *Res J Pharm Biol Chem Sci*. 2010;1(3):631–638.
114. Kehtari M, Karimi-Jaberi Z. A convenient synthesis of 3,5-diaryl-2-pyrazoline-1-carboxamides through the reactions of chalcones with semicarbazide in the presence of potassium carbonate. *Chem Biol Interface*. 2016;6(2):64–68.
115. Kumar R, Singh H, Mazumder A, Salahuddin, Yadav RK. Synthetic approaches, biological activities, and structure–activity relationship of pyrazolines and related derivatives. *Top Curr Chem*. 2023;381(3):12. doi:10.1007/s41061-023-00422-z
116. Nikalje AP, Malhotra P, Ghodke M. Ultrasound-promoted green synthesis and pharmacological screening of some novel 4-(3, 5-diaryl substituted)-4,5-dihydro-1H-pyrazol-1-yl) benzene sulfonamide. *Asian J Res Chem*. 2011;4(11):1712–1716. doi:10.5958/0974-4150
117. Sharma PK, Kumar S, Kumar P, et al. Synthesis of 1-(4-aminosulfonylphenyl)-3,5-diarylpyrazoline derivatives as potent antiinflammatory and antimicrobial agents. *Med Chem Res*. 2012;21(10):2945–2954. doi:10.1007/s00044-011-9823-x
118. Herfindo N, Frimayanti N, Ikhtiarudin I, Eryanti Y, Zamri A. Synthesis and evaluation of some sulfonamide-substituted of 1,3,5-triphenyl pyrazoline derivatives as tyrosinase enzyme inhibitors. *Molekul*. 2023;18(2):218–226. doi:10.20884/1.jm.2023.18.2.6936
119. Bilginer S, Bardaweel SK, Demir Y, Gulcin I, Kazaz C. Synthesis, cytotoxicities, and carbonic anhydrase inhibition activities of pyrazoline–benzenesulfonamide derivatives harboring phenol/polyphenol moieties. *Med Chem Res*. 2022;31(6):925–935. doi:10.1007/s00044-022-02893-z
120. Thach TD, Nguyen TMT, Nguyen TAT, et al. Synthesis and antimicrobial, antiproliferative and anti-inflammatory activities of novel 1,3,5-substituted pyrazoline sulphonamides. *Arab J Chem*. 2021;14(11):103408. doi:10.1016/j.arabjc.2021.103408
121. Gul HI, Yamali C, Yesilyurt F, et al. Microwave-assisted synthesis and bioevaluation of new sulfonamides. *J Enzyme Inhib Med Chem*. 2017;32(1):369–374. doi:10.1080/14756366.2016.1254207

122. Hassan SY. Synthesis, antibacterial and antifungal activity of some new pyrazoline and pyrazole derivatives. *Molecules*. 2013;18(3):2683–2711. doi:10.3390/molecules18032683
123. Yan XQ, Wang ZC, Li Z, et al. Sulfonamide derivatives containing dihydropyrazole moieties selectively and potently inhibit MMP-2/MMP-9: design, synthesis, inhibitory activity and 3D-QSAR analysis. *Bioorg Med Chem Lett*. 2015;25(20):4664–4671. doi:10.1016/j.bmcl.2015.08.026
124. Abdelall EKA, Lamie PF, Ali WAM. Cyclooxygenase-2 and 15-lipoxygenase inhibition, synthesis, anti-inflammatory activity and ulcer liability of new celecoxib analogues: determination of region-specific pyrazole ring formation by NOESY. *Bioorg Med Chem Lett*. 2016;26 (12):2893–2899. doi:10.1016/j.bmcl.2016.04.046
125. Fadhil HR, Raauf AMR, Mahdi MF. Synthesis, characterization, preliminary molecular docking, pharmacological activity, and ADME studies of some new pyrazoline derivatives as anti-breast cancer agents. *Pharmacia*. 2024;71:1–10. doi:10.3897/pharmacia.71.e133015
126. Raauf AMR, Omar TNA, Mahdi MF, Fadhil HR. Synthesis, molecular docking and anti-inflammatory evaluation of new trisubstituted pyrazoline derivatives bearing benzenesulfonamide moiety. *Nat Prod Res*. 2024;38(2):253–260. doi:10.1080/14786419.2022.2117174
127. Tuğrak M, Gül Hİ, Sakagami H, Kaya R, Gülçin İ. Synthesis and biological evaluation of new pyrazolebenzene-sulphonamides as potential anticancer agents and hCA I and II inhibitors. *Turk J Chem*. 2021;45(3):528–539. doi:10.3906/kim-2009-37
128. Özdemir A, Sever B, Altıntop MD, Tilki EK, Dikmen M. Design, synthesis, and neuroprotective effects of a series of pyrazolines against 6-hydroxydopamine-induced oxidative stress. *Molecules*. 2018;23(9):2151. doi:10.3390/molecules23092151
129. Rathish IG, Javed K, Ahmad S, et al. Synthesis and antiinflammatory activity of some new 1,3,5-trisubstituted pyrazolines bearing benzene sulfonamide. *Bioorg Med Chem Lett*. 2009;19(1):255–258. doi:10.1016/j.bmcl.2008.10.105
130. Abdellatif KRA, Abdelall EKA, Elshemy HAH, Lamie PF, Elnahaas E, Amin DME. Design, synthesis of new anti-inflammatory agents with a pyrazole core: COX-1/COX-2 inhibition assays, anti-inflammatory, ulcerogenic, histopathological, molecular Modeling, and ADME studies. *J Mol Struct*. 2021;1240:130554. doi:10.1016/j.molstruc.2021.130554
131. Faidallah HM, Rostom SAF, Khan KA. Synthesis and biological evaluation of pyrazole chalcones and derived bipyrazoles as anti-inflammatory and antioxidant agents. *Arch Pharmacal Res*. 2015;38(2):203–215. doi:10.1007/s12272-014-0392-7
132. Fioravanti R, Desideri N, Carta A, et al. Inhibitors of yellow fever virus replication based on 1,3,5-triphenyl-4,5-dihydropyrazole scaffold: design, synthesis and antiviral evaluation. *Eur J Med Chem*. 2017;141:15–25. doi:10.1016/j.ejmech.2017.09.060
133. Abdellatif KRA, Abdelgawad MA, Elshemy HAH, Alsayed SSR, Kamel G. Synthesis and anti-inflammatory evaluation of new 1,3,5-triaryl-4,5-dihydro-1H-pyrazole derivatives possessing an aminosulphonyl pharmacophore. *Arch Pharmacal Res*. 2015;38(11):1932–1942. doi:10.1007/s12272-015-0606-7
134. Amin NH, Hamed MIA, Abdel-Fattah MM, Abusabaa AHA, El-Saadi MT. Design, synthesis and mechanistic study of novel diarylpyrazole derivatives as anti-inflammatory agents with reduced cardiovascular side effects. *Bioorg Chem*. 2021;116:105394. doi:10.1016/j.bioorg.2021.105394
135. Chaudhary JK, Jain AP, Tiwari OP. Preparation and analysis of new 1,3,5-trisubstituted-2-pyrazolines derivative for their analgesic potential. *J Pharm Res Int*. 2021;33(57A):153–164. doi:10.9734/jpri/2021/v33i57A33979
136. Eid NM, George RF. Facile synthesis of some pyrazoline-based compounds with promising anti-inflammatory activity. *Future Med Chem*. 2018;10(2):183–199. doi:10.4155/fmc-2017-0144
137. Hussain T, Ullah S, Alrokayan S, et al. Synthesis, characterization and biological evaluation of pyrazole-based benzene sulfonamides as inhibitors of human carbonic anhydrase II, IX and XII. *RSC Adv*. 2023;13(27):18461–18479. doi:10.1039/D3RA03276K
138. Kucukoglu K, Oral F, Aydin T, et al. Synthesis, cytotoxicity and carbonic anhydrase inhibitory activities of new pyrazolines. *J Enzyme Inhib Med Chem*. 2016;31(sup4):20–24. doi:10.1080/14756366.2016.1217852
139. Mete E, Comez B, Inci Gul H, Gulcin I, Supuran CT. Synthesis and carbonic anhydrase inhibitory activities of new thienyl-substituted pyrazoline benzenesulfonamides. *J Enzyme Inhib Med Chem*. 2016;31(sup2):1–5. doi:10.1080/14756366.2016.1181627
140. Ovais S, Bashir R, Yaseen S, Rathore P, Samim M, Javed K. Synthesis and pharmacological evaluation of some novel 2-pyrazolines bearing benzenesulfonamide as anti-inflammatory and blood glucose lowering agents. *Med Chem Res*. 2013;22(3):1378–1385. doi:10.1007/s00044-012-0130-y
141. ChK K, Trivedi R, Ravi Kumar K, Giribabu L, Sridhar B. Synthesis, characterization, electrochemistry and optical properties of new 1,3,5-trisubstituted ferrocenyl pyrazolines and pyrazoles containing sulfonamide moiety. *J Organomet Chem*. 2012;718:64–73. doi:10.1016/j.jorganchem.2012.08.011
142. Yan XQ, Wang ZC, Zhang B, Qi PF, Li GG, Zhu HL. Dihydropyrazole derivatives containing benzo oxygen heterocycle and sulfonamide moieties selectively and potently inhibit COX-2: design, synthesis, and anti-colon cancer activity evaluation. *Molecules*. 2019;24(9):1685. doi:10.3390/molecules24091685
143. Lamie PF, Philoppes JN, Azouz AA, Safwat NM. Novel tetrazole and cyanamide derivatives as inhibitors of cyclooxygenase-2 enzyme: design, synthesis, anti-inflammatory evaluation, ulcerogenic liability and docking study. *J Enzyme Inhib Med Chem*. 2017;32(1):805–820. doi:10.1080/14756366.2017.1326110
144. Qiu HY, Wang PF, Li Z, et al. Synthesis of dihydropyrazole sulphonamide derivatives that act as anti-cancer agents through COX-2 inhibition. *Pharmacol Res*. 2016;104:86–96. doi:10.1016/j.phrs.2015.12.025
145. Abdelall EKA, Aboelnaga LS, Hassan RM, Lamie PF. Methanesulfonamide derivatives as gastric safe anti-inflammatory agents: design, synthesis, selective COX-2 inhibitory activity, histopathological and histochemical studies. *Bioorg Chem*. 2023;140:106787. doi:10.1016/j.bioorg.2023.106787
146. Kumar G, Tanwar O, Kumar J, et al. Pyrazole-pyrazoline as promising novel antimalarial agents: a mechanistic study. *Eur J Med Chem*. 2018;149:139–147. doi:10.1016/j.ejmech.2018.01.082
147. Amin KM, Eissa AAM, Abou-Seri SM, Awadallah FM, Hassan GS. Synthesis and biological evaluation of novel coumarin–pyrazoline hybrids endowed with phenylsulfonyl moiety as antitumor agents. *Eur J Med Chem*. 2013;60:187–198. doi:10.1016/j.ejmech.2012.12.004
148. Pandey AK, Sharma S, Pandey M, Alam MM, Akhter M, Shaquiquzzaman M. 4,5-Dihydrooxazole-pyrazoline hybrids: synthesis and their evaluation as potential antimalarial agents. *Eur J Med Chem*. 2016;123:476–486. doi:10.1016/j.ejmech.2016.07.055
149. Gul HI, Yamali C, Bulbuller M, et al. Anticancer effects of new dibenzenesulfonamides by inducing apoptosis and autophagy pathways and their carbonic anhydrase inhibitory effects on hCA I, hCA II, hCA IX, hCA XII isoenzymes. *Bioorg Chem*. 2018;78:290–297. doi:10.1016/j.bioorg.2018.03.027

150. Kumar P, Chandak N, Kaushik P, et al. Benzenesulfonamide bearing pyrazolylpyrazolines: synthesis and evaluation as anti-inflammatory–antimicrobial agents. *Med Chem Res*. 2014;23(2):882–895. doi:10.1007/s00044-013-0679-0
151. Ragab FAEF, Mohammed EI, Abdel Jaleel GA, Abd El-Rahman AA, Nissan YM. Synthesis of hydroxybenzofuranyl-pyrazolyl and hydroxyphenyl-pyrazolyl chalcones and their corresponding pyrazoline derivatives as COX inhibitors, anti-inflammatory and gastroprotective agents. *Chem Pharm Bull*. 2020;68(8):742–752. doi:10.1248/cpb.c20-00193
152. Dekhane DV, Pawar SS, Gupta S, Shingare MS, Patil CR, Thore SN. Synthesis and anti-inflammatory activity of some new 4,5-dihydro-1,5-diaryl-1H-pyrazole-3-substituted-heteroazole derivatives. *Bioorg Med Chem Lett*. 2011;21(21):6527–6532. doi:10.1016/j.bmcl.2011.08.061
153. Sharma PK, Kumar S, Kumar P, et al. Synthesis and biological evaluation of some pyrazolylpyrazolines as anti-inflammatory–antimicrobial agents. *Eur J Med Chem*. 2010;45(6):2650–2655. doi:10.1016/j.ejmech.2010.01.059
154. Thach TD, Le TTV, Nguyen HTA, Dang CH, Dang VS, Nguyen TD. Synthesis of sulfonamides bearing 1,3,5-triarylpyrazoline and 4-thiazolidinone moieties as novel antimicrobial agents. *J Serb Chem Soc*. 2020;85(2):155–162. doi:10.2298/JSC180621057T
155. Ozgun DO, Alak G, Ucar A, et al. Effects of a novel benzenesulfonamide 4-(3-(4-bromophenyl)-5-(2,4-dimethoxyphenyl)-4,5-dihydro-1H-pyrazol-1-yl) on antioxidant enzymes and hematological parameters of rainbow trout (Oncorhynchus mykiss). *Pak J Zool*. 2021;53(6):2083–2089. doi:10.17582/journal.pjz/20191118081134
156. Khloya P, Ceruso M, Ram S, Supuran CT, Sharma PK. Sulfonamide bearing pyrazolylpyrazolines as potent inhibitors of carbonic anhydrase isoforms I, II, IX and XII. *Bioorg Med Chem Lett*. 2015;25(16):3208–3212. doi:10.1016/j.bmcl.2015.05.096
157. Abdellatif KRA, Fadaly WAA. Design, synthesis, cyclooxygenase inhibition and biological evaluation of new 1,3,5-triaryl-4,5-dihydro-1*H*-pyrazole derivatives possessing amino/methanesulfonyl pharmacophore. *Bioorg Chem*. 2017;70:57–66. doi:10.1016/j.bioorg.2016.11.008
158. Wang PF, Qiu HY, Baloch SK, Gong HB, Wang ZC, Zhu HL. Synthesis, biological evaluation, and docking of dihydropyrazole sulfonamide containing 2-hydroxyphenyl moiety: a series of novel MMP-2 inhibitors. *Chem Biol Drug Des*. 2015;86(6):1405–1410. doi:10.1111/cbdd.12604
159. Ozgun DO, Gul HI, Yamali C, et al. Synthesis and bioactivities of pyrazoline benzensulfonamides as carbonic anhydrase and acetylcholinesterase inhibitors with low cytotoxicity. *Bioorg Chem*. 2019;84:511–517. doi:10.1016/j.bioorg.2018.12.028
160. Yamali C, Gul HI, Ece A, Taslimi P, Gulcin I. Synthesis, molecular modeling, and biological evaluation of 4-[5-aryl-3-(thiophen-2-yl)-4,5-dihydro-1H-pyrazol-1-yl] benzenesulfonamides toward acetylcholinesterase, carbonic anhydrase I and II enzymes. *Chem Biol Drug Des*. 2018;91(4):854–866. doi:10.1111/cbdd.13149
161. Yamali C, Gul HI, Kazaz C, Levent S, Gulcin I. Synthesis, structure elucidation, and in vitro pharmacological evaluation of novel polyfluoro substituted pyrazoline type sulfonamides as multi-target agents for inhibition of acetylcholinesterase and carbonic anhydrase I and II enzymes. *Bioorg Chem*. 2020;96:103627. doi:10.1016/j.bioorg.2020.103627
162. Gul HI, Mete E, Taslimi P, Gulcin I, Supuran CT. Synthesis, carbonic anhydrase I and II inhibition studies of the 1,3,5-trisubstituted-pyrazolines. *J Enzyme Inhib Med Chem*. 2017;32(1):189–192. doi:10.1080/14756366.2016.1244533
163. Yadav CS, Azad I, Rahman Khan A, et al. Recent advances in the synthesis of pyrazoline derivatives from chalcones as potent pharmacological agents: a comprehensive review. *Results Chem*. 2024;7:101326. doi:10.1016/j.rechem.2024.101326
164. Bano S, Javed K, Ahmad S, Rathish IG, Singh S, Alam MS. Synthesis and biological evaluation of some new 2-pyrazolines bearing benzene sulfonamide moiety as potential anti-inflammatory and anti-cancer agents. *Eur J Med Chem*. 2011;46(12):5763–5768. doi:10.1016/j.ejmech.2011.08.015
165. Gul HI, Mete E, Eren SE, Sakagami H, Yamali C, Supuran CT. Designing, synthesis and bioactivities of 4-[3-(4-hydroxyphenyl)-5-aryl-4,5-dihydro-pyrazol-1-yl]benzenesulfonamides. *J Enzyme Inhib Med Chem*. 2017;32(1):169–175. doi:10.1080/14756366.2016.1243536
166. Gul HI, Yamali C, Sakagami H, et al. New anticancer drug candidates sulfonamides as selective hCA IX or hCA XII inhibitors. *Bioorg Chem*. 2018;77:411–419. doi:10.1016/j.bioorg.2018.01.021
167. Fadhil HR, Mahdi MF, Raauf AMR. Molecular docking, synthesis, characterization and antiproliferative evaluation of pyrazoline derivatives. *Biochem Cell Arch*. 2022;22(1):2927–2936.